

Aus dem Institut für Neuroimmunologie und Multiple-Sklerose-Forschung  
(Prof. Dr. med. A. Flügel)  
der Medizinischen Fakultät der Universität Göttingen

# **Analysis of teriflunomide therapy on EAE**

INAUGURAL-DISSERTATION

zur Erlangung des Doktorgrades  
der Medizinischen Fakultät der  
Georg-August-Universität zu Göttingen

vorgelegt von

**Jasemin Beate Dannheim**

aus

Stade

Göttingen 2020

Dekan:	Prof. Dr. med. W. Brück
Referent	Prof. Dr. med. A. Flügel
Ko-Referent:	Prof. Dr. rer. nat. L. Walter
Drittreferent:	Prof. Dr. mult. T. Meyer

Datum der mündlichen Prüfung: 08.03.2022

Hiermit erkläre ich, die Dissertation mit dem Titel "Analysis of teriflunomide therapy on EAE" eigenständig angefertigt und keine anderen als die von mir angegebenen Quellen und Hilfsmittel verwendet zu haben.

Göttingen, den 08.05.2020

.....

(Unterschrift)

## Table of contents

<b>List of tables</b> .....	<b>III</b>
<b>List of figures</b> .....	<b>IV</b>
<b>Abbreviations</b> .....	<b>VI</b>
<b>1 Introduction</b> .....	<b>1</b>
1.1 Central Nervous System — an immune-privileged organ? .....	1
1.2 Multiple sclerosis .....	2
1.2.1 Etiology and clinical phenotypes .....	2
1.2.2 Histopathology .....	4
1.2.3 MS etiopathogenesis: the autoimmune hypothesis .....	5
1.3 Experimental autoimmune encephalomyelitis as an animal model of MS .....	7
1.4 Infiltration route of T <sub>MBP-GFP</sub> cells during EAE course .....	9
1.5 Disease-modifying treatments in multiple sclerosis .....	11
1.5.1 Established treatments .....	11
1.5.2 Teriflunomide .....	15
1.6 Aims of the study .....	19
<b>2 Materials and Methods</b> .....	<b>20</b>
2.1 Materials .....	20
2.2 Methods .....	22
2.2.1 Animals .....	22
2.2.2 Generation and culturing of GFP <sup>+</sup> antigen-specific T cells .....	22
2.2.3 Animal experiments .....	24
2.2.4 Adoptive transfer EAE .....	25
2.2.5 Teriflunomide solution .....	25
2.2.6 Administration of teriflunomide and uridine .....	26
2.2.7 Cell isolation .....	27
2.2.8 Flow cytometry cell quantification .....	28
2.2.9 Surface staining .....	28
2.2.10 Proliferation assay .....	28
2.2.11 Quantitative real-time polymerase chain reaction (QRT-PCR) .....	29
2.2.12 Cell sorting .....	31
2.2.13 Apoptosis detection assay .....	32
2.2.14 Histology .....	32
2.2.15 Acute slicing and imaging .....	33
2.2.16 ReInjection of T cells isolated from mediastinal lymph nodes .....	33
<b>3 Results</b> .....	<b>35</b>
3.1 Analysis of T <sub>MBP-GFP</sub> cell proliferation .....	35
3.2 Effect of teriflunomide on T <sub>MBP-GFP</sub> cell activation .....	37

---

3.3	The effect of teriflunomide on the production of pro-inflammatory cytokines IFN $\gamma$ and IL-17 in T <sub>MBP-GFP</sub> cells.....	40
3.4	The effect of teriflunomide on the preclinical phase in the EAE model in Lewis rats .....	41
3.4.1	Pharmacokinetics with different doses of teriflunomide .....	41
3.4.2	Clinical development of EAE under the influence of teriflunomide .....	42
3.4.3	Effect of teriflunomide on T <sub>MBP-GFP</sub> cell infiltration in the spinal cord.....	43
3.4.4	Effect of teriflunomide on the inflammatory milieu in the spinal cord .....	44
3.4.5	Effect of teriflunomide on the migratory pattern of T <sub>MBP-GFP</sub> cells .....	45
3.4.6	Distribution of T cells in the peripheral organs .....	49
3.4.7	Effect of teriflunomide on the migratory behavior of T cells within the lung tissue .....	51
3.4.8	Effect of teriflunomide on the emigration of T <sub>MBP-GFP</sub> cells out of the lung .....	53
3.4.9	Effect of teriflunomide on the reactivation potential of <i>ex vivo</i> -isolated T <sub>MBP-GFP</sub> cells .....	54
3.5	Effect of teriflunomide on the clinical phase in the EAE model in Lewis rats.....	58
<b>4</b>	<b>Discussion .....</b>	<b>63</b>
4.1	Effect of teriflunomide on T <sub>MBP-GFP</sub> cells <i>in vitro</i> .....	63
4.2	<i>In vivo</i> effect of teriflunomide on transfer EAE.....	64
4.3	Impairment of T cell migration .....	66
4.4	Teriflunomide in therapeutic treatment .....	68
<b>5</b>	<b>Summary and conclusion.....</b>	<b>70</b>
<b>6</b>	<b>Abstract.....</b>	<b>71</b>
<b>7</b>	<b>References .....</b>	<b>72</b>
	<b>Acknowledgments .....</b>	<b>86</b>
	<b>Lebenslauf.....</b>	<b>87</b>

**List of tables**

Table 1 Medium prepared for the present study.....	20
Table 2 Scoring system for rat experimental autoimmune encephalomyelitis .....	25
Table 3 Reaction batch per well for QRT-PCR .....	30
Table 4 Primer sequences for <i>in vitro</i> analyses .....	31
Table 5 Clinical table .....	43

**List of figures**

Figure 1 Neuroanatomy of the vascular blood–brain barrier .....	2
Figure 2 Representative disease score of a monophasic disease during atEAE in Lewis rat.....	9
Figure 3 Migratory pattern of i.v. injected T <sub>MBP-GFP</sub> cells during atEAE.....	10
Figure 4 Changed mRNA expression profile of migratory T cells versus T cell blasts .....	11
Figure 5 German DGNM guideline for disease-modifying treatments in MS.....	14
Figure 6 The role of DHODH in the <i>de novo</i> pyrimidine synthesis.....	15
Figure 7 Impact of teriflunomide on the pyrimidine synthesis .....	16
Figure 8 Proliferation assay of T <sub>MBP-GFP</sub> cells in the absence and presence of MBP.....	24
Figure 9 Mode and scheme of administration of teriflunomide and uridine I .....	26
Figure 10 Mode and scheme of administration of teriflunomide and uridine II .....	27
Figure 11 <i>In vitro</i> proliferation of T <sub>MBP-GFP</sub> cells with different concentrations of teriflunomide .....	36
Figure 12 Proliferation assay of T <sub>MBP-GFP</sub> cells in presence of different concentrations of teriflunomide measured by 3H-thymidine incorporation.....	37
Figure 13 Levels of activation markers in T <sub>MBP-GFP</sub> cells stimulated in the presence of teriflunomide .....	39
Figure 14 Quantitative PCR of pro-inflammatory cytokine expression in T <sub>MBP-GFP</sub> cells cultured with different concentrations of teriflunomide.....	41
Figure 15 Pharmacokinetic with 3, 5, and 10 mg/kg/d teriflunomide.....	42
Figure 16 Infiltration of T <sub>MBP-GFP</sub> cells in the spinal cord on day 5 p.t. (peak of atEAE) with or without teriflunomide treatment.....	44
Figure 17 Quantitative RNA analyses of pro-inflammatory cytokines in total tissue of spinal cord parenchyma and meninges from naïve animals and from teriflunomide-treated animals on day 4 and 5 .....	45
Figure 18 Quantification of T <sub>MBP-GFP</sub> cells in different organs under different treatments during atEAE .....	48
Figure 19 Higher percentage of T <sub>MBP-GFP</sub> cells in the lung in teriflunomide-treated animals compared to vehicle-treated animals.....	50

---

Figure 20 Homing of T <sub>MBP-GFP</sub> cells to bronchi in teriflunomide-treated and vehicle-treated animals .....	52
Figure 21 Annexin V and propidium iodide staining of T <sub>MBP-GFP</sub> cells in the lung on day 3 p.t. ....	53
Figure 22 Quantitative PCR analyses for expression of KLF2, S1P1, CCR7, and CXCR3 in sorted T <sub>MBP-GFP</sub> cells from the lung .....	54
Figure 23 Re-stimulation of <i>ex vivo</i> -isolated T <sub>MBP-GFP</sub> cells from mediastinal lymph nodes ..	55
Figure 24 T <sub>MBP-GFP</sub> cells extracted from mediastinal lymph nodes from animals treated with vehicle- or teriflunomide and re-stimulated <i>in vitro</i> with MBP show the same activation levels .....	56
Figure 25 Expression levels of inflammatory cytokines in T <sub>MBP-GFP</sub> cells extracted from vehicle- or teriflunomide-treated animals on day 2 after antigen encounter.....	57
Figure 26 Clinical effect of teriflunomide administered either as therapeutic or prophylactic treatment during atEAE.....	59
Figure 27 Number of T <sub>MBP-GFP</sub> cells in the s.c. parenchyma, s.c. meninges, and blood under vehicle treatment, prophylactic treatment, and therapeutic treatment at day 4 p.t. ....	60
Figure 28 Quantitative RNA analyses of pro-inflammatory cytokines in T <sub>MBP-GFP</sub> cells sorted from s.c. parenchyma and blood from either vehicle-treated or therapeutically treated animals on day 4 p.t. ....	61
Figure 29 Quantitative RNA analyses of pro-inflammatory cytokines in the total tissue of s.c. parenchyma and meninges on day 4 p.t. ....	62



**Abbreviations**

APC	antigen-presenting cell
atEAE	adoptive transfer experimental autoimmune encephalomyelitis
BBB	blood-brain barrier
Beta-IFN	betainterferon
CNP	cyclic nucleotide phosphodiesterase
CNS	central nervous system
DHODH	dihydroorotate dehydrogenase
FCS	fetal calf serum
GA	glatiramer acetate
GFP	green fluorescent protein
GM	grey matter
GWASs	genome-wide association studies
i.v.	intravenously
MAG	myelin-associated glycoprotein
MBP	myelin basic protein
MHC	major histocompatibility complex
MOA	mode of action
MOG	myelin oligodendrocyte glycoprotein
MS	multiple sclerosis
PLP	myelin proteolipid protein
pMSCV	plasmid murine stem cell virus
PPMS	primary progressive multiple sclerosis
p.t.	post transfer
RRMS	relapsing-remitting multiple sclerosis
S1P1	sphingosine-1-phosphate receptor 1
s.c.	spinal cord

s.e.m.	standard error of the mean
SPMS	secondary progressive multiple sclerosis
WM	white matter

## 1 Introduction

### 1.1 Central Nervous System — an immune-privileged organ?

Traditionally, the central nervous system (CNS) was considered an immune-privileged organ. In 1948, Medawar was the first to publish on the groundbreaking discovery that foreign tissue grafts are not rejected by the brain. This initial observation was supported by several following findings, e.g. the lack of classical antigen-presenting cells (APCs) such as dendritic cells in the CNS parenchyma (Matyszak and Perry 1996), the low expression of major histocompatibility complex (MHC) I and II complexes on (Wekerle and Sun 2010) parenchymal cells (Perry 1998; Bartholomäus et al. 2009), a severely limited spectrum of cytokines and chemokines (Wekerle and Sun 2010), and the seclusion from the periphery by specialized barriers (Engelhardt and Ransohoff 2005, 2012). Based on these observations it was thought that the CNS was entirely secluded from the peripheral organs and that immune cells could not traffic to this tissue under healthy conditions. Hitherto, it is common knowledge that both solutes and cells are able to travel in and out of the CNS, and thus it is more appropriate to classify the CNS as an “immune-specialized” organ (Engelhardt and Ransohoff 2005, 2012).

Under healthy conditions, the number of immune cells present in the CNS is very limited compared to peripheral organs (Ousman and Kubes 2012). Immune cells are typically located in perivascular spaces checking for antigens presented by MHC II positive perivascular macrophages (Cross et al. 1990; Engelhardt and Ransohoff 2012). Under pathological conditions of the CNS (e.g. viral infections, ischemia, or inflammatory diseases such as multiple sclerosis (MS) the trafficking of leukocytes into the brain increases significantly (Engelhardt and Ransohoff 2012). This constant surveillance also of CNS tissue presumably plays an important role because if the trafficking of leukocytes is inhibited by drugs such as natalizumab or fingolimod (see 1.5), then the risk of developing a progressive multifocal leukoencephalopathy caused by human polyomavirus 2 (JC virus) or another fatal CNS infection is increased.

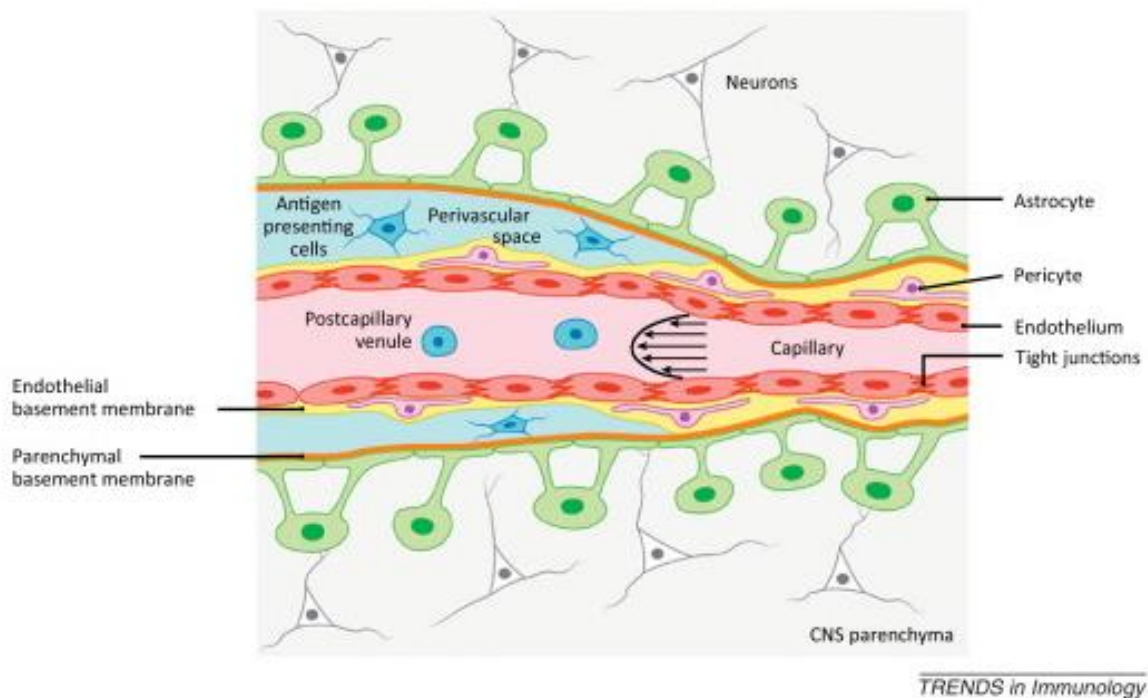


**Figure 1 Neuroanatomy of the vascular blood–brain barrier**

The blood–brain barrier (BBB) is localized at the CNS microvessels, capillaries, and post-capillary venules. It consists of highly specialized endothelial cells (red), the endothelial basement membrane (yellow) in which pericytes (pink) are located, the parenchymal basement membrane (orange), and astrocytes (green). The perivascular space between the endothelial basement membrane and the parenchymal basement membrane is filled with cerebrospinal fluid containing antigen-presenting cells (blue). Reprinted with permission from *Trends in Immunology* (Engelhardt and Ransohoff 2012). Printed with permission by Elsevier.

## 1.2 Multiple sclerosis

Multiple sclerosis is the most common inflammatory disease of the CNS. Complete details of the pathomechanism of MS have not yet been elucidated. However, there is strong evidence for MS being a T cell-mediated autoimmune disease (see 1.2.2, 1.2.3, 1.3). As the name indicates, MS is a demyelinating and neurodegenerative disease leading to multiple plaques of axonal, neuronal, and astroglial injury in the CNS of MS patients (Compston and Coles 2002; Hemmer et al. 2002; Compston and Coles 2008) (see 1.2.2). The clinical symptoms of patients are due to the affected areas in the CNS. The first symptoms are often impaired vision caused by optic neuritis and deficits in sensation, and are often followed by movement disorder (e.g. spasticity and ataxia), fatigue, and incontinence (Köhler und Hoffmann 2015).

### 1.2.1 Etiology and clinical phenotypes

Multiple sclerosis is the most common cause of neurological disability in young people (Compston and Coles 2002). The global mean age of onset is about 30 years (Atlas of MS 2013). MS occurs twice as frequently in women than in men (Compston and Coles

2008; Atlas of MS 2013) and has a higher incidence in the northern hemisphere compared to the southern hemisphere (Garg and Smith 2015; Atlas of MS 2013; Compston and Coles 2008). The number of deaths caused by MS worldwide increased from approx. 12,000 in 1990 to approx. 20,000 in 2013 (GBD 2013 Mortality and Causes of Death Collaborators 2015), and the global median prevalence increased from 30 (in 2008) to 33 per 100,000 (in 2013) (Atlas of MS 2013). This leads to the prediction that further increases in incidence can be expected in the future.

Although the etiology of MS is poorly understood, both genetic and environmental factors are supposed to play a role. Indeed, various genetic regions –mainly immune-related loci– were identified by genome-wide association studies, and these identified regions are linked to disease risk. One of these gene complexes is the well-known human leukocyte antigen (HLA) encoding for MHC (Gourraud et al. 2012). Recent studies showed non-MHC variants like BCL10, a gene encoding a protein, playing a role in the activation of (NF)- $\kappa$ B signaling. This is important for controlling gene expression in inflammation, immunity, cell proliferation, and apoptosis (Beecham et al. 2013; Kempainen et al. 2011).

The genetic basis for MS susceptibility is further supported by population-based studies that show that the disease concordance rate for monozygotic twins is approx. 15 %–30 % as opposed to approx. 2 %–7 % for dizygotic twins and siblings in general (Kamm et al. 2014).

This modest familial risk provides evidence for the importance of lifestyle/environmental factors in determining MS. Epidemiological studies have repeatedly shown that environmental factors (e.g. smoking, light exposure), viral infections (e.g. Epstein–Barr virus infection), and lifestyle (e.g. adolescent body mass index, shift work) influence MS risk (Hedström et al. 2015). Furthermore, vitamin D levels have been shown to be a predictor for disease activity and progression (Ascherio et al. 2014; Martinelli et al. 2014; Munger et al. 2014), just as low melatonin levels negatively correlate with disease relapses (Farez et al. 2015b). Epidemiological studies have also indicated that viral upper respiratory tract infections increase MS relapses. Among the viruses, EBV is a risk factor for MS since patients with EBV in the past, or with an acute EBV-triggered infection, possess an increased risk of developing MS (Levin et al. 2010; Pender and Burrows 2014). Several lifetime parameters such as high sodium intake (Farez et al. 2015a),

cigarette smoking (Salzer et al. 2013; O'Gorman and Broadley 2014; Hernán et al. 2005), and obesity (Munger et al. 2013; Langer-Gould et al. 2013) were identified as risk factors.

The clinical presentation of MS may vary. According to the newest classification, three different phenotypes can be described: (1) clinically isolated syndrome (CIS), (2) relapsing-remitting disease (RRMS), and (3) chronic progressive disease, the latter of which can be subdivided into primary progressive (PPMS) and secondary progressive multiple sclerosis (SPMS). RRMS and CIS can be either characterized as active or inactive (Lublin et al. 2014).

The CIS is the first clinical presentation of the disease showing characteristics of inflammatory demyelination in MRI. However, it does not fulfill criteria of dissemination in time to confirm the diagnosis of MS even though CIS patients have a high risk of fulfilling diagnostic criteria of MS in the future (Lublin et al. 2014; Compston and Coles 2008). RRMS is the most common phenotype (Compston and Coles 2002, 2008), and over time 25 %–65 % of patients develop a SPMS (Garg and Smith 2015; Compston and Coles 2008). In PPMS, disability accumulates from disease onset and is present in 20 % of the cases (Compston and Coles 2008).

---

### 1.2.2 Histopathology

The histopathology of MS is characterized by the presence of inflammatory infiltration, which is associated with structural changes such as demyelination and a variable degree of axonal destruction. The rescue of function and attempt to repair the CNS parenchyma results in glial scarring (Compston and Coles 2008) since the axonal loss cannot be repaired. The latter might be responsible for the accumulation of disability in the progression of MS (Bjartmar et al. 2000; Kuhlmann et al. 2002).

The lesions detected by MRI in the CNS of MS patients are called plaques. They consist of T cells, activated macrophages/microglia, B cells, and plasma cells (Lassmann et al. 2007; Lassmann 2013). The plaques are localized in the white matter (WM) of the cerebrum, optic nerve, cerebellum, brainstem, and spinal cord (s.c.). Depending on their location, plaques cause different clinical signs (Compston and Coles 2008) and can be classified as active, chronic remyelinated plaques by histopathology and MRI (Lassmann 2013). The technical advances of MRI, e.g. high-field MRI, emphasize grey matter (GM) lesions in the patient's brain (Peterson et al. 2001).

The active WM demyelinating lesions in MS are subdivided into four patterns. All types of lesions have a strong infiltration of T cells and macrophages. Pattern I and II lesions are characterized by infiltration of T cells and macrophages centered on small veins and venules with sharply demarcated edges with perivenous extensions. Pattern II lesions are distinguished from pattern I lesions by the presence of IgG and the activation of the complement system. Pattern III lesions are characterized by the localization around inflamed vessels and a diffuse spreading of the active lesion into the surrounding WM. Another characteristic is the preferential loss of myelin-associated glycoprotein (MAG); meanwhile, other myelin proteins like myelin proteolipid protein (PLP), myelin basic protein (MBP), or cyclic nucleotide phosphodiesterase (CNP) are preserved. At the margin of the plaque a pronounced loss of oligodendrocytes (myelin oligodendrocyte glycoprotein (MOG)) is typically observed. The rare pattern IV lesions are also characterized by the loss of oligodendrocytes in the periplaque zone. However, differences in the expression of myelin proteins (MAG, MBP, PLP, CNP, MOG) cannot be observed. Pattern I and II lesions show close similarities to a T cell-mediated or T cell plus antibody-mediated autoimmune encephalomyelitis, respectively. Pattern III and IV lesions are more suggestive of oligodendrocyte dystrophy (Lucchinetti et al. 2000).

---

### 1.2.3 MS etiopathogenesis: the autoimmune hypothesis

With respect to the histopathology of MS the occurrence of demyelinating processes as well as axonal degeneration are recognized facts. The etiopathogenesis, however, is still under discussion. Possible processes are (1) inflammation as an exclusive trigger, (2) neurodegeneration occurring first and followed by inflammation, (3) inflammation and neurodegeneration occurring simultaneously, or (4) intrinsic neurodegeneration occurring as a consequence of inflammation (Compston and Coles 2008).

The infiltration of cells into the CNS is one of the crucial steps in the development of MS (Kebir et al. 2009). It has been shown that autoreactive T cells against MBP have been part of the lymphocyte repertoire both in MS patients and healthy donors (Goebels 2000). For unknown reasons these autoreactive T cells become activated. There are several mechanisms that might empower pathogens to trigger an autoimmune disease: molecular mimicry, bystander activation, exposure to cryptic antigens, and so-called superantigens. For example, lymphocytes encounter non-self antigens as viral peptides in secondary lymphatic organs. These antigens are similar to those antigens in the CNS which may lead to a cross-reaction (molecular mimicry) (Oldstone 1987; McRae et al. 1995). When

presented to either T or B cells in the context of the MHC, lymphocytes get erroneously reactivated, clonally expand, and circulate through the body; they end up accumulating in the CNS (Wucherpfennig and Strominger 1995; Gonsette 2012).

Traditionally, autoreactive and IFN- $\gamma$  producing T helper type 1 (Th1 CD4<sup>+</sup>) cells were thought to be the major player in the development of MS. Further research showed that IL17-producing Th17 cells also play a major role (Steinman 2007; Stromnes et al. 2008). Furthermore, an impairment of regulatory T cells (T<sub>reg</sub>) might lead to pathogenicity and dysregulation of the autoimmune CD4<sup>+</sup> T cells (Schneider et al. 2013; Rodi et al. 2016). Some of these aspects were used to create animal models of MS. One of these models is the Th1 CD4<sup>+</sup> T cell-driven experimental autoimmune encephalomyelitis (EAE).

Over the last decade, the role of other immune cells besides autoreactive Th1 CD4<sup>+</sup> T cells have been investigated in more detail, showing that both the innate and adoptive immune system are involved in the pathology of MS.

Apart from the role of CD4<sup>+</sup> T cells, there is also evidence for the involvement of CD8<sup>+</sup> T cells. The histopathologic examinations of MS patients' CNS parenchyma showed an even higher amount of CD8<sup>+</sup> T cells than CD4<sup>+</sup> T cells (Booss et al. 1983; Babbe et al. 2000). Furthermore, the histopathology of biopsied demyelinated lesions in early stages of MS showed, apart from infiltration of T cells, a high presence of macrophages, and fewer B cells and plasma cells (Popescu et al. 2013). In addition, the results of Lucchinetti and colleagues showed that antibody-mediated and complement-mediated mechanisms might be linked to the demyelination process (see 1.2.2). The role of B cells in the development of MS and EAE was further evaluated as, firstly, a producer of autoantibodies as well as pro- and anti-inflammatory cytokines, and, secondly, an agent involved in antigen-presentation (Kitamura et al. 1991; Linington et al. 1988). Macrophages have a shared responsibility. On one hand they promote neuroinflammation and neurodegeneration by releasing inflammatory cytokines and stimulating leukocyte trafficking and infiltration into the CNS; on the other hand, they support CNS repair by phagocytosing myelin debris and producing neurotrophic factors (Bogie et al. 2014).

Cortical lesions in chronic MS lack the breakdown of the BBB, inflammatory infiltrations, and complement deposition. Here, microglia are doing the phagocytosing. Furthermore, atrophy and apoptosis of neurons and oligodendrocytes are present. In the late stage of progressive disease, there is a profound meningeal inflammatory infiltration by T cells, B cells, and macrophages. This is true for both PPMS and SPMS. Additionally,



in SPMS, infiltration of the meninges by B cells resembling ectopic follicular structures have been described (Popescu et al. 2013).

To summarize, there is no final proof for MS being an autoimmune disease, but there is strong evidence supporting this thesis. Firstly, the massive infiltration of immune cells including T cells, B cells, and macrophages in lesions of MS patients (see 1.2.2). Secondly, the presence of autoreactive T cells and autoantibodies in MS patients and the evidence for molecular mimicry (e.g. through association of MS with virus infections, especially EBV (see 1.2.1)) suggests that MS is an autoimmune disease (see 1.2.3). Furthermore, the genome-wide association studies (GWASs) support the role of the immune system in MS: virtually all GWASs show a highly significant association of MS with the MHC region (see 1.2.1). Moreover, the fact that MS can be suppressed by immunomodulatory treatments supports the thesis of the immune system's pathogenic role (see 1.5).

In other words, the presence of myelin-reactive T cells with encephalitogenic potential undergoing clonal expansion might play a role in the development of MS in humans. However, these findings do not explain the specific role of myelin-specific T cells in disease progression, nor do they explain the complete pathogenesis of MS, which has been proved to be much more complex.

### 1.3 Experimental autoimmune encephalomyelitis as an animal model of MS

Most of our knowledge about the histopathology and the concept of MS being an autoimmune disease was derived from the development and use of animal models mimicking different aspects of MS. The most commonly used animal model is the experimental autoimmune encephalomyelitis (EAE) (Ben-Nun et al. 1981; Freund and McDermott 1942; Gold et al. 2006).

The origin of the EAE model dates back to the 1920s when Koritschoner and Schweinburg induced paralysis in rabbits after immunization with human s.c. homogenate (Koritschoner and Schweinburg 1925).

This paralysis was further investigated in 1933/35, when T. M. Rivers performed animal experiments to analyze the ascending paralysis seen in humans after rabies vaccination. In the histopathological analyses, inflammatory demyelinating lesions in the CNS were discovered (Schwentker and Rivers 1934; Rivers 1935). This discovery was the basis for the development of the rodent active EAE model by Lipton et al. (1953). The model was

induced by immunizing animals with a combination of CNS homogenates and adjuvants to provoke an immune response. A hallmark for showing EAE to be a model for an immune cell-mediated disease were the experiments of Ben-Nun et al. (1981). In these experiments, lymphocytes were isolated from immunized rats, then cultured under CD4<sup>+</sup> T cell polarizing conditions, and finally transferred into healthy recipient animals. The animals developed a monophasic disease with complete recovery (Ben-Nun et al. 1981). The development of this adoptive transfer experimental autoimmune encephalomyelitis (atEAE) allowed for explicitly studying the role of CD4<sup>+</sup> T cells during neuroinflammation. It provided formal evidence that MBP-specific T cells can induce an autoimmune-mediated disease in the CNS (Gold et al. 2006). Later, it was shown that the induction of EAE is not restricted to T cells reactive against myelin antigens but can also be initiated by T cells reactive against astroglial, neuronal and oligodendrocyte-specific antigens (Wekerle and Sun 2010).

The atEAE model in Lewis rats was also used in this study. T cells specific for the CNS antigen MBP were retrovirally labelled with green fluorescent protein (GFP) (T<sub>MBP-GFP</sub> cells) (Flügel et al. 1999), and after activation were transferred into Lewis rats to induce disease. The GFP allowed for the monitoring and unequivocal identification of the injected CD4<sup>+</sup> T cells.

Another big advantage of the atEAE model is the high reproducibility of the disease course with an incidence of nearly 100 % (Gold et al. 2006). The disease in Lewis rats starts after an obligatory asymptomatic phase called prodromal phase of about 3–4 days. The disease is monophasic and characterized by a loss of body weight, followed by a progressive ascending paresis and a spontaneous full recovery after 9–10 days (**Fig. 2**).

The atEAE with MBP-specific CD4<sup>+</sup> T cells reflects mainly an acute inflammatory phase. The lesions are primarily occurring in the WM of the s.c. Hence, the atEAE primarily reflects the WM lesions in MS patients and pathologically overlaps with the aforementioned pattern I and II lesions of Lucchinetti et al. (Linker and Lee 2009).

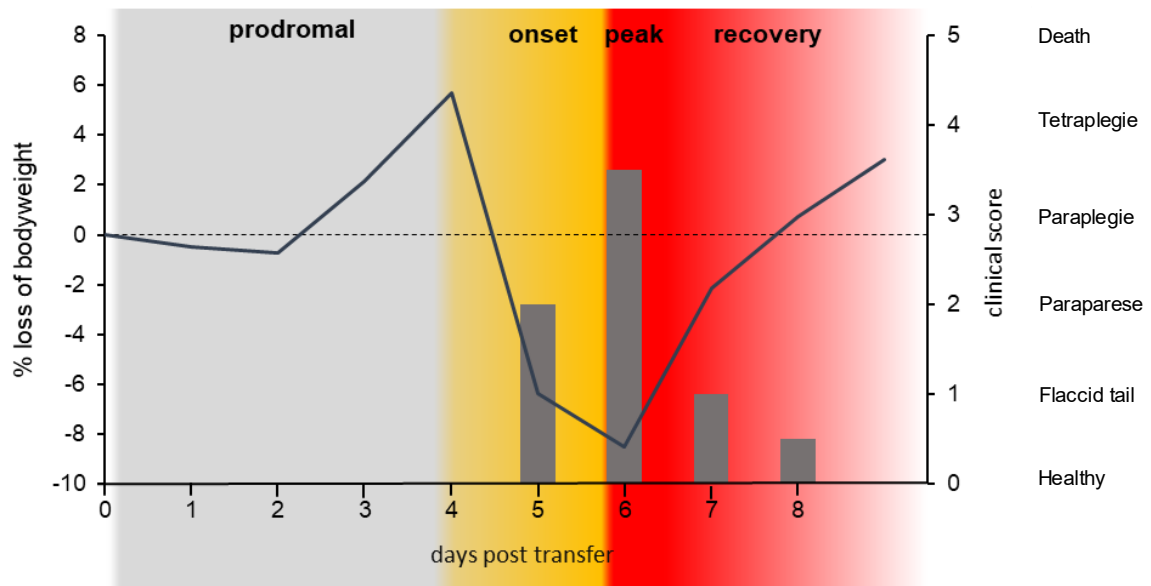


**Figure 2** Representative disease score of a monophasic disease during atEAE in Lewis rat

About 3-4 days after intravenous (i.v.) T cell transfer the clinical disease starts with a loss of bodyweight. Approximately 12 h later motor symptoms start. Peak of disease develops 1 or 2 days after disease onset and is followed by a recovery phase of 2-3 more days. Shown is a representative EAE course. Loss of body weight (in %) displayed as line on the left axis; clinical score (from 1-5) and the corresponding clinical symptoms are displayed as bars and correspond to the right axis. The color code indicates the different phases of the disease.

#### 1.4 Infiltration route of $T_{\text{MBP-GFP}}$ cells during EAE course

As described above, the CNS-reactive T cells retrovirally engineered to express fluorescent markers make it possible to track and functionally characterize these cells during the course of the immune attack.

Shortly after injection of the activated T cell blasts, they vanish from the blood and home into the lung. The cells persist in the lung for 24–36 h. After this period, they are drained to the local mediastinal lymph nodes. About 48 h post transfer (p.t.) the cells reappear in the blood and spleen, before they invade the CNS at about day 3–4 p.t. During their journey in the peripheral organs the T cells change their expression profile and acquire a migratory phenotype (**Fig. 3**). They downregulate activation markers (e.g.  $\text{IFN-}\gamma$ , IL-17) and simultaneously upregulate cell adhesion molecules, chemokine receptors, and migration markers (e.g. sphingosine-1-phosphate receptor 1 (S1P1)) (**Fig. 4**). This profile switch allows the T cells to overcome the BBB and therefore to enter their target organ, – i.e. the CNS (Flügel et al. 2001; Odoardi et al. 2012).

Before entering the CNS parenchyma,  $T_{\text{MBP-GFP}}$  cells extravasate from leptomeningeal vessels of the s.c., where they become reactivated by interacting with local antigen-presenting cells. After their reactivation the T cells infiltrate the CNS parenchyma and induce inflammation (Lodygin et al. 2013).

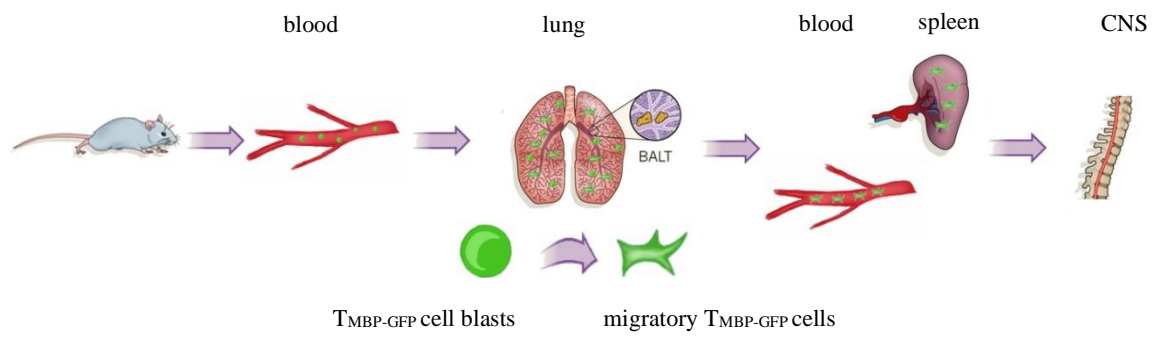


**Figure 3 Migratory pattern of i.v. injected  $T_{MBP-GFP}$  cells during atEAE**

*In vitro*-activated  $T_{MBP-GFP}$  cells promptly vanish from the blood and home into the lung following i.v. transfer. About 48 h later they reappear in the blood circulation and in the spleen before they enter the CNS. Adapted with permission from Nature (Ransohoff 2012). Printed with permission by Springer Nature.

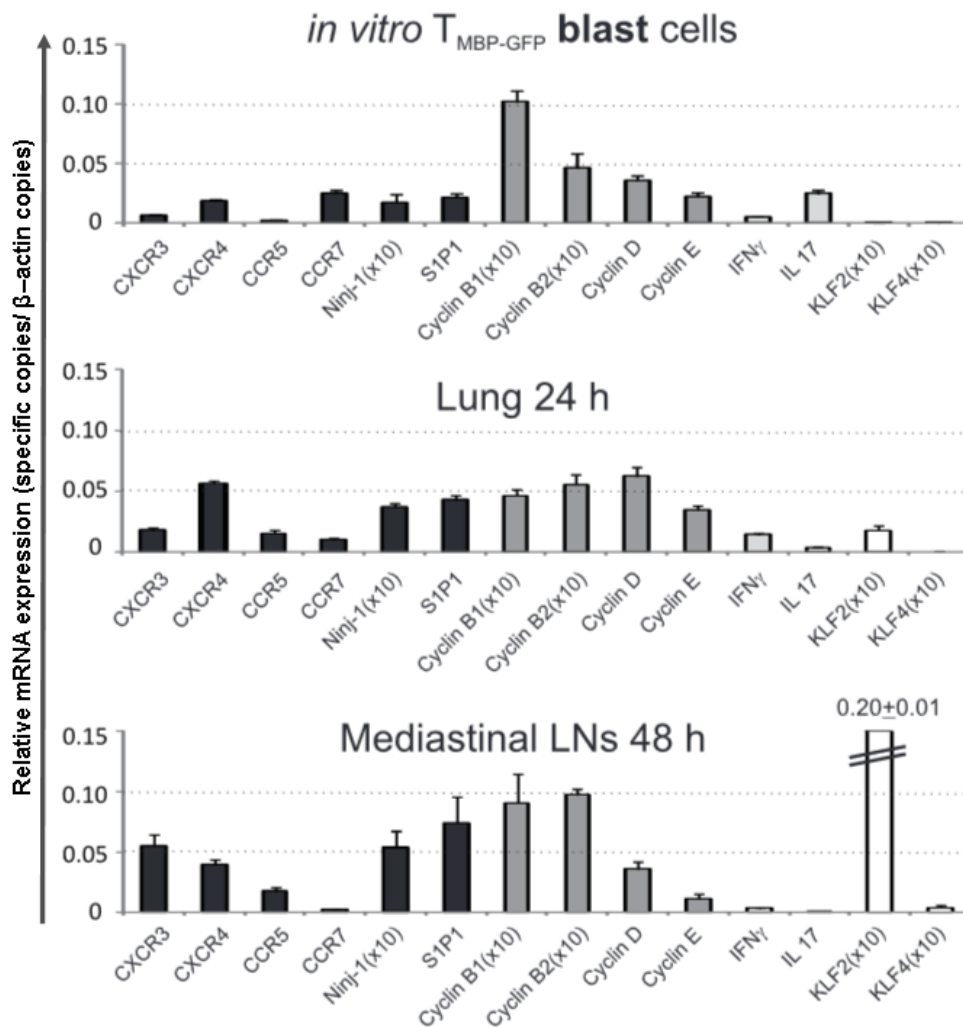


**Figure 4** Changed mRNA expression profile of migratory T cells versus T cell blasts

Graphs show the mRNA expression profile of T<sub>MBP-GFP</sub> blasts (top) compared to *ex vivo* sorted T<sub>MBP-GFP</sub> cells from the lung (middle) and the mediastinal LNs (bottom) 24 h and 48 h after injection. Adapted with permission from Nature (Odoardi et al. 2012). Printed with permission by Springer Nature.

## 1.5 Disease-modifying treatments in multiple sclerosis

Based on the hypothesis that the immune system plays a major role in MS pathogenesis, several disease-modifying treatments (DMTs) aimed to modulate different aspects of the immune response have been developed. This allows for more personal treatment options for MS patients depending on factors such as the activity level of the disease and the pathological particularity of each patient.

### 1.5.1 Established treatments

The first DMT for RRMS was beta-interferon (beta-IFN) 1b, and was approved in the USA in 1993 and in the European Union in 1995 (Cross and Naismith 2014). In the last

two decades, eight more DMTs have been approved in the European Union (Kolber et al. 2015).

Nevertheless, the injectable beta-IFNs (Avonex®, Betaferon®, Extavia®, Rebif®) are still the first-line treatment of MS due to their known and favorable safety profile as well as for their long-term clinical experience. They are indicated both for CIS and RRMS with a mild activity. Furthermore, beta-IFNs are also established in treatment of SPMS with relapses (Leitlinie MS 2014, **Fig. 5**). The mode of action (MOA) of the beta-IFNs is not completely understood, and several mechanisms have been proposed: (1) impairment of antigen presentation leading to a reduction of T cell activation and proliferation, (2) decrease of pro-inflammatory cytokine production, (3) impairment of T cell adhesion and migration across the BBB through a blockage of VLA-4 interaction, and (4) potential antiviral activity (Yong et al. 1998; Kasper and Reder 2014; Dhib-Jalbut and Marks 2010).

Apart from the group of interferons, the other injectable DMT is glatiramer acetate (GA). It is a synthetic analog of the MBP (Teitelbaum et al. 1971) and is indicated for CIS and for RRMS with mild activity (Leitlinie MS 2014, **Fig. 5**). The exact mechanism of action is unclear, but several modes were proposed. GA is supposed to induce specific T cells predominantly of the Th2 phenotype (Neuhaus et al. 2000; Duda et al. 2000; Weber et al. 2007), which infiltrate and accumulate in the CNS, where they might release anti-inflammatory cytokines (Aharoni et al. 2000; Sarchielli et al. 2007). Another MOA might be the induction of T<sub>reg</sub> cells (Hong et al. 2005).

Recently, some oral drugs have been approved for MS treatment. In 2011, fingolimod (Gilenya®) was the first oral drug to be approved by the European Commission. In Europe it is mainly used as escalation therapy for RRMS with high activity (Leitlinie MS 2014; **Fig. 5**). Fingolimod downregulates the expression of S1P1, thus inhibiting the egress of lymphocytes from the lymph nodes resulting in lymphopenia. Through this mechanism, it reduces immune cell infiltration into the CNS and thus interrupts inflammatory processes in the CNS. Furthermore, the interruption of inflammation might be supported by a modulation of astrocyte and oligodendrocyte action (Mandala et al. 2002; Brinkmann 2009). The second oral drug recently approved for MS treatment for mild RRMS (autumn 2013) is teriflunomide (Aubagio®). The main and best-known MOA of teriflunomide is the reversible inhibition of the dihydroorotate dehydrogenase

(DHODH), a key enzyme in the pyrimidine synthesis (see 1.5.2). At the beginning of 2014 dimethyl fumarate (Tecfidera®), a drug already used for treatment of psoriasis was approved for MS treatment in patients with RRMS in mild cases. Dimethyl fumarate seems to have an anti-inflammatory and cytoprotective effect, which is probably mediated by the activation of Nrf2 (nuclear factor erythroid 2-related factor 2) (Linker et al. 2011) and HCA-receptor-2 (hydroxycarboxylic acid receptor 2) (Chen et al. 2014).

Currently, two antibodies are authorized for MS treatment in the EU: alemtuzumab (Lemtrada®) and natalizumab (Tysabri®), both indicated for patients with high MS activity (Leitlinie MS 2014; **Fig. 5**). Natalizumab was the first monoclonal antibody approved for MS. It is directed against the  $\alpha$ -4-subunit of  $\alpha$ 4 $\beta$ 1- and  $\alpha$ 4 $\beta$ 7-integrins expressed on the surface of human leukocytes (Rice et al. 2005). In MS it is supposed to block interaction between  $\alpha$ 4 $\beta$ 1-integrin (known as very late antigen-4, VLA-4) expressed on the leukocyte plasma membrane, and the vascular cell adhesion molecule-1 (VCAM-1) leading to a reduced leukocyte migration into the CNS (Engelhardt and Kappos 2008). Alemtuzumab is a humanized IgG1 monoclonal antibody against CD52 (Hu et al. 2009). CD52 is expressed at high levels on T and B lymphocytes and to a lower extent on monocytes and eosinophil granulocytes (Rodig et al. 2006). Alemtuzumab leads to a lysis of CD52 positive cells (Hu et al. 2009).

Additionally, mitoxantrone, azathioprine, and cyclophosphamide (all belong to the cytostatic group) are approved and indicated as second-line therapy in SPMS treatment (Leitlinie MS 2014; **Fig. 5**).

	indication	CIS	RRMS		SPMS	
<b>Disease-modifying treatments</b>	<b>(high) active MS</b>		<b>first-line treatment</b> – alemtuzumab – fingolimod – natalizumab	<b>second-line treatment</b> – mitoxantrone – (cyclophosphamide)	No relapses	Including relapses
	<b>mild MS</b>	– glatiramer acetate – beta-interferon 1a i.m. – beta-interferon 1a s.c. – beta-interferon 1b s.c.	– dimethylfumarate – glatiramer acetate – beta-interferon 1a im – beta-interferon 1a sc – beta-interferon 1b sc – PEG beta- interferon 1a sc – teriflunomide – (azathioprin) – (IVIg)		– beta-interferon 1a s.c. – beta-interferon 1b s.c. – mitoxantrone – (cyclophosphamide)	– mitoxantrone – (cyclophosphamide)

**Figure 5 German DGNM guideline for disease-modifying treatments in MS**  
 Approved drugs indicated for disease-modifying treatment in MS (adapted from Leitlinie MS 2014)



### 1.5.2 Teriflunomide

Teriflunomide (A77 1726) is the active metabolite of leflunomide, an anti-inflammatory drug that has been used for a long time in the treatment of rheumatoid arthritis and psoriasis (Boyd 2012). Leflunomide is rapidly and nearly entirely converted to teriflunomide after oral ingestion (Oh and O'Connor 2014). As an agricultural pesticide named HWA 486, leflunomide was originally developed in the 1980s by Hoechst (Bartlett 1986).

So far, it is not completely understood how exactly teriflunomide acts. However, it is a known fact that teriflunomide primarily inhibits cell proliferation through the inhibition of the enzyme DHODH (Bruneau et al. 1998; Greene et al. 1995; Cherwinski et al. 1995b). DHODH is a mitochondrial protein located at the outer surface of the inner mitochondrial membrane (Chen and Jones 1976). It is an enzyme catalyzing the oxidation of dihydroorotate to orotate in *de novo* pyrimidine biosynthesis (Munier-Lehmann et al. 2013; Levine et al. 1974; Jones 1980). Furthermore, it has been shown that the DHODH enzyme might be the rate-limiting enzyme in *de novo* pyrimidine synthesis (Löffler et al. 1997).

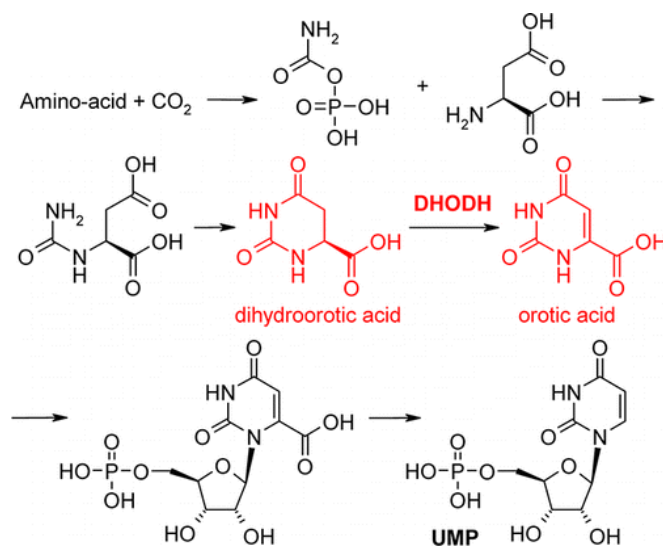


**Figure 6** The role of DHODH in the *de novo* pyrimidine synthesis

Pathway of *de novo* pyrimidine synthesis. Highlighted in red is the oxidation of dihydroorotate to orotate as catalyzed by DHODH. Reprinted with permission from Journal of Medicinal Chemistry (Munier-Lehmann 2013). Printed with permission by American Chemical Society.

Pyrimidine is essential for the synthesis of DNA and RNA. Cells with high proliferative capacity need to replenish their pyrimidine pool by *de novo* pyrimidine synthesis (**Fig. 6**); conversely, homeostatically expanding lymphocytes can supply their pyrimidine consumption through the salvage pathway (Peters and Veerkamp 1983). The salvage

pathway generates pyrimidine bases directly from uracil. It is therefore DHODH-independent (Levine et al. 1974; Jones 1980) (**Fig. 7**).

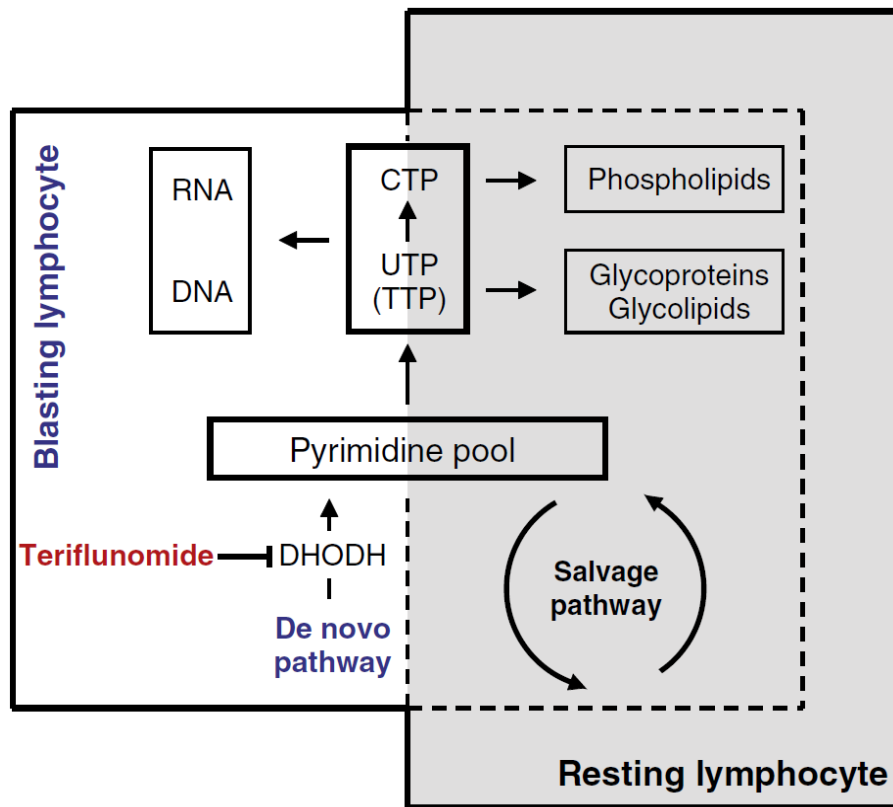


**Figure 7** Impact of teriflunomide on the pyrimidine synthesis

Inhibitory effect of teriflunomide on DHODH and thus the abrogation of *de novo* pyrimidine synthesis, which in turn effects the metabolism of activated lymphocytes. Reprinted with permission from Clinical Immunology (Claussen and Korn 2012). Printed with permission by Elsevier.

The dose-dependent antiproliferative effect of teriflunomide *in vitro* has been frequently demonstrated (Cherwinski et al. 1995a; Cherwinski et al. 1995c; Cao et al. 1995; Chong et al. 1996; Elder et al. 1997; Siemasko et al. 1996; Silva et al. 1996; Williamson et al. 1995; Williamson et al. 1996; Xu et al. 1996; Zielinski et al. 1995). Other studies went into greater detail and showed that the antiproliferative effect is mediated through the inhibition of the DHODH (Williamson et al. 1995, 1995; Williamson et al. 1996; Kuo et al. 1996; Davis et al. 1996). In a publication by Korn et al. (2004) the antiproliferative effect of teriflunomide was shown on MBP-specific T cells. Ringheim et al. (2013) showed a strong reduction of CD4<sup>+</sup> T cells, CD8<sup>+</sup> T cells, B cells, and natural killer (NK) cells in peripheral blood during active EAE in Dark Agouti rats (Ringheim et al. 2013). These results also hold true in humans: a reduced number of white blood cell counts could be observed under teriflunomide therapy, whereby the immunological answer to a flu vaccine was not diminished (Bar-Or 2014).

Other *in vitro* experiments showed that teriflunomide strongly inhibits the proliferation of T cells with a high avidity to ovalbumin (OVA) *in vitro* (Posevitz et al. 2012). This is important because high-avidity T cells are assumed to play a major role in autoimmune diseases including MS (Bielekova et al. 2004). It might be an additional explanation for teriflunomide's good safety profile because low-avidity T cells are still present for a normal immune response against pathogens.

Furthermore, several other targets of teriflunomide were identified in *in vitro* studies (Claussen and Korn 2012). For example, teriflunomide might have additional inhibitory effects on Jak1 and Jak3 (Elder et al. 1997; Siemasko et al. 1998), two major tyrosine kinases, playing an important role in interferon signal transduction. The relevance of this finding for clinical MS therapy is under discussion because of relatively high *in vitro* concentrations of about 100  $\mu\text{M}$  teriflunomide which are necessary to induce effects and the lack of *in vivo* experiments (Claussen and Korn 2012; Bar-Or et al. 2014). Thus, the block of DHODH remains the main target of teriflunomide therapy (Munier-Lehmann et al. 2013; Sykes et al. 2016).

To evaluate the effectiveness of teriflunomide as a drug it was first tested in active EAE. Prophylactic and therapeutic treatment with teriflunomide in Dark Agouti rat EAE showed a delay in disease onset, reduced maximal and cumulative scores and improved disease outcomes. Furthermore, a reduction in inflammation, demyelination, and axonal loss has been observed in the histopathology (Merrill et al. 2009). Moreover, teriflunomide reduces infiltration of macrophages and T cells in the CNS in active EAE as well as atEAE (Korn et al. 2004; Ringheim et al. 2013). In atEAE it was also shown that rats developed a less severe EAE if cells were preincubated with teriflunomide before transfer (Korn et al. 2004).

These promising results obtained from rat EAE experiments generated an interest in using teriflunomide in clinical studies. The efficiency of teriflunomide was tested in different phase III trials. The first two studies were the TEMSO and TOWER clinical trials. There the treatment of MS patients with 7 or 14 mg teriflunomide was compared to placebo treatment. The relative reduction of the annualized relapse rate (ARR) compared with placebo was between 31.5 % and 36.0 %, respectively (O'Connor et al. 2011; Confavreux et al. 2014). In another clinical trial, the TOPIC study, MS patients with a first clinical demyelinating event were checked for a second relapse and showed a significantly reduced risk of new clinical relapse by 43 % compared to placebo under the treatment of

14 mg teriflunomide (Miller et al. 2014). The treatment with 14 mg teriflunomide and the subcutaneous injection with interferon- $\beta$ -1a showed no difference in the ARR in the phase III TENERE study (Vermersch et al. 2014).

The quality of the evidence for the effect of teriflunomide treatment over placebo is currently under discussion. The evidence was rated rather low due to (1) a high risk of detection bias for relapse assessment, (2) a high risk of bias due to conflicts of interest, (3) a high dropout rate, and (4) an unclear attrition bias. The study using control treatment with IFN $\beta$ -1a had a high risk of performance bias and a lack of power because of limited sample size (324 patients in total). Even for the long-lasting phase II study, there was a problem of high drop out and therefore a limited interpretation of the low remaining ARR and minimal disability progression. According to He et al. (2016), there is a need for new studies with a higher quality and longer follow-up (follow-up was between 1 and 2 years) (He et al. 2016).

Nevertheless, teriflunomide seems to be quite efficient as was shown by comparable ARR with IFN $\beta$  and GA combined with a good safety profile (Xu et al. 2016). In addition, the long term experience with leflunomide in RA patients makes it a good treatment choice for MS patients (Warnke et al. 2013).

To sum up, teriflunomide's mechanism of action indicates that it is most efficient in highly proliferating lymphocytes but spares homeostatically proliferating or resting hematopoietic cell types (Bar-Or et al. 2014; Tanasescu et al. 2013; Claussen and Korn 2012; Rückemann et al. 1998). This might be the reason for teriflunomide's good safety profile. EAE experiments suggest that teriflunomide might be suitable for MS treatment. The clinical studies showed a convincing reduction of the ARR and comparable efficiency under teriflunomide in comparison to other oral treatments. Finally, teriflunomide can be given orally, which is generally better accepted and associated with a higher quality of life for patients. This would certainly also factor into the decision of doctors and patients for treatment options (Tanasescu et al. 2013).

## 1.6 Aims of the study

The overall aims of this study are as follows:

- 1) To investigate the effect of teriflunomide on activation and proliferation of CD4<sup>+</sup> myelin-reactive T cells *in vitro*.
- 2) To investigate the effect of teriflunomide on migration, activation, and proliferation of CD4<sup>+</sup> myelin-reactive T cells in Lewis rat EAE
  - during the preclinical phase;
  - during the clinical phase.

## 2 Materials and Methods

### 2.1 Materials

If not indicated otherwise, the buffers were prepared in Milli-Q purified H<sub>2</sub>O (MILLIPORE GmbH, Schwalbach, Germany).

**Table 1 Medium prepared for the present study**

medium	ingredients	
DMEM	66.9 g/5 l 18.59 g/5 l	Gibco DMEM Powder (52100-021) (INVITROGEN, Carlsbad USA) NaHCO <sub>3</sub> (CARL ROTH GmbH, Karlsruhe, Germany)
EH	375 ml 125 ml	DMEM Gibco HEPES 1M (INVITROGEN, Carlsbad USA)
T cell medium (TCM)	1 l 10 ml 10 ml 10 ml 10 ml 10 ml 4 µl	DMEM Gibco Non-essential Amino Acids (INVITROGEN, Carlsbad, USA) Gibco Penicillin/ Streptomycin (INVITROGEN, Carlsbad, USA) Gibco Sodium Pyruvate (INVITROGEN, Carlsbad, USA) L-Glutamine, PAN (Biotech GMBH, Aidenbach, Germany) L-Asparagine Monohydrate (SIGMA-ALDRICH, Munich, Germany) 2-β-Mercaptoethanol (13.6 mol/l) (INVITROGEN, Carlsbad, USA)
Re-stimulation medium (RM)	100 ml 1 ml	TCM Rat serum (in-house production)

medium	ingredients	
T cell growth factor (TCGF)	500 ml 50 ml 25 ml	TCM heat-inactivated horse serum (BIOCHROM GMBH, Berlin, Germany) conditioned medium from splenocytes treated with the mitogen Concanavalin A (ConA supernatant)
Phosphor buffered salt solution (PBS, 10x)	8.10 mM 1.47 mM 137 mM 2.68 mM	Na <sub>2</sub> HPO <sub>4</sub> (CARL ROTH GmbH, Karlsruhe, Germany) NaH <sub>2</sub> PO <sub>4</sub> (CARL ROTH GmbH, Karlsruhe, Germany) NaCl (CARL ROTH GmbH, Karlsruhe, Germany) KCl (CARL ROTH GmbH, Karlsruhe, Germany) adjusted to pH 7.2
FACS PBS	100 ml 5 ml	1x PBS Rat serum (in-house production)
Freezing medium	40 ml 50 ml 10 ml	TCM Horse serum (in-house production) DMSO (CARL ROTH GmbH, Karlsruhe, Germany)
ACK buffer	0.15 mol/l 1 mmol/l 0.1 mmol/l	NH <sub>4</sub> Cl (CARL ROTH GmbH, Karlsruhe, Germany) KHCO <sub>3</sub> NH <sub>4</sub> Cl (CARL ROTH GmbH, Karlsruhe, Germany) Na <sub>2</sub> EDTA/Titriplex (CARL ROTH GmbH, Karlsruhe, Germany) Adjust to pH 7.2 – 7.4 with 1N HCl
Isotonic percoll	9x Vol. 1x Vol.	Percoll (GE HEALTHCARE, Munich, Germany) PBS 10x

medium	ingredients	
Underlay percoll (70 %)	7 ml 3.9 ml	Isotonic Percoll PBS 1x
Percoll (40 %)	4 ml 5.9 ml	Isotonic Percoll PBS 1x
Complete Freund's adjuvant	10 ml 100 mg	Incomplete Freund's adjuvant (DIFCO LABORATORIES, Detroit, USA) Mycobacteria M. Tuberculosis H37Ra, (DIFCO LABORATORIES, Detroit, USA)
MBP		Isolated from guinea pig brains as described (Eylar et al. 1974)

## 2.2 Methods

### 2.2.1 Animals

Rats on a Lew/Crl background (*Rattus norvegicus*) were supplied by the Animal Facility of the Medical School Göttingen (Göttingen, Germany) and kept under standardized conditions. All animal experiments carried out in this study were approved by the responsible authorities.

### 2.2.2 Generation and culturing of GFP<sup>+</sup> antigen-specific T cells

CD4<sup>+</sup> T cells reactive against MBP and retrovirally transduced to express GFP (T<sub>MBP-GFP</sub> cells) were established as previously described (Flügel et al. 1999). In brief, eight to ten week-old female Lewis rats were immunized with 100 µg guinea pig MBP (Flügel et al. 1999). The paste containing 1 volume of complete Freund's adjuvant (CFA, 4 mg/ml) and 1 volume MBP antigen (1 mg/ml) was injected into both sides of the tail-base, 50 µl on each side, and an additional 50 µl on each side in the popliteal cavities. After 10 days, the animals were sacrificed using CO<sub>2</sub>. Subsequently, the draining lymph nodes (paraaortal, popliteal and inguinal) were taken out. The lymph nodes were prepared as a cell suspension through a metal mesh. Lymphocytes obtained in this manner were co-cultured with packaging cells in a 96 u-bottom well plate (THERMOFISHER SCIENTIFIC INC., Braunschweig, Germany) at a concentration of 2x10<sup>6</sup>/ml T cells and 3x10<sup>5</sup>/ml packaging cells at 37 °C and 10 % CO<sub>2</sub> under sterile conditions (Heraeus



Heracell 240 incubator, THERMOFISHER SCIENTIFIC INC., Braunschweig, Germany). Each of the 96 wells contained 100  $\mu$ l RM and 6  $\mu$ g/ml of the respective antigen. As packaging cells, GPE+86 mouse fibroblasts (Markowitz et al. 1988) previously transduced with a retroviral vector encoding for both eGFP and neomycin-resistant gene were used (Flügel et al. 1999). The packaging cells were seeded in the plates two hours before adding the lymphocyte suspension. Two days after antigen encounter, 50  $\mu$ l of TCGF was added to each well. Two days later, 100  $\mu$ l of the supernatant was discarded and the cells were transferred into 96-well flat-bottom plates. Furthermore, 100  $\mu$ l of TCGF containing 0.4 mg/ml Geneticin/ G418 (PAA LABORATORIES GmbH, Pasching, Austria) were added to each well for negative selection. Seven days after antigen encounter, T cells were challenged again with the cognate antigen. For this purpose, 100  $\mu$ l of the supernatant was substituted by fresh RM containing irradiated thymocytes ( $1.4 \times 10^6$ ), MBP (6  $\mu$ g/ml) and Geneticin/ G418 (0.4 mg/ml). Two days later, 50  $\mu$ L of TCGF containing 0.4 mg/ml Geneticin/ G418 was added to each well. Another day later, the wells containing the most fluorescent  $T_{\text{MBP-GFP}}$  cells were selected for further procedure by using an Axiovert 200M fluorescence microscope (CARL-ZEISS MICROIMAGING, Jena, Germany). The  $T_{\text{MBP-GFP}}$  cells were pooled in 6 cm dishes (SARSTEDT AG & CO., Nürnbrecht, Germany) and cultured in TCGF. Four days later, the cells were further stimulated with the cognate antigen. For this purpose,  $3.5 \times 10^6$   $T_{\text{MBP-GFP}}$  cells were cultured in presence of  $70 \times 10^6$  irradiated thymocytes, 6  $\mu$ g antigen, and 0.4 mg/ml Geneticin in 5 ml RM. The stimulation procedure was repeated up to three times following a 6–7 day cycle. The  $T_{\text{MBP-GFP}}$  cells were either frozen on day 2 as fully activated  $T_{\text{MBP-GFP}}$  cell blasts, or on day 6/7 as resting  $T_{\text{MBP-GFP}}$  cells. They were stored in liquid nitrogen. Alternatively, they were directly used for injection for atEAE experiments on day 2.

To ensure the specificity of the established cell line against MBP, the  $T_{\text{MBP-GFP}}$  cells were tested *in vitro* by a proliferation assay. The cognate antigen MBP was used as the relevant antigen. The cells were cultured with APCs in the presence or absence of MBP. The  $T_{\text{MBP-GFP}}$  cells strongly proliferate in the presence of MBP, whereas in absence of antigen (no MBP), almost no proliferation could be measured. The graph clearly shows a specific reaction of the  $T_{\text{MBP-GFP}}$  cells against MBP presented by professional APCs *in vitro* (Fig. 8).

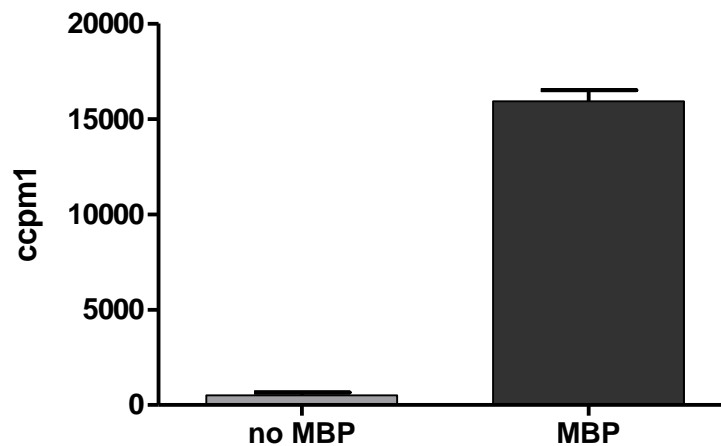


**Figure 8** Proliferation assay of  $T_{\text{MBP-GFP}}$  cells in the absence and presence of MBP

For the proliferation assay  $1 \times 10^5$   $T_{\text{MBP-GFP}}$  cells were restimulated on day 6 with  $1 \times 10^6$  thymocytes in 100  $\mu\text{L}$  RM per well. The specific antigen was added in a concentration of 30  $\mu\text{M}$ / 5 ml. After incubating the cells for 36 h, 3H-thymidine was added and the proliferation was measured after an additional 16 h of incubation. The result of one representative experiment is shown. Data were acquired in triplicates.

### 2.2.3 Animal experiments

For all experiments except for the abovementioned primary culture experiments 6–8 weeks-old rats on a Lew/Crl background (*Rattus norvegicus*) were supplied by the animal facility of the Medical School of Göttingen (Göttingen, Germany) and kept under standardized conditions. Male and female Lewis rats were used in the EAE experiments. No differences were noted between the sexes. All experiments abided to Lower Saxony's local regulations for animal welfare. The animals were weighed and scored on a daily basis during the running experiment. From the date of the disease's onset the animals were weighed twice a day. If an animal reached the score 3.5 or lost more than 20 % of its body weight, it was euthanized and taken out of the experiment.

**Table 2 Scoring system for rat experimental autoimmune encephalomyelitis**

<b>Score</b>	<b>Clinical symptom</b>
<b>0</b>	No symptoms
<b>0.5</b>	Partial loss of tail tonus
<b>1</b>	Flaccid tail
<b>2</b>	Gait disorder
<b>3</b>	Hind-limb paralysis Animals were still able to move forward with their front limbs
<b>3.5</b>	Weakness of fore limbs leading to impaired forward movement
<b>4</b>	Tetraplegia
<b>5</b>	Death

#### 2.2.4 Adoptive transfer EAE

For induction of adoptive transfer EAE (atEAE) Lewis rats were injected with  $3\text{-}5 \times 10^6$  encephalitogenic  $T_{\text{MBP-GFP}}$  cell blasts (2 days after antigen encounter). Freshly re-stimulated  $T_{\text{MBP-GFP}}$  cells or previously frozen  $T_{\text{MBP-GFP}}$  cells were used for the experiments. In order to minimize the stress of the thawing procedure, the frozen T cells were rapidly thawed in a  $37^\circ\text{C}$  water bath and immediately diluted with EH-buffer containing 10 % fetal calf serum (FCS).  $T_{\text{MBP-GFP}}$  cells were then centrifuged down for 6 min at  $4^\circ\text{C}$  with 300 xg (Multifuge Heraeus S IS-R, THERMOFISCHER SCIENTIFIC INC., Braunschweig, Germany). Next,  $3\text{-}5 \times 10^6$  cells in 1 ml were injected of EH into the tail vein of the rats. In accordance with the experimental set up, the animals were sacrificed by exposure to carbon dioxide.

#### 2.2.5 Teriflunomide solution

For *in vitro* culture teriflunomide powder (SANOFI, Paris, France) was solved in dimethyl sulfoxide (DMSO) and used for cell culture at a concentration of 0.1 molar. Teriflunomide was diluted to 1, 10, 50, and 100  $\mu\text{M}$  with TCM. Uridine (CARL ROTH GmbH + Co KG, Karlsruhe, Germany) was solved in TCM as 0.2 molar solution and added to each well in a concentration of 200  $\mu\text{M}$ . For assessing  $T_{\text{MBP-GFP}}$  cell proliferation in this study resting  $T_{\text{MBP-GFP}}$  cells were stimulated in 96-well flat-bottom plates. Each well contained  $5 \times 10^4$  T cells,  $1 \times 10^6$  irradiated thymocytes in 100  $\mu\text{l}$  RM, and 6  $\mu\text{g/ml}$  of

MBP. Teriflunomide and uridine was added. Another two days later, 50  $\mu$ L of TCGF was added to each well. The T<sub>MBP-GFP</sub> cells were used for analysis on days three, four, and five post antigen encounter.

### 2.2.6 Administration of teriflunomide and uridine

For animal treatment, teriflunomide was solved in DMSO and EH + 10 % FCS.

The drug was administered at a concentration of 3, 5 or 10 mg/kg/d in a volume of 500  $\mu$ l per animal. It was orally administered by gavage in awake rats once a day. In order to evaluate the clinical effects of teriflunomide in a preventive setting, the treatment with teriflunomide started simultaneously with the injection of activated T<sub>MBP-GFP</sub> cell blasts at day zero and continued until the end of the experiment (**Fig. 9**).

The uridine was solved in 1 ml of sterile EH and given in excess (500 mg/animal). It was administered intraperitoneal twice a day (**Fig. 9**).

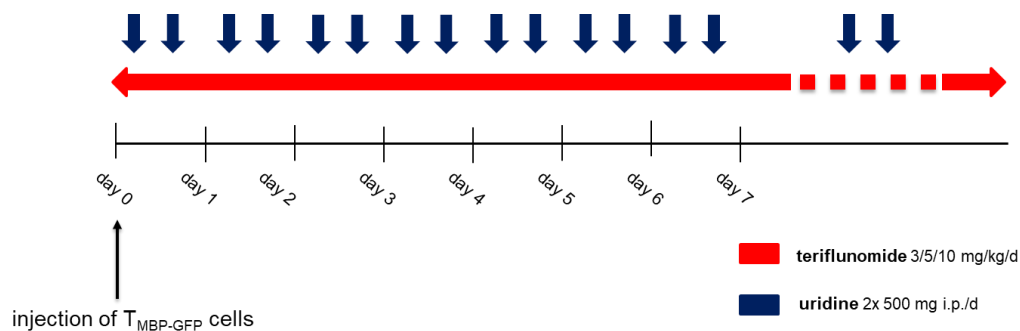


**Figure 9** Mode and scheme of administration of teriflunomide and uridine I

In order to evaluate the differences between the preventive and therapeutic setting, the treatment with teriflunomide was started at different time points. As described above, teriflunomide was started at day 0 for a preventive treatment. For a therapeutic treatment, teriflunomide was started at the onset of the disease, i.e. when animals started to lose body weight. Teriflunomide was given in a concentration between 3–7 mg/kg/d. Treatment was then continued until the end of the experiment (**Fig. 10**).

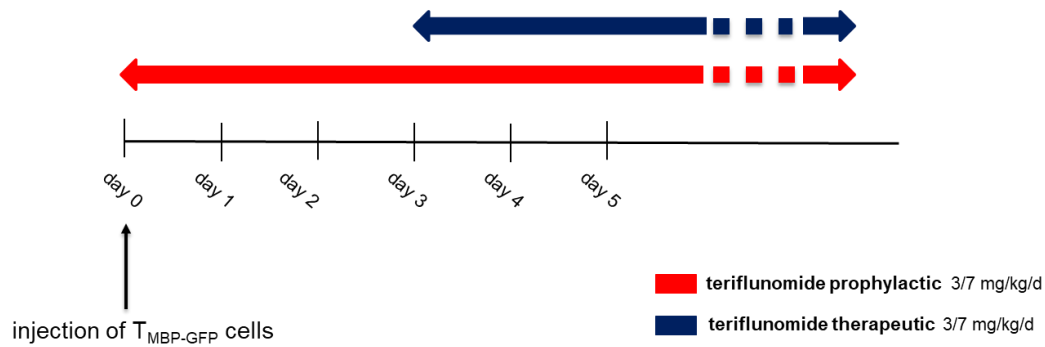


**Figure 10** Mode and scheme of administration of teriflunomide and uridine II

### 2.2.7 Cell isolation

Lung, mediastinal lymph nodes, spleen, s.c. meninges, and s.c. parenchyma were isolated immediately after having euthanized the animals. Blood samples were collected by cardiac puncture with a syringe filled with 0.5 ml of EDTA (CARL ROTH GmbH, Karlsruhe, Germany) in order to prevent clotting. All samples were kept in EH on ice.

Single cell suspensions were obtained by passing lymph nodes, spleen, s.c. meninges, and s.c. parenchyma through a metal mesh cell strainer (UMG Göttingen, in-house machine shop) using a pistil (Braun Melsungen AG, Sempach, Switzerland). After centrifugation (6 min, 4 °C, 300 xg), samples were re-suspended in a certain volume of EH medium and stored on ice. Additionally, in the cell suspension of the spleen, erythrocyte-lysis was achieved by incubating the cells in ACK-buffer for 5 min on ice. The reaction was then blocked by adding ice cold PBS. The samples were then centrifuged (6 min, 4 °C, 300 xg) and resuspended in ice cold EH.

Mononuclear cells were isolated from the blood by a density gradient separation. In order to do so, blood samples were mixed at a ratio of 1:1 with room temperature PBS and carefully underlaid by half the amount of lymphocyte separation medium (LSM1077, PAA LABORATORIES GmbH, Pasching, Austria). The samples were then centrifuged for 30 min at 2000 rpm at room temperature with minimal acceleration and deceleration (Multifuge Heraeus 1S-R, THERMOFISHER SCIENTIFIC INC., Braunschweig, Germany). The interphase containing the mononuclear cells was carefully collected with a pipette and transferred in a fresh tube, washed once with ice cold PBS, centrifuged down, and resuspended in ice cold EH medium.

S.c. parenchyma and s.c. meninges were purified by using a Percoll gradient. For this purpose, single cell suspensions were (1) kept in EH medium (s.c. parenchyma 35 ml, s.c.

meninges 7 ml), (2) were mixed with isotonic Percoll (s.c. parenchyma 15 ml, s.c. meninges 7 ml), and (3) centrifugated (20 °C, 30 min, 3780 rpm with minimal acceleration and deceleration). The pellet was resuspended in ice cold EH.

---

### 2.2.8 Flow cytometry cell quantification

In order to quantify  $T_{\text{MBP-GFP}}$  cells *in vitro* and *ex vivo*, defined volumes of cell suspension were mixed with a definite number of fluorescence beads (BECTON DICKINSON GmbH, Heidelberg, Germany). The samples were measured by use of flow cytometry (BD FACSCalibur<sup>TM</sup>, BECTON DICKINSON GmbH, Heidelberg, Germany).

---

### 2.2.9 Surface staining

In order to determine the activation level of  $T_{\text{MBP-GFP}}$  cells *in vitro*, surface staining was performed using the following mouse anti-rat monoclonal antibodies (both from SEROTEX, Kidlington, UK): OX-40 antigen (CD134) and OX-39 antigen (CD25, IL2 receptor  $\alpha$  chain). Mouse IgG (SIGMA-ALDRICH, Munich, Germany) was used as isotype control. For every surface marker  $1 \times 10^6$  cultured  $T_{\text{MBP-GFP}}$  cells were transferred in a 96-well v-bottom plate and centrifuged for 2 min at 1200 rpm. Subsequently, the pellet was washed one time with PBS (100  $\mu$ l) and one time with FACS PBS (100  $\mu$ l). Pellets were then incubated on ice in 100  $\mu$ l of FACS PBS containing the respective antibody in a dilution of 1:100 for 30 min. Next,  $T_{\text{MBP-GFP}}$  cells were washed two times in FACS PBS, and incubated for another 30 min with the secondary antibody in a dilution of 1:100. Finally, they were washed one time with FACS PBS, one time with PBS, taken up in 100  $\mu$ l of PBS, and transferred to 500  $\mu$ l FACS tubes (BD Biosciences, San Jose, CA, US) for analysis.

---

### 2.2.10 Proliferation assay

$T_{\text{MBP-GFP}}$  cell proliferation *in vitro* upon teriflunomide treatment was measured by <sup>3</sup>H-thymidine proliferation assay. For this purpose,  $T_{\text{MBP-GFP}}$  cells were cultured in presence of the cognate antigen or a sham antigen in 96-well u-bottom plates. Irradiated thymocytes were used as APCs. Twenty-four hours after antigen encounter, <sup>3</sup>H-thymidine (2 Ci/mmol) was added to each well. The proliferation was measured with a beta counter 24 h later.

### 2.2.11 Quantitative real-time polymerase chain reaction (QRT-PCR)

In order to isolate the RNA of *in vitro* cultured T<sub>MBP-GFP</sub> cells, total tissue of s.c. meninges and total tissue of s.c. parenchyma samples were lysed using QIAzol<sup>®</sup> Lysis Reagent (QIAGEN GmbH, Hilden, Germany) according to the standard protocols from SIGMA-ALDRICH and INVITROGEN. The samples were taken up in 500 µl of QIAzol<sup>®</sup> Lysis Reagent. Complete cell lysis was reached by repetitive pipetting. Afterwards the cells were either stored at -80 °C or immediately centrifuged at 12 000 rpm for 10 min at 4 °C to obtain the soluble part. The tube with the pellet was discharged. The supernatant was transferred to a fresh tube and incubated for 10 min at room temperature to allow the complete dissociation of nucleoprotein complexes. Subsequently, 0.1 ml chloroform were added and mixed by repetitive pipetting for about 15 s until the chloroform was solved completely. Another incubation of 15 min at room temperature followed. After that, the samples were centrifuged for 15 min at 12 000 rpm and at 4 °C. The spinning separated the samples into three phases: a lower phenol-chloroform phase, an interphase, and an upper aqueous phase, which contained the RNA. The upper phase was transferred carefully in a new tube and was mixed with 0.25 ml of 100 % isopropanol and 1 µl glycogen in order to precipitate the RNA. This precipitation step was carried out over night at -20 °C when the samples contained a small number of cells (less than 10000). All samples with a number of cells higher than 10000 were incubated for 10 min at room temperature. Samples were then centrifuged for 10 min at 12000 rpm at 4 °C. The RNA pellet was washed with 1 ml of 70 % ethanol. Therefore, the sample was vortexed briefly and centrifuged for 5 min at 7500 rpm at 4 °C. The ethanol was then removed. The pellet was dried at room air for about 5 to 10 min and resuspended in 11 µl of RNase-free water by gentle repetitive pipetting.

In order to isolate the RNA from *ex vivo* sorted cells the RNeasy Micro Kit (QIAGEN, Hilden, Germany) was used following the standard manufacturer's protocol. A maximum of 5x10<sup>6</sup> cells was harvest and homogenized in 350 µl RLT buffer. The samples were stored at -80 °C. After unfreezing the samples, the cell lysate was mixed with 1 volume 70 % ethanol by pipetting. The sample was directly transferred to a RNeasy MinElute spin column in a 2 ml collection tube. The tube was centrifuged with closed lid for 15 s at ≥ 8000 xg. The flow-through was discarded. Afterward, 350 µl of RW1 buffer was added to the RNeasy MinElute spin column. The lid was closed and again centrifuged for 15 s at ≥ 8000 xg. On each column, a mixture of 10 µl DNase I stock solution and 70 µl RDD buffer was added. The benchtop was incubated at room temperature for 15 min.

Another washing step with RW1 buffer followed as previously described. The RNeasy MinElute spin column was placed in a new collection tube. For the next step, 500  $\mu$ l RPE buffer was added to the spin column and again centrifuged for 15 s at  $\geq 8000$  xg with the lid closed. The flow-through was discarded. Afterward, 500  $\mu$ L of 80 % ethanol was added to the RNeasy MinElute spin column and centrifuged as described above. The RNeasy MinElute spin column was placed in a new collection tube and spun with an open lid for 5 min to dry the membrane. Finally, the RNeasy MinElute spin column was placed in a new collection tube and 14  $\mu$ l of RNase-free water was added directly to the center of the membrane. The tube was centrifuged with a closed lid for 1 min at full speed to elute the RNA.

In this study, the RNA was used for the direct transfer into cDNA.

The synthesis of cDNA from RNA was performed by using the FermentasRevertAid™ First Strand cDNA Synthesis Kit (THERMO FISCHER Scientific Inc., Waltham, US) according to the company's standard protocol. The cDNA synthesis reaction was done using the EPPENDORF Mastercycler EP Gradient with the following PCR protocol: 5 min at 25 °C, 60 min at 42 °C, 5 min at 70 °C, and 4 °C for the terminal phase. cDNA samples were directly used as templates for qPCR reactions or stored at -20 °C.

In order to quantify the gene expression level of (1) cytokines, (2) cytokine receptors, (3) chemokines, and (4) chemokine receptors, a semi-quantitative real time PCR (qPCR) was performed. For QRT-PCR analysis, qPCR mastermix and primermix were mixed separately and successively pipetted into a 96-well Flat Deck Thermo-Fast detection plate (SARSTEDT AG & Co, Nürnbrecht, Germany). The cDNA was subsequently added. The reaction batch per well is depicted in **Table 3**.

**Table 3** Reaction batch per well for QRT-PCR

Reagent	Volume
qPCR mastermix	12.5 $\mu$ l
Primermix	5 $\mu$ l
cDNA template (1:10 or 1:20 diluted with Aqua Dest depending on cDNA concentration)	7.5 $\mu$ l
Total volume	25 $\mu$ L

The samples were analyzed as duplicates with the Delta-delta Ct method for quantification using the StepOnePlus Real Time PCR System (APPLIED BIOSYSTEMS, Darmstadt, Germany), and the corresponding StepOne Software v2.0.  $\beta$ -



actin was used as the housekeeping gene. The probes (SIGMA-ALDRICH, Munich, Germany) worked with FAM-TAMRA as fluorophore-quencher pairs. The following primer were used for total tissue analyses *in vitro* and *ex vivo*:  $\beta$ -actin, Interferon- $\gamma$ , and Interleukin 17. For *ex vivo*-sorted cells, S1P1, KLF2, CXCR3, and CCR7 were also used.

Table 4 Primer sequences for *in vitro* analyses

Gene	Forward primer 5'-3'	Reverse primer 5'-3'	Probe FAM-5' – 3'-TAMRA
<b>Beta-actin</b> ( $\beta$ -actin)	GTACAACCTCCTT GCAGCTCCT	TTGTCGACGACGAG CGC	CGCCACCAGTTCGCCA TGGAT
<b>Interferon-<math>\gamma</math></b> (IFN- $\gamma$ )	AACAGTAAAGCAA AAAAGGATGCATT	TTCATTGACAGCTTT GTGCTGG	CGCCAAGTTCGAGGTG AACAACCC
<b>Interleukin 17</b> (IL-17)	GAGTCCCCGGAGA ATTCCAT	GAGTACCGCTGCCT TCACTGT	ATGTGCCTGATGCTGTT
<b>S1P1</b> (Bartholomäus et al. 2009)	GATCGCGCGCGGT GTAGAC	TTTCCTTGGCTGGAG AGG	TTGAGCGAGGCTGCTG TTTCTC
<b>KLF2</b> (Bartholomäus et al. 2009)	GCACCTAAAGGCG CATCTG	AGCGCGCGAACTTC CA	AGGTGAGAAGCCTTAT C
<b>CXCR3</b> (Bartholomäus et al. 2009)	AGCAGCCAAGCCA TGTACCTT	TAGGGAGATGTGCT GTTTTCCA	AGGTCAGTGAACGTCA AGTGC TAGATGCCTC
<b>CCR7</b> (Bartholomäus et al. 2009)	GTGTAGTCCACGG TGGTGTTCCTC	CTGGTCATTTTCCAG GTGTGCT	CCGATGTAGTCGTCTGT GA

### 2.2.12 Cell sorting

Samples were prepared as described in 2.2.7. In order to enrich a pure lymphocyte fraction, the spleen and lung were further treated.

Spleen single cell suspensions were centrifuged down (6min, 4 °C, 300 xg), taken up in 20 ml of TCM, and incubated at 37 °C and 10 % CO<sub>2</sub> (Heraeus Heracell 240 incubator,

THERMOFISHER SCIENTIFIC INC., Braunschweig, Germany) for 20 min in 10 cm dishes (SARSTEDT AG&CO., Nürnberg, Germany). They were stored in the incubator to let the macrophages attach to the dishes. Subsequently, the supernatant was transferred into a fresh falcon, centrifuged again, and taken up in 5 ml of EH containing 1 % of EDTA to prevent T cell-to-cell adhesion.

In order to purify mononuclear cells from the lung, samples were taken up in 5 ml of 40 % Percoll. After that 5 ml underlay Percoll were cautiously underlain the mixture. The samples were then centrifuged (30 min, 2000 rpm, RT, minimal acceleration and deceleration). The obtained interphase was cautiously collected with a pipette and transferred in a fresh falcon. A single washing step with PBS followed. Finally, the samples were taken up in EH plus EDTA.

---

#### 2.2.13 Apoptosis detection assay

In order to quantify the percentage of apoptotic/ necrotic T<sub>MBP-GFP</sub> cells in tissue samples, Annexin- propidium iodide (PI) staining was performed;  $1 \times 10^6$  cells were used for the staining in a 96-well v-bottom plate. Cells were washed once with ice cold PBS and incubated in one-time binding buffer 50  $\mu$ L/well (BD Biosciences, San Jose, CA US) containing 2.5  $\mu$ L Annexin V-APC (BD Biosciences, San Jose, CA US) for 15 min at room temperature and in the dark. The reaction was blocked by transferring the samples into 500  $\mu$ l FACS tubes containing 200  $\mu$ L binding and 1  $\mu$ L of PI (BD Biosciences, San Jose, CA US). The samples were acquired using BD FACS Calibur. Analysis of the percentage of Annexin and PI positive cells was done with FlowJo V10 software.

---

#### 2.2.14 Histology

In order to verify the T cell infiltration into and distribution within the s.c., histological analyses were performed. Animals were perfused with PBS followed by 4 % paraformaldehyde (PFA). After post-fixation in 4 % paraformaldehyde the s.c. was prepared out of the vertebral column and cut on a CM305S cryostat CM 3050 S (LEICA, Wetzlar, Germany) into 16  $\mu$ m thick slices. Images were obtained with an Axio Observer Z1 fluorescent microscope (CARL ZEISS, Jena, Germany) equipped with a 10x air objective. Images were acquired and processed by using Axiovision 4.8 software.

---

### 2.2.15 Acute slicing and imaging

In order to prepare acute slices of the lung, the whole lung including the trachea was isolated from the rat thorax and stored in ice cold EH. The airways were then filled with warm (37 °C) 2 % low-melting agarose (CARL ROTH GmbH, Karlsruhe, Germany) in TCM by using a cannula inserted into the trachea. Filling up the lung was considered complete when both the lungs were inflated to a volume comparable to the *in vivo* situation. Lungs were kept on ice to allow the agar to polymerize. After cooling, the lung was cut into smaller pieces that were embedded in 7 % low-melting agarose in TCM. Subsequently, 1 mm thick slices were obtained by using a 752M Vibroslicer (CAMPDEN INSTRUMENTS LTD, Loughborough, England) equipped with a fresh razor blade. The slices were incubated in 4 °C TCM infused with carbogen to ensure suitable environment conditions for the T cells.

All images were recorded with a LSM710/Axio Examiner Z1 microscope (CARL-ZEISS Microimaging) combined with a > 2.5 Watt Ti:Sapphire Chameleon Vision II Laser device (COHERENT GmbH, Dieburg, Germany). The excitation wavelength was tuned to 880 nm and routed through a 20x water NA1.0 immersion objective W Plan Apochromat (CARL ZEISS, Jena, Germany). Emitted fluorescence was detected using non-descanned detectors (CARL ZEISS, Jena, Germany) equipped with 442/46 nm, 483/32 nm, 525/50 nm, and 607/70 nm band-pass filters (SEMROCK Inc., Rochester, NY US). Collagen was detected by two-photon generated second-harmonic signals.

---

### 2.2.16 Reinjection of T cells isolated from mediastinal lymph nodes

AtEAE was induced as described in 2.2.4. One group of animals was treated with 3 mg/kg/d teriflunomide, whereas the other group received only the vehicle.

On day 2 the mediastinal lymph nodes were isolated in sterile conditions and kept in ice cold EH. Single cell suspension was obtained as described in 2.2.2. Subsequently, the cells were stimulated in 96-well flat-bottom plates on a concentration of  $30 \times 10^6$  T cells per plate either with the cognate antigen (MBP, 30  $\mu$ M/ml) or with a shame antigen (OVA, 40  $\mu$ M/ml). The absolute number of plated T<sub>MBP-GFP</sub> cells was measured by FACS Calibur.

Two days later the cells were again counted by FACS Calibur. Subsequently, the amplification rate between day 0 and day 2 was calculated. Moreover, the expression of the surface activation markers CD134 and CD25 was detected by FACS staining as

---

described in 2.2.9. The activation level was further investigated by qPCR analysis for several genes (IFN $\gamma$  and IL-17) as described above in 2.2.11.

## 3 Results

### 3.1 Analysis of T<sub>MBP-GFP</sub> cell proliferation

In order to assess teriflunomide effects on T<sub>MBP-GFP</sub> cell proliferation *in vitro*, two different approaches were pursued.

First, the effect of teriflunomide on the proliferation of T<sub>MBP-GFP</sub> cells was assessed *in vitro* by flow cytometry. T<sub>MBP-GFP</sub> cells were stimulated with MBP in the presence of different concentrations of teriflunomide with or without the addition of uridine. Proliferation was measured by flow cytometry on days 2, 3, and 4 after antigen stimulation. As shown in **Figure 11**, teriflunomide impaired T<sub>MBP-GFP</sub> cell proliferation in a dose-dependent manner, starting at 1  $\mu\text{M}$ . At higher teriflunomide concentrations, cell proliferation was completely abrogated. Exogenous addition of uridine could rescue the blocking of proliferation at concentrations of 1, 10, and 50  $\mu\text{M}$  teriflunomide, but not at 100  $\mu\text{M}$  (**Fig. 11**).

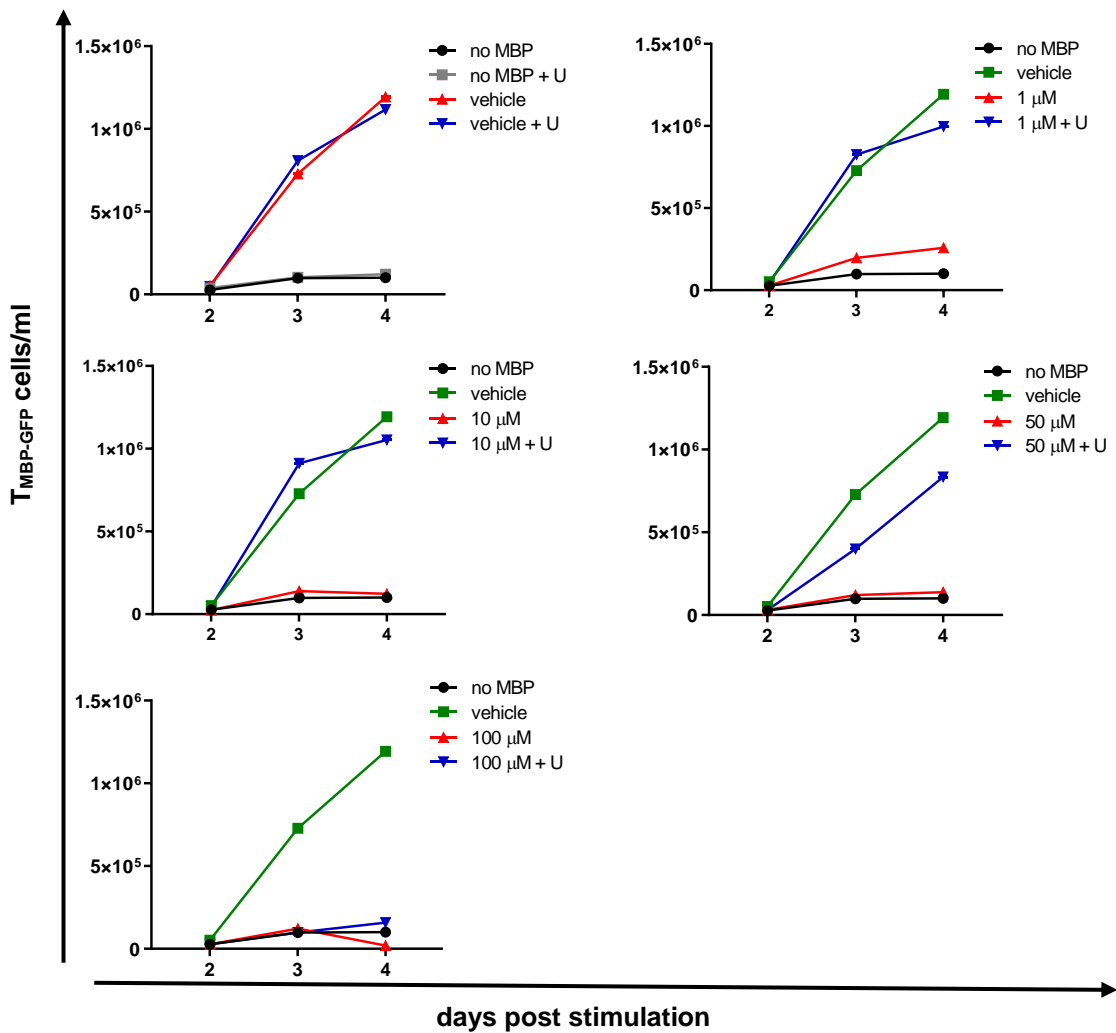


**Figure 11** *In vitro* proliferation of T<sub>MBP-GFP</sub> cells with different concentrations of teriflunomide

1 × 10<sup>5</sup> resting T<sub>MBP-GFP</sub> cells were cultured with MBP and 1 × 10<sup>6</sup> thymocytes per well. Teriflunomide was added at 1, 10, 50, and 100 μM with or without the addition of 200 μM uridine (U). Proliferation was measured flow cytometrically after 48 h, 72 h, and 96 h of incubation. A representative experiment is shown. The experiment was done in triplicate.

Second, the effect of teriflunomide on the proliferation of  $T_{\text{MBP-GFP}}$  cells *in vitro* was measured by incorporation of  $^3\text{H}$ -thymidine in the presence of different concentrations of teriflunomide with or without the addition of uridine. Proliferation was measured 48 h after antigen encounter (**Fig. 12**). Proliferation without MBP was minimal and was used as negative control to define basic proliferation rate.

Under these conditions, the proliferation decreased with increasing teriflunomide concentrations. Exogenous uridine could completely rescue this effect at a concentration of 1  $\mu\text{M}$  and 10  $\mu\text{M}$ , and partially at 50  $\mu\text{M}$  teriflunomide. At 100  $\mu\text{M}$  teriflunomide, the proliferation did not exceed the baseline level and could not be rescued by uridine.

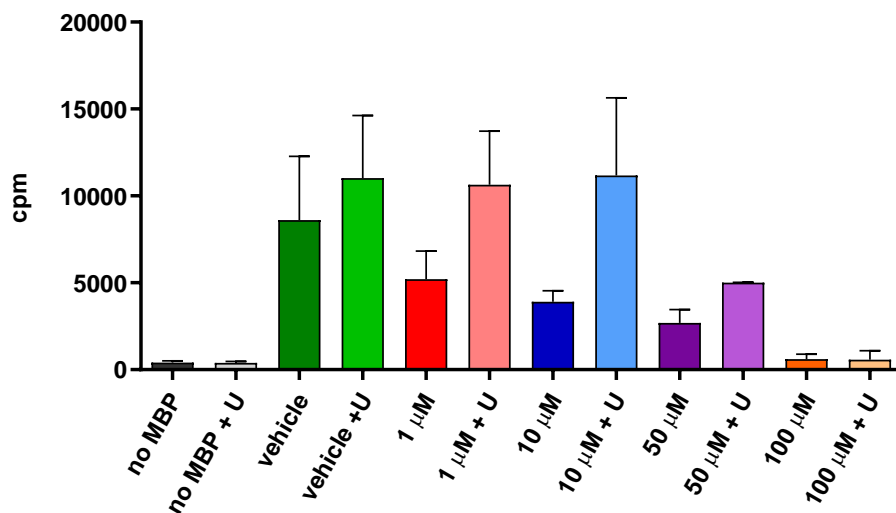


**Figure 12** Proliferation assay of  $T_{\text{MBP-GFP}}$  cells in presence of different concentrations of teriflunomide measured by  $^3\text{H}$ -thymidine incorporation

$1 \times 10^5$  resting  $T_{\text{MBP-GFP}}$  cells were cultured with MBP and  $1 \times 10^6$  thymocytes per well. Teriflunomide was added in concentrations of 1, 10, 50, and 100  $\mu\text{M}$ . Uridine (U) was added at a concentration of 200  $\mu\text{M}$ . 36 h after stimulation with MBP,  $^3\text{H}$ -thymidine was added. Incorporation was measured 16 h after addition of  $^3\text{H}$ -thymidine by a beta-counter. The diagram shows the results of three independent experiments.  $n \geq 2$  per group per experiment. Mean + s.e.m.

### 3.2 Effect of teriflunomide on $T_{\text{MBP-GFP}}$ cell activation

In order to investigate the effect of teriflunomide on T cell activation *in vitro*,  $T_{\text{MBP-GFP}}$  cells were stained for surface activation markers CD134 and CD25 and afterwards were measured flow cytometrically on day 2 after antigen encounter. As expected, upon MBP stimulation,  $T_{\text{MBP-GFP}}$  cells upregulated both CD134 and CD25 (**Fig. 13**).

Under the treatment with teriflunomide in concentrations ranging from 1  $\mu\text{M}$  to 100  $\mu\text{M}$ , no differences in levels of CD134 could be observed. Levels of CD25 were slightly elevated after treatment of cells with teriflunomide. This increase might be due to a

delayed proliferation and activation of cells cultured with teriflunomide because of a decreasing concentration of teriflunomide in the culture medium due to consumption. In the presence of exogenous uridine, no changes in activation could be detected (**Fig. 13**).



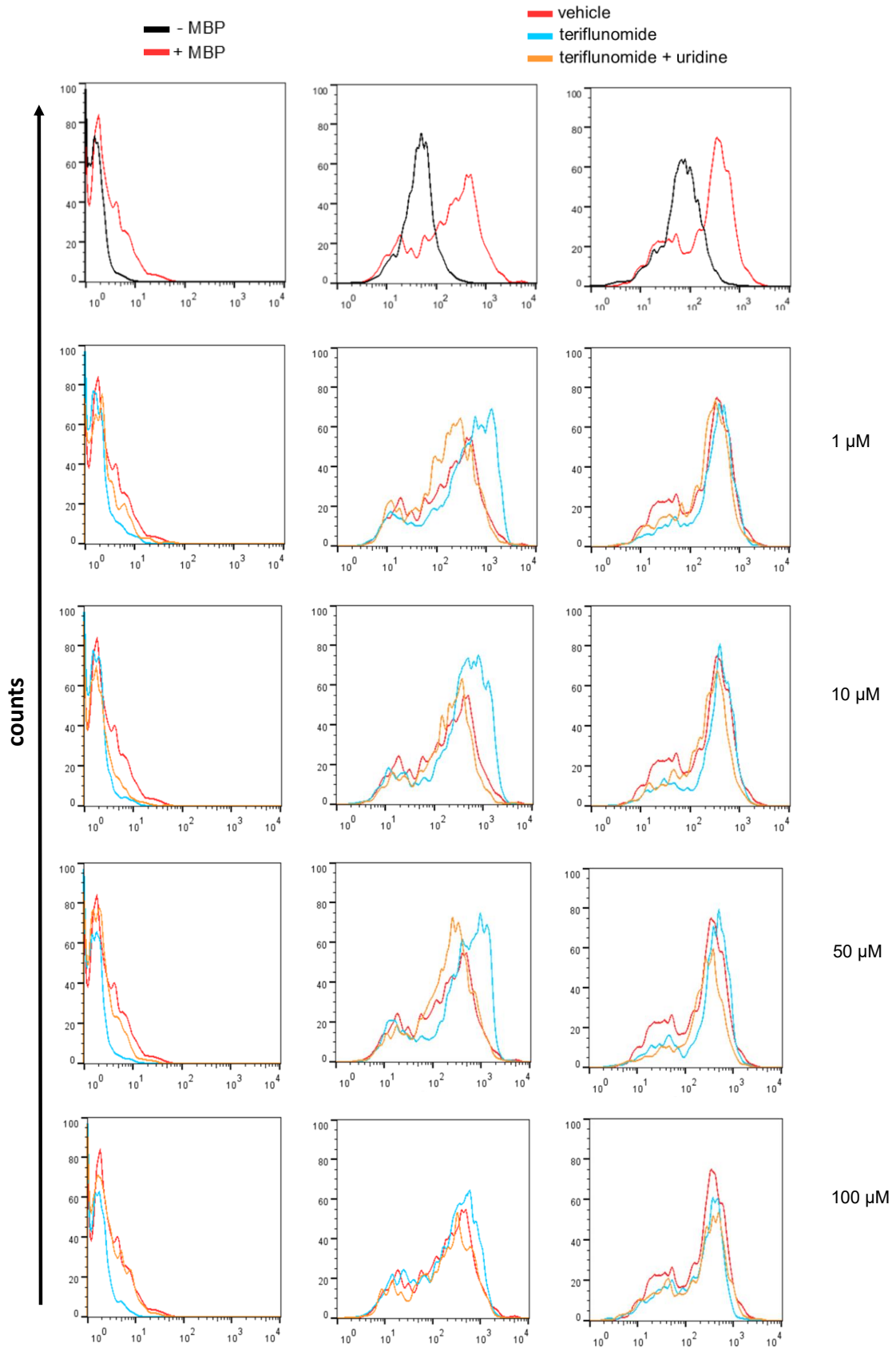


**Figure 13** Levels of activation markers in  $T_{MBP-GFP}$  cells stimulated in the presence of teriflunomide. Two days after *in vitro* stimulation with MBP  $T_{MBP-GFP}$  cells were stained for expression of surface markers CD134 and CD25. As control, cells were stained with isotype control antibody (IgG). The top row shows surface marker levels after stimulation with (red) or without (black) MBP. Shown are overlay histograms gated for  $T_{MBP-GFP}$  cells treated with vehicle (red), teriflunomide (blue) and teriflunomide plus uridine (orange) of a representative experiment. The experiment was done in triplicate.

### 3.3 The effect of teriflunomide on the production of pro-inflammatory cytokines IFN $\gamma$ and IL-17 in T<sub>MBP-GFP</sub> cells

Pro-inflammatory cytokine production of IFN $\gamma$  and IL-17 was measured in T<sub>MBP-GFP</sub> cells on day 2 after stimulation with MBP by real time PCR. As expected, upon stimulation an increase of both cytokines was observed. Interestingly, T<sub>MBP-GFP</sub> cells cultured with increasing concentrations of teriflunomide (1–100  $\mu$ M) did not show any reduction in the expression of inflammatory cytokines compared to T<sub>MBP-GFP</sub> cells cultured in the presence of vehicle. Additionally, when adding uridine to the cells no statistically different changes in cytokine expression compared to the control could be detected (**Fig. 14**). The high IFN $\gamma$  values at 50 and 100  $\mu$ M of teriflunomide could be due to a high fluctuation of expression level between experiments. This is also evidenced by the high arrow bars in **Figure 14**.

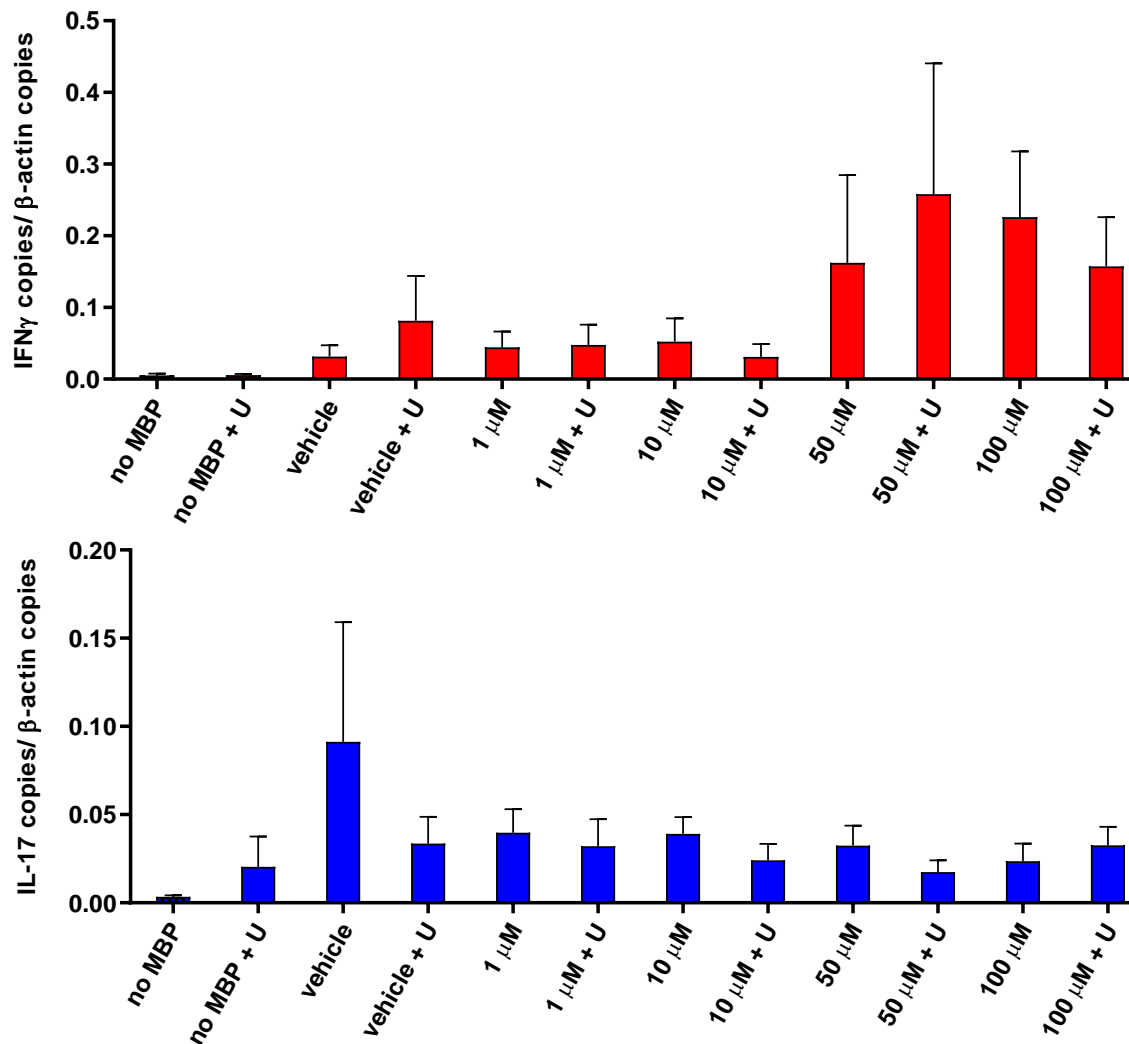


**Figure 14** Quantitative PCR of pro-inflammatory cytokine expression in T<sub>MBP-GFP</sub> cells cultured with different concentrations of teriflunomide

$1 \times 10^5$  resting T<sub>MBP-GFP</sub> cells were cultured with  $1 \times 10^6$  thymocytes and MBP per well. As negative controls, T<sub>MBP-GFP</sub> cells were plated without MBP. The expression level of IFN $\gamma$  (red) in the upper diagram and IL-17 (blue) in the lower diagram was measured on day 2 after re-stimulation by qPCR. The results of five independent experiments are shown with  $n \geq 4$ , mean + s.e.m.

### 3.4 The effect of teriflunomide on the preclinical phase in the EAE model in Lewis rats

#### 3.4.1 Pharmacokinetics with different doses of teriflunomide

In order to investigate the effect of teriflunomide *in vivo*, Lewis rats were treated with different concentrations of teriflunomide starting from day 0 (T cells transfer). The drug was well tolerated by the rats also at the highest concentration of 10 mg/kg/d. Regarding the effects, animals treated with a dose of 3, 5, and 10 mg/kg/d of teriflunomide did not show any clinical score (neither loss of body weight nor motility deficits). As expected,

the vehicle-treated group showed a typical EAE that started on day 4 and peaked between day 5 and 6 with paralysis of the lower limbs (**Fig. 15**).

When the animals were treated with 0.5 and 1 mg/kg/d of teriflunomide there was a dose-dependent amelioration of the clinical disease. In both groups teriflunomide-treated animals developed a clinic more or less similar to the vehicle-treated group (data not shown).

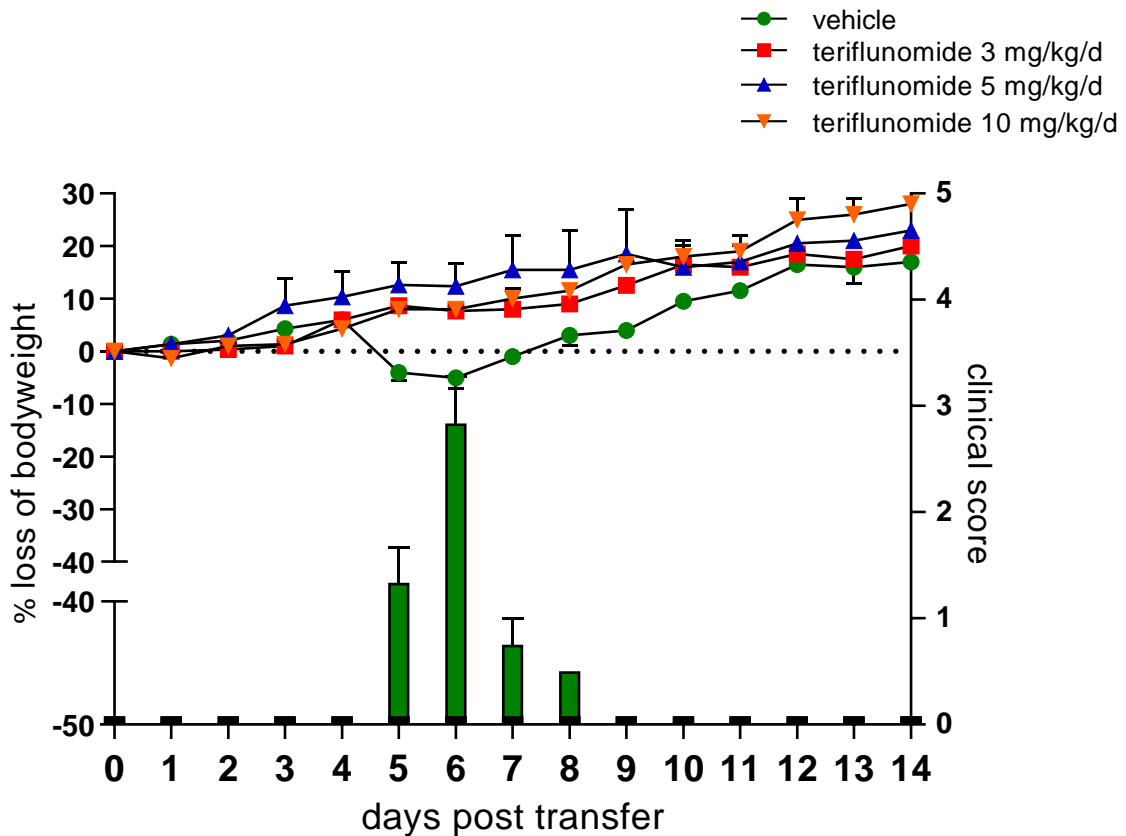


**Figure 15** Pharmacokinetic with 3, 5, and 10 mg/kg/d teriflunomide

Left and right axis display clinical disease score (bars) and percentage of loss of body weight (lines) over time, respectively. Shown are mean + s.e.m. of three animals per group: vehicle-treated group (green), teriflunomide 3 mg/kg/d (red), teriflunomide 5 mg/kg/d (blue), and teriflunomide 10 mg/kg/d (orange).

### 3.4.2 Clinical development of EAE under the influence of teriflunomide

The next step was to evaluate the effect of teriflunomide on a greater cohort of animals. Therefore, animals were divided into three groups: a vehicle-treated group, a teriflunomide-treated group (3 mg/kg/d), and a teriflunomide (3 mg/kg/d) plus uridine (500 mg i.p. twice per day) treated group. The dose of teriflunomide 3 mg/kg/d was chosen based on the previous pharmacokinetics (see 3.4.1.). The dose of uridine was chosen according to the literature (Korn et al. 2004). The clinical data are summarized in **Table 5**. Under the treatment with teriflunomide incidence of disease was significantly

reduced. Upon teriflunomide treatment the disease onset was delayed compared to the vehicle-treated group. An additional treatment with uridine had no influence on the start of disease compared to a treatment with teriflunomide alone; it also had no influence on the peak or incidence of disease. The disease duration and severity of clinical symptoms were significantly reduced by teriflunomide. Uridine seemed to ameliorate the effect of teriflunomide on disease duration and the maximum score to a certain extent. In total, the cumulative score during teriflunomide treatment was reduced. This effect was alleviated by treatment with exogenous uridine. For ethical reasons, six animals of the vehicle-treated group were taken out of the experiment (**Table 5**).

**Table 5 Clinical table**

	incidence of disease	onset of disease	peak of disease	disease duration	highest score	cumulative score	fatality
		day (S.D.)	day (S.D.)	days (S.D.)	score (S.D.)	score (S.D.)	
vehicle	<b>96 %</b> (n=27)	<b>3.1</b> (0.19) (n=6)	<b>4.9</b> (0.78) (n=11)	<b>2.4</b> (1.24) (n=9)	<b>2.7</b> (n=11)	<b>3.9 (2.51)</b> (n=9)	<b>6</b> (n=27)
teriflunomide	<b>25 %</b> (n=24)	<b>4.2</b> (0.52) (n=6)	<b>5 (0)</b> (n=2)	<b>0.54</b> (1.21) (n=11)	<b>0.55</b> (n=11)	<b>1 (2.33)</b> (n=11)	<b>0</b> (n=24)
teriflunomide + uridine	<b>46 %</b> (n=13)	<b>4.3</b> (0.42) (n=6)	<b>5 (0)</b> (n=2)	<b>1.2</b> (1.64) (n=5)	<b>1.2</b> (n=5)	<b>2.7 (3.7)</b> (n=5)	<b>0</b> (n=13)

Shown is the mean + S.D. for all acquired clinical parameters. P-values for incidence of disease were calculated by Fisher's exact test. P-values for disease duration and highest score were calculated by ANOVA and multiple comparison by Turkey's HSD. \*p<0.05 \*\*p<0.01 \*\*\*p<0.001

### 3.4.3 Effect of teriflunomide on T<sub>MBP-GFP</sub> cell infiltration in the spinal cord

Since the severity of clinical symptoms in transfer EAE could be significantly reduced by the treatment with teriflunomide, the infiltration of T<sub>MBP-GFP</sub> cells into the s.c. was measured. Infiltration was analyzed at the peak of disease on day 5 post transfer.

The histological examination showed a marked reduction of T<sub>MBP-GFP</sub> cell infiltration into the s.c. parenchyma in teriflunomide-treated animals (**Fig. 16B**) compared to vehicle-treated animals (**Fig. 16A**). In vehicle-treated animals T<sub>MBP-GFP</sub> cells could be observed in GM and WM of the s.c. parenchyma, whereas in teriflunomide-treated animals T<sub>MBP-GFP</sub> cells were few and remained in the submeningeal area.

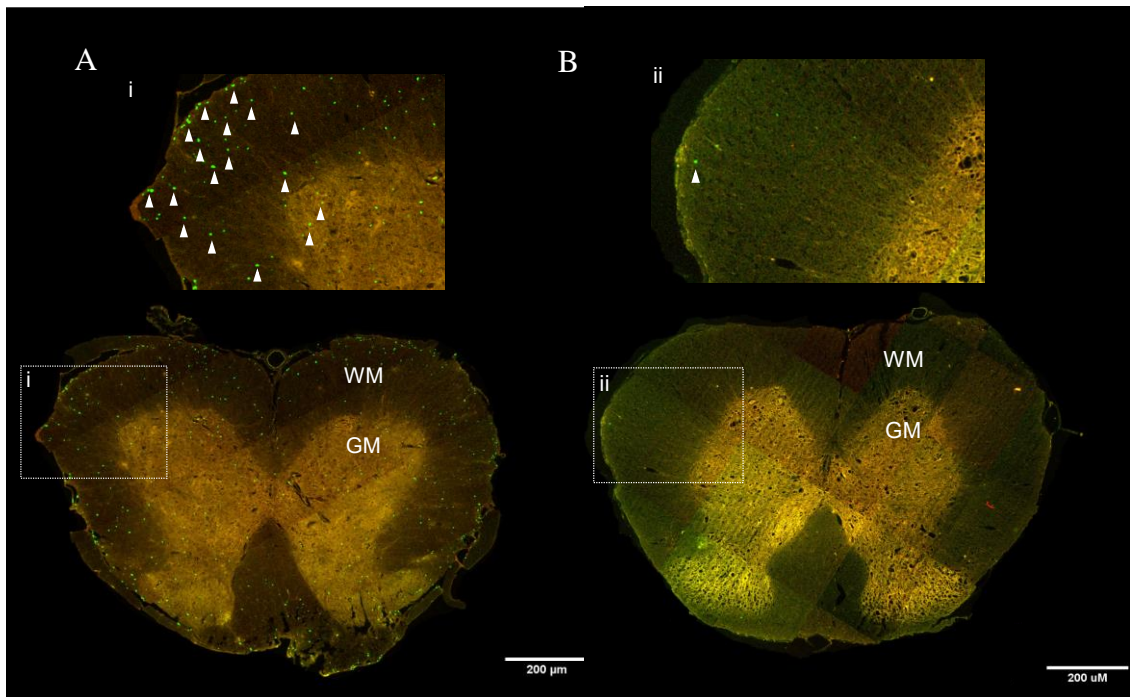


**Figure 16 Infiltration of T<sub>MBP-GFP</sub> cells in the spinal cord on day 5 p.t. (peak of atEAE) with or without teriflunomide treatment**

Shown are representative fluorescence microscopy images of the s.c. with WM and GM. Animals were i.v. injected with T<sub>MBP-GFP</sub> cells and either treated with 3 mg/kg/d teriflunomide (B) or only with vehicle (A). Pictures show infiltration of green T<sub>MBP-GFP</sub> cells (white arrows) into WM and GM in a vehicle-treated animal (A) and a teriflunomide-treated animal (B). However, in teriflunomide-treated animals there is only low submeningeal T cell infiltration. The inserts show a magnification of representative areas with T<sub>MBP-GFP</sub> cells indicated by white arrows.

#### 3.4.4 Effect of teriflunomide on the inflammatory milieu in the spinal cord

The next step was to investigate whether teriflunomide affects the level of inflammation in the s.c. To this end, RNA was extracted from s.c. total tissue samples of animals treated with teriflunomide (3 mg/kg/d) or vehicle. The expression levels of the pro-inflammatory cytokines IFN $\gamma$  and IL-17 were measured by qPCR on day 4 and day 5 post transfer.

A reduction in the expression of IFN $\gamma$  and IL-17 both on day 4 (**Fig. 17B**) and day 5 (**Fig. 17C**) in the s.c. parenchyma could be detected under the treatment with teriflunomide in comparison to vehicle-treated animals. In the s.c. meninges the expression of IL-17 was clearly reduced under treatment with teriflunomide both on day 4 and 5. The level of IFN $\gamma$ , however, was only slightly reduced under teriflunomide treatment on both days (**Fig. 17B, C**).

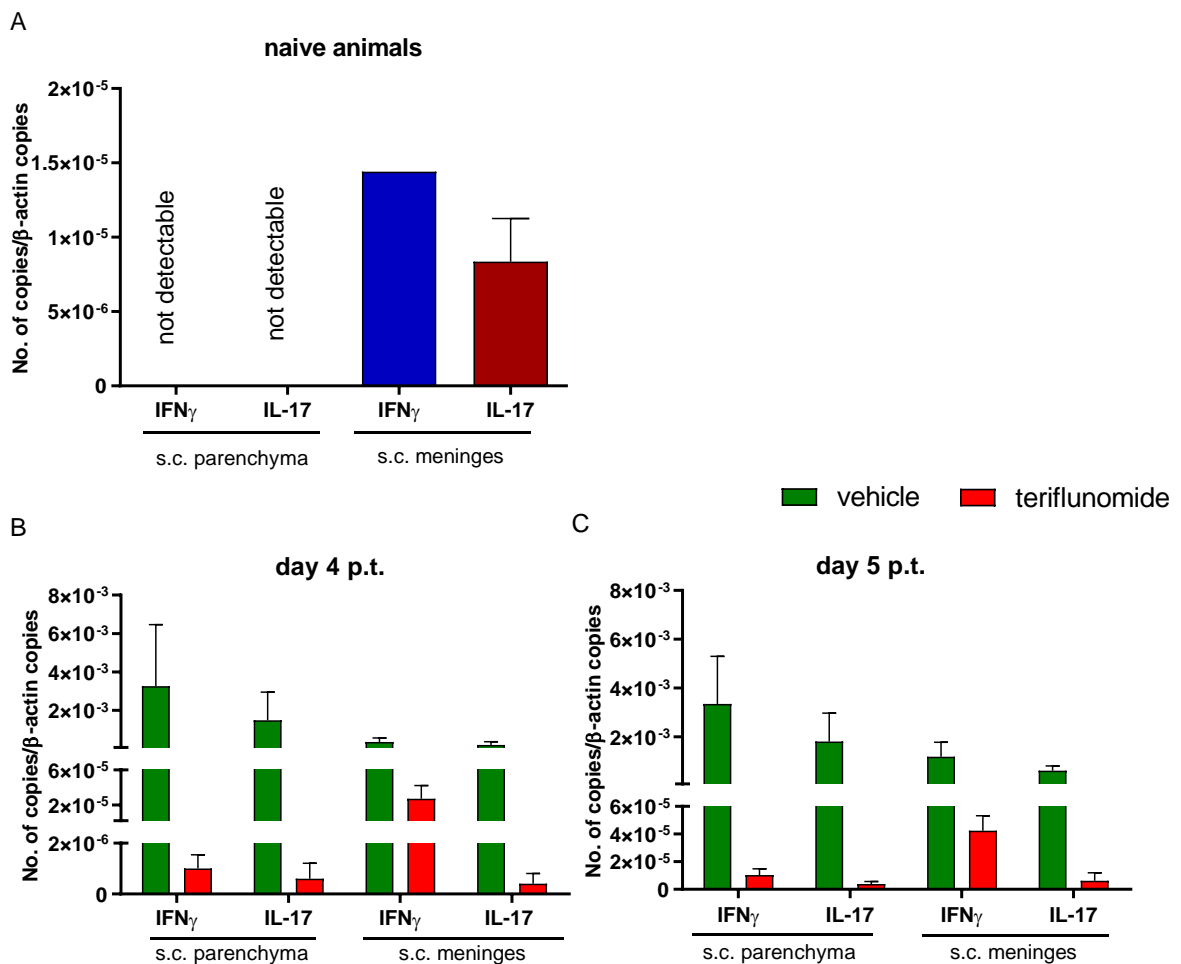


**Figure 17** Quantitative RNA analyses of pro-inflammatory cytokines in total tissue of spinal cord parenchyma and meninges from naive animals and from teriflunomide-treated animals on day 4 and 5

Spinal cords were explanted from naive Lewis rats (A) and from animals on day 4 (B) and day 5 (C) post transfer of T<sub>MBP-GFP</sub> cells. One group of transferred animals was treated with 3 mg/kg/d teriflunomide (red) the other group received only the vehicle (green). The naive animals did not receive any treatment. Expression of IFN $\gamma$  and IL-17 was measured by quantitative PCR. The relative copy numbers compared to  $\beta$ -actin copies (housekeeping gene) are shown. Mean + s.e.m. of at least 3 (day 4) or 4 (day 5) different experiments per time point are shown. The data from the naive animals were provided by Dr. Francesca Odoardi.

### 3.4.5 Effect of teriflunomide on the migratory pattern of T<sub>MBP-GFP</sub> cells

Next, the effect of teriflunomide on T cell proliferation and migration during EAE was investigated. In Lewis rat transfer EAE, T cells follow a precise migratory pattern: they

first enter the lung and then migrate to the mediastinal lymph nodes. Three days p.t. the  $T_{\text{MBP-GFP}}$  cells appear in blood and spleen just before infiltrating the CNS. Therefore, the absolute numbers of  $T_{\text{MBP-GFP}}$  cells were quantified in the peripheral organs (lung, mediastinal lymph nodes, spleen, blood) and the CNS (s.c. meninges, s.c. parenchyma) with and without teriflunomide treatment (**Fig. 18**).

Regarding T cell numbers in the first two days p.t., differences were observed only in the mediastinal lymph nodes, where a higher number of  $T_{\text{MBP-GFP}}$  cells in the vehicle-treated animals could be detected (**Fig. 18B**) compared to the other two groups.

On day 3 compared to day 2, an increase in T cell number could be detected in the lung with both vehicle and teriflunomide treatment. Thus, teriflunomide did not impair the entry of T cells into the lung. Between the teriflunomide-treated groups and the vehicle-treated group only minor differences could be observed. However, in the mediastinal lymph nodes, a clearly higher number of T cells could be detected in the vehicle-treated animals compared to the teriflunomide( $\pm$ uridine)-treated groups (**Fig. 18A, B**). These differences were even stronger in blood and spleen, where the cell number was clearly reduced under teriflunomide treatment (**Fig. 18C, D**). In the blood the difference in T cell number reached significance on day 3 and 4. Conversely, in the s.c. the first T cells appeared in the meninges and the parenchyma on day 3. The number of T cells in vehicle-treated animals was much higher than in teriflunomide-treated animals (**Fig. 18E, F**).

On day 4, an increase in the number of T cells in the lung of vehicle-treated animals could be observed, whereas the number of T cells in the lung of teriflunomide( $\pm$  uridine)-treated animals remained stable (**Fig. 18A**). The number of  $T_{\text{MBP-GFP}}$  cells in the mediastinal lymph nodes decreased in teriflunomide( $\pm$  uridine)-treated animals, whereas in vehicle-treated animals the numbers increased and reached a significant difference between vehicle and teriflunomide treatment and vehicle and teriflunomide/uridine treatment (**Fig. 18B**). Furthermore, in the blood and spleen, a significantly higher number of T cells could be observed in the vehicle-treated group compared to teriflunomide( $\pm$  uridine)-treated groups (**Fig. 18C, D**). In the s.c. vehicle-treated animals showed noticeably higher numbers of T cells compared to teriflunomide-treated animals (**Fig. 18E, F**).

On day 5, the number of T cells in the lung was decreasing in the vehicle as well as in the teriflunomide-treated group (**Fig. 18A**). In the mediastinal lymph nodes, the number of



T cells remained stable in the vehicle-treated group, whereas no T cells could be detected in the teriflunomide-treated group. This difference proved statistically significant (**Fig. 18B**). In the blood and spleen, T cells could almost exclusively be found in vehicle-treated animals (statistically significant for spleen). The same held true for the number of T cells in the s.c. parenchyma and s.c. meninges (**Fig. 18E, F**), which could also be shown by histological examination (**Fig. 16**).

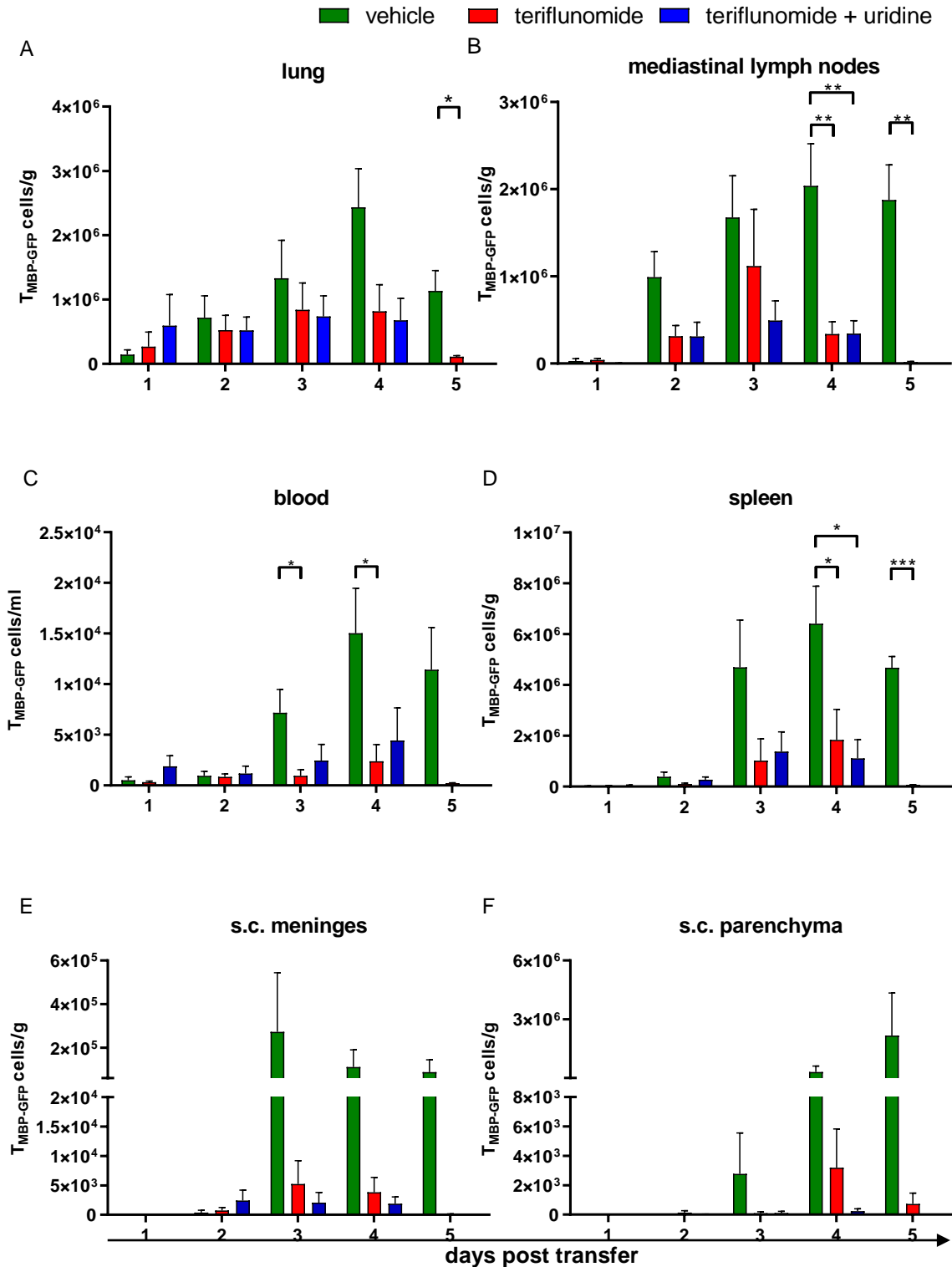


**Figure 18** Quantification of T<sub>MBP</sub>-GFP cells in different organs under different treatments during atEAE

Animals were treated with teriflunomide (red), teriflunomide plus uridine (blue), or vehicle (green). T<sub>MBP</sub>-GFP cells per g or ml organ quantified by flow cytometry at the indicated days post transfer. Gated for GFP<sup>+</sup> lymphocytes. Each time point and group with n<sub>3</sub> from at least 7 independent experiments. The statistical significance was tested by ANOVA and multiple comparison by Turkey's HSD. Results on day 5 were compared by unpaired t-test, since no data were acquired for the group of animals treated with teriflunomide plus uridine. \*p<0.05 \*\*p<0.01 \*\*\*p<0.001.

### 3.4.6 Distribution of T cells in the peripheral organs

Based on the findings concerning teriflunomide's influence on migration patterns, the following task was to answer the question of whether teriflunomide treatment influences the distribution of T cells in the peripheral organs. Therefore, the number of T cells was analyzed in the lung (**Fig. 19A**) and spleen (**Fig. 19B**) of vehicle and teriflunomide-treated animals during transfer EAE. After  $T_{\text{MBP-GFP}}$  cells from lung, mediastinal lymph nodes, blood, spleen, s.c. meninges, and s.c. parenchyma were quantified flow cytometrically on days 1 to 5, the percentage of cells in lung and spleen was calculated.

In the lung an increase of percentage of  $T_{\text{MBP-GFP}}$  cells on days 2 to 5 in teriflunomide-treated animals compared to vehicle-treated animals could be observed (**Fig. 19A**). However, this difference was statistically significant only on day 5. The percentage of cells in vehicle-treated animals steadily decreased from 80 % on day 1 to 10 % on day 5; meanwhile, the percentage of cells in the teriflunomide group started at around 53 %, dropped to 36 % on day 4, and increased to 55 % on day 5.

In the spleen, during the first two days, the percentage of  $T_{\text{MBP-GFP}}$  cells in vehicle and teriflunomide-treated animals was comparable at a level of 15 %–20 %. In the vehicle-treated animals the percentage of T cells increased from about 20 % on day 2 to about 55 % on day 3, and then remained stable until day 5. Under the treatment with teriflunomide, only a slight increase in  $T_{\text{MBP-GFP}}$  cells from 16 % on day 3 to 32 % on day 4 and 38 % on day 5 could be observed (**Fig. 19B**).

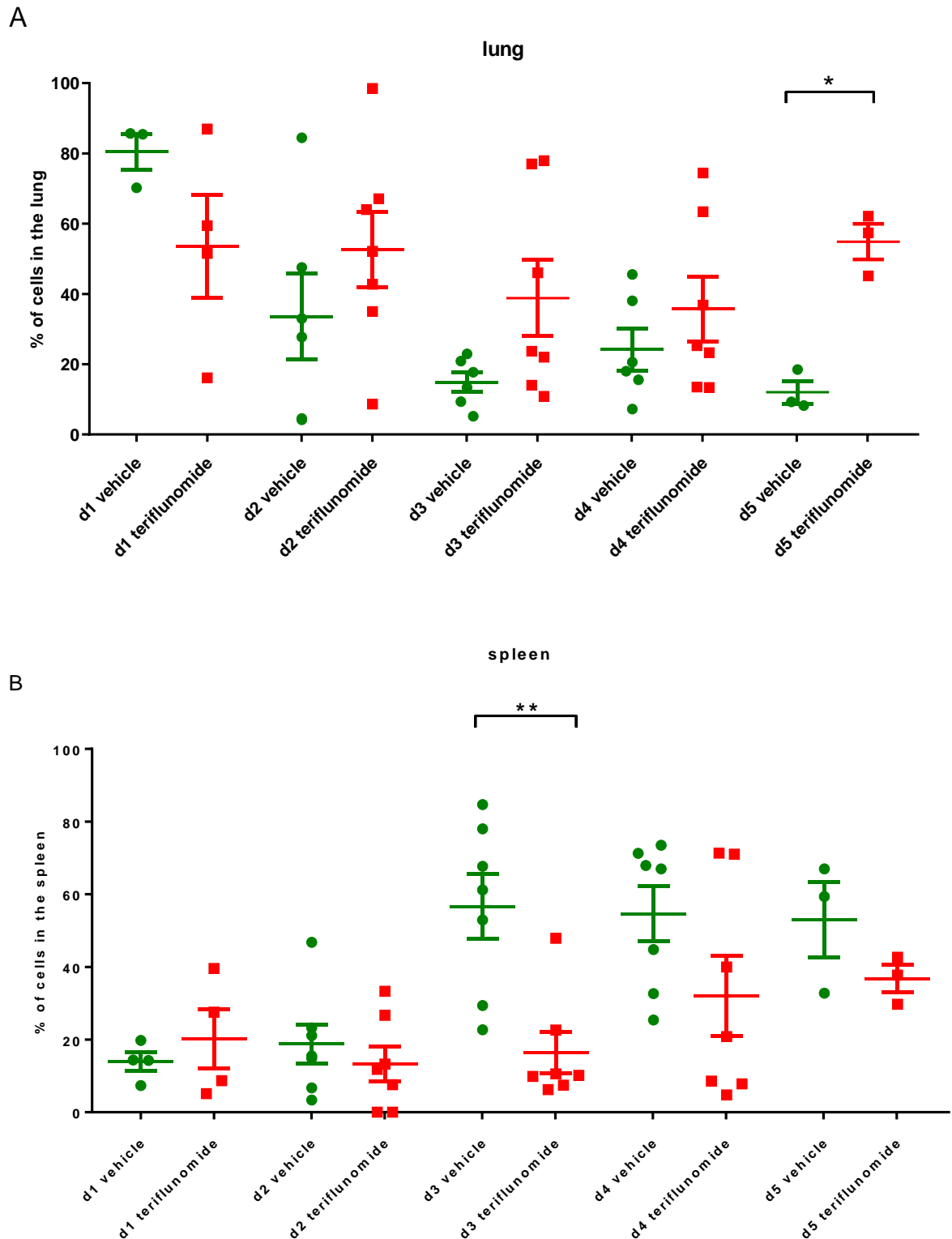


**Figure 19 Higher percentage of T<sub>MBP-GFP</sub> cells in the lung in teriflunomide-treated animals compared to vehicle-treated animals**

Percentage of T<sub>MBP-GFP</sub> cells in the lung and the spleen of teriflunomide-treated animals (red) compared to vehicle-treated animals (green) calculated from the absolute numbers of T<sub>MBP-GFP</sub> cells in all organs analyzed. Absolute numbers of T cells were acquired by FACS analysis and measured per g or ml per organ. Shown are mean ± s.e.m. Each data point represents one animal. Significance was determined by unpaired t-test. \* $p < 0.05$  \*\* $p < 0.01$  \*\*\* $p < 0.001$ .

---

### 3.4.7 Effect of teriflunomide on the migratory behavior of T cells within the lung tissue

Considering that T cells upon teriflunomide treatment tended to persist in the lung, their migratory capacity was analyzed in more detail. Firstly, a histological analysis was performed to detect the distribution of T cells in the lung tissue.

In the vehicle-treated group, T cells tended to accumulate around the bronchi and the bronchus-associated lymphoid tissues at day 3 p.t., as already described in the literature (Odoardi et al. 2012). Teriflunomide treatment did not change this pattern of distribution:  $T_{\text{MBP-GFP}}$  cells localized around the bronchi at day 3 p.t. also in teriflunomide-treated animals. Although the relative numbers of  $T_{\text{MBP-GFP}}$  cells in the lung in teriflunomide-treated animals were higher compared to vehicle-treated ones, the absolute numbers of  $T_{\text{MBP-GFP}}$  cells were lower in the teriflunomide-treated animals than in vehicle-treated ones (**Fig. 20**).

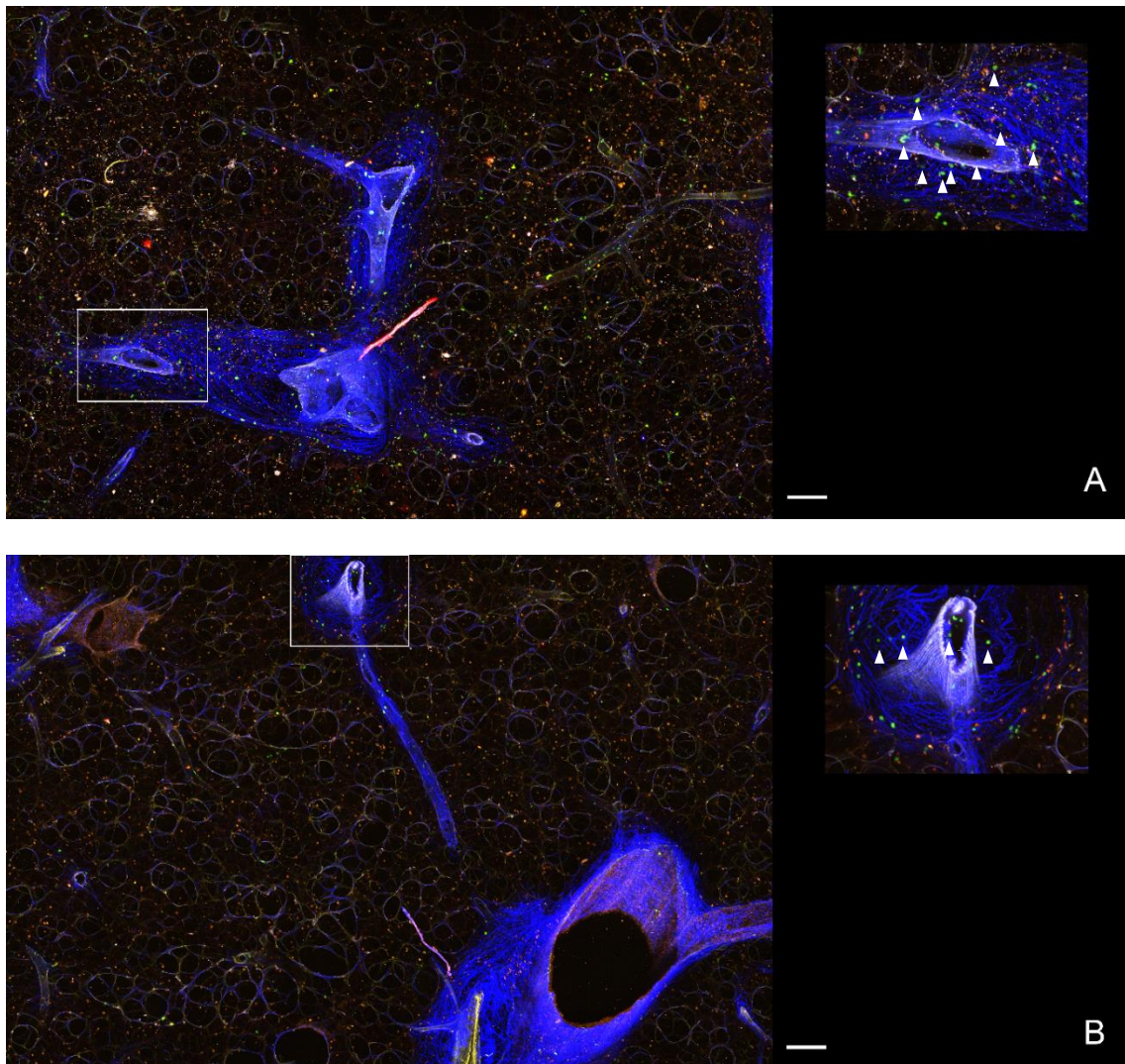


**Figure 20 Homing of  $T_{MBP-GFP}$  cells to bronchi in teriflunomide-treated and vehicle-treated animals**

Representative 2-photon microscopic images of acute lung slices at day 3 p.t. Lung of vehicle-treated animal (A). Lung of teriflunomide-treated animal (B). Insets show magnification of  $T_{MBP-GFP}$  cell infiltration (white arrows) around the bronchi. Scale bar 200  $\mu$ m.

Due to lower absolute numbers of  $T_{MBP-GFP}$  cells in the lung under teriflunomide treatment, the effect of teriflunomide on inducing apoptosis or necrosis in T cells in the lung was investigated. For this purpose, a flow cytometric analysis of Annexin V (AnnV) and propidium iodide (PI) staining was performed. The results are shown in **Figure 21**. No differences in percentage of apoptotic or necrotic  $T_{MBP-GFP}$  cells isolated from lung were detected in the vehicle-treated group versus the teriflunomide-treated groups. The percentage of non-apoptotic cells (PI-, AnnV-) was around 60 % in both groups. The percentage of apoptotic cells (PI-, AnnV+) was around 35 %, and the percentage of necrotic cells (PI+, AnnV-) was around 5 % (**Fig. 21**).

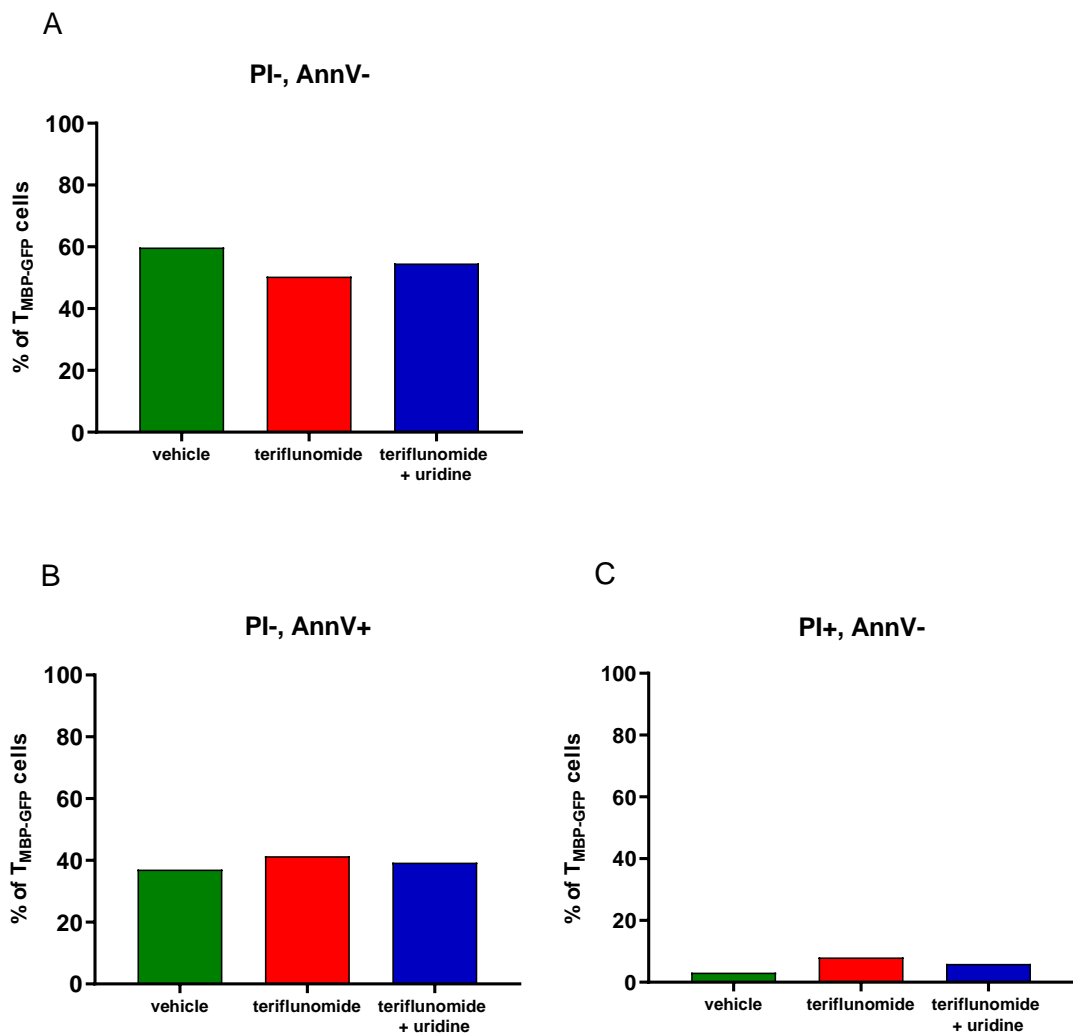


**Figure 21 Annexin V and propidium iodide staining of  $T_{MBP-GFP}$  cells in the lung on day 3 p.t.**

Percentage of  $T_{MBP-GFP}$  cells in the lung of vehicle-treated (green), teriflunomide-treated (red) and teriflunomide plus uridine-treated (blue) animals at day 3 p.t., analyzed by flow cytometry. Non-apoptotic  $T_{MBP-GFP}$  cells (AnnV-, PI-) (A). Apoptotic  $T_{MBP-GFP}$  cells (AnnV+, PI-) (B). Necrotic  $T_{MBP-GFP}$  (PI+, AnnV-) (C). Result of one experiment (n=1). Gated for  $T_{MBP-GFP}$  cells.

### 3.4.8 Effect of teriflunomide on the emigration of $T_{MBP-GFP}$ cells out of the lung

Next, the influence of teriflunomide treatment on the expression profile of  $T_{MBP-GFP}$  cells was analyzed. In particular, genes known to be involved in T cell trafficking were measured, which might explain the higher percentage of  $T_{MBP-GFP}$  cells remaining in the lung. Therefore, the expression of the emigration factors KLF2 and S1P1 as well as the chemokines CCR7 and CXCR3 were analyzed; which change their expression during T cell migration in peripheral organs (Odoardi et al. 2012).

$T_{MBP-GFP}$  cells were sorted from lung on day 2, 3, and 4 p.t. Under treatment with teriflunomide, expression levels of KLF2 (Fig. 22A) and S1P1 (Fig. 22B) were reduced compared to the vehicle-treated group on all days analyzed.

In the expression profiles of CCR7 and CXCR3, no differences between vehicle treatment and teriflunomide treatment could be detected (Fig. 22C, D).

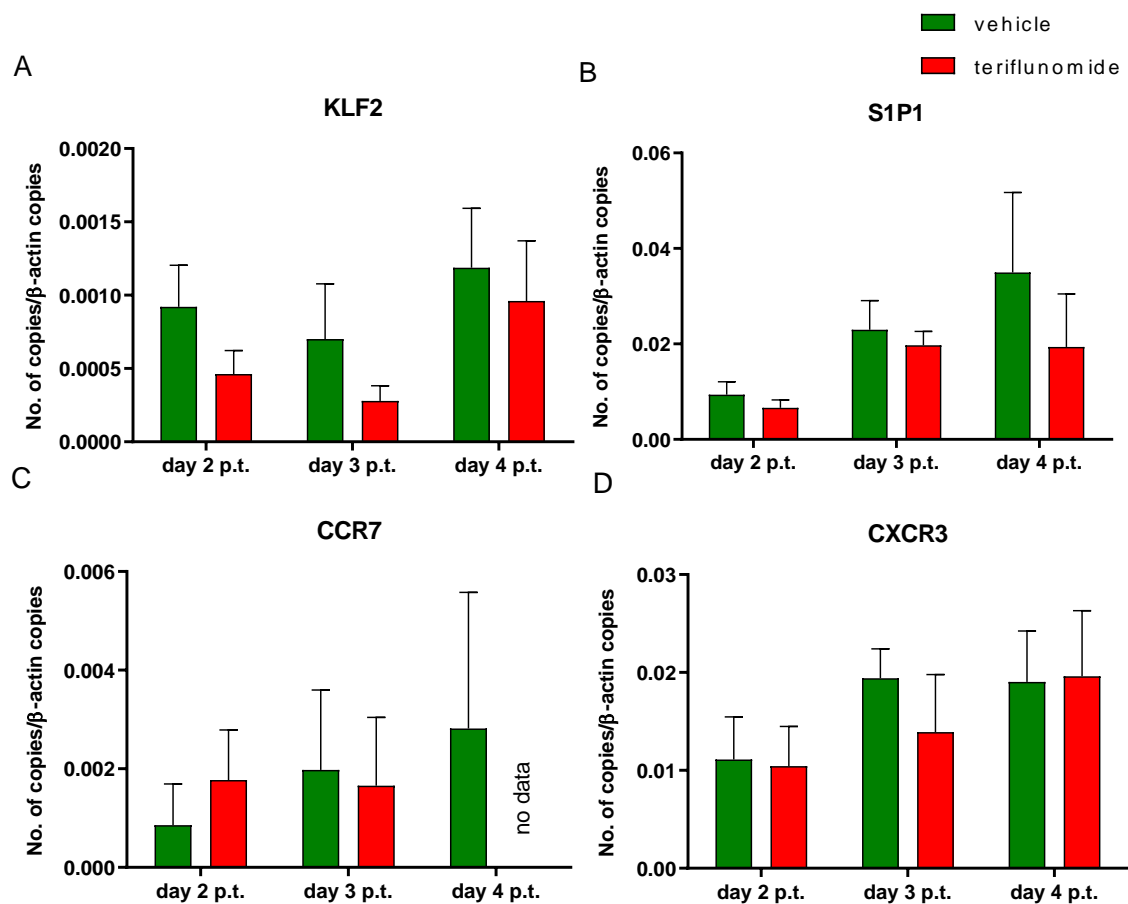


**Figure 22** Quantitative PCR analyses for expression of KLF2, S1P1, CCR7, and CXCR3 in sorted  $T_{MBP-GFP}$  cells from the lung

$T_{MBP-GFP}$  cells were sorted from the lung of vehicle-treated (green) and teriflunomide-treated (red) animals at day 2, 3, and 4 p.t. The teriflunomide group was treated with 3 mg/kg/d. Relative copy numbers of KLF2 (A), S1P1 (B), CCR7 (C), and CXCR3 (D) in relation to  $\beta$ -actin are shown.  $n \geq 3$  per time point and group. Graphs are mean + s.e.m.

### 3.4.9 Effect of teriflunomide on the reactivation potential of *ex vivo*-isolated $T_{MBP-GFP}$ cells

In the following step, induction of T cell anergy by teriflunomide was investigated.  $T_{MBP-GFP}$  cells were isolated from the mediastinal lymph nodes of vehicle- or teriflunomide-treated animals on day 2 p.t. The cells were either challenged with the cognate antigen (MBP) or with a control antigen (OVA) *in vitro*.



MBP specific proliferation of  $T_{\text{MBP-GFP}}$  cells isolated both from vehicle-treated animals and teriflunomide-treated animals could be observed. The proliferation of cells from vehicle-treated animals, however, reached higher levels (**Fig. 23B**). As expected, no proliferation was observed when only OVA was added to the T cell culture (**Fig. 23A**).

Taken together, these data indicate that  $T_{\text{MBP-GFP}}$  cells extracted from teriflunomide-treated animals were not anergic (**Fig. 23A, B**).

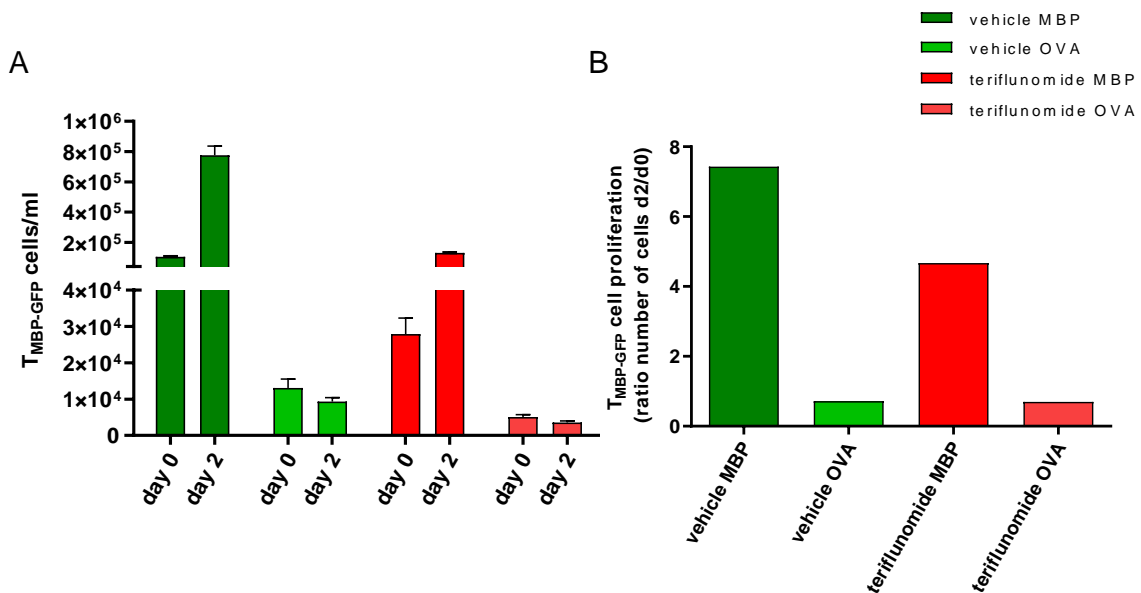


**Figure 23** Re-stimulation of *ex vivo*-isolated  $T_{\text{MBP-GFP}}$  cells from mediastinal lymph nodes

$T_{\text{MBP-GFP}}$  cells were extracted from mediastinal lymph nodes on day 2 p.t. from animals either treated with vehicle (green) or teriflunomide 3 mg/kg/d (red). The isolated cells were re-stimulated *in vitro* in the presence of MBP or OVA. OVA was used as the negative control. Absolute numbers of  $T_{\text{MBP-GFP}}$  cells (A) measured by flow cytometry on day 0 and day 2 after antigen encounter. Mean + s.e.m. Ratio of proliferation (B) of day 2/day 0 of the same experiment. Representative data of one experiment (n=1). Experiment was done in triplicate.

Next, the influence of teriflunomide on the reactivation potential of  $T_{\text{MBP-GFP}}$  cells was tested. Therefore, two days after isolation from mediastinal lymph nodes with subsequent re-stimulation *in vitro*, T cells were stained for CD134 and CD25, which are classical surface activation markers. When challenged with MBP, the expression of CD134 and CD25 was increased compared to T cells stimulated with OVA both in T cells extracted from vehicle-treated animals and for T cells extracted from teriflunomide-treated

animals. However, no differences in the activation levels between these two groups were observed (**Fig. 24**).

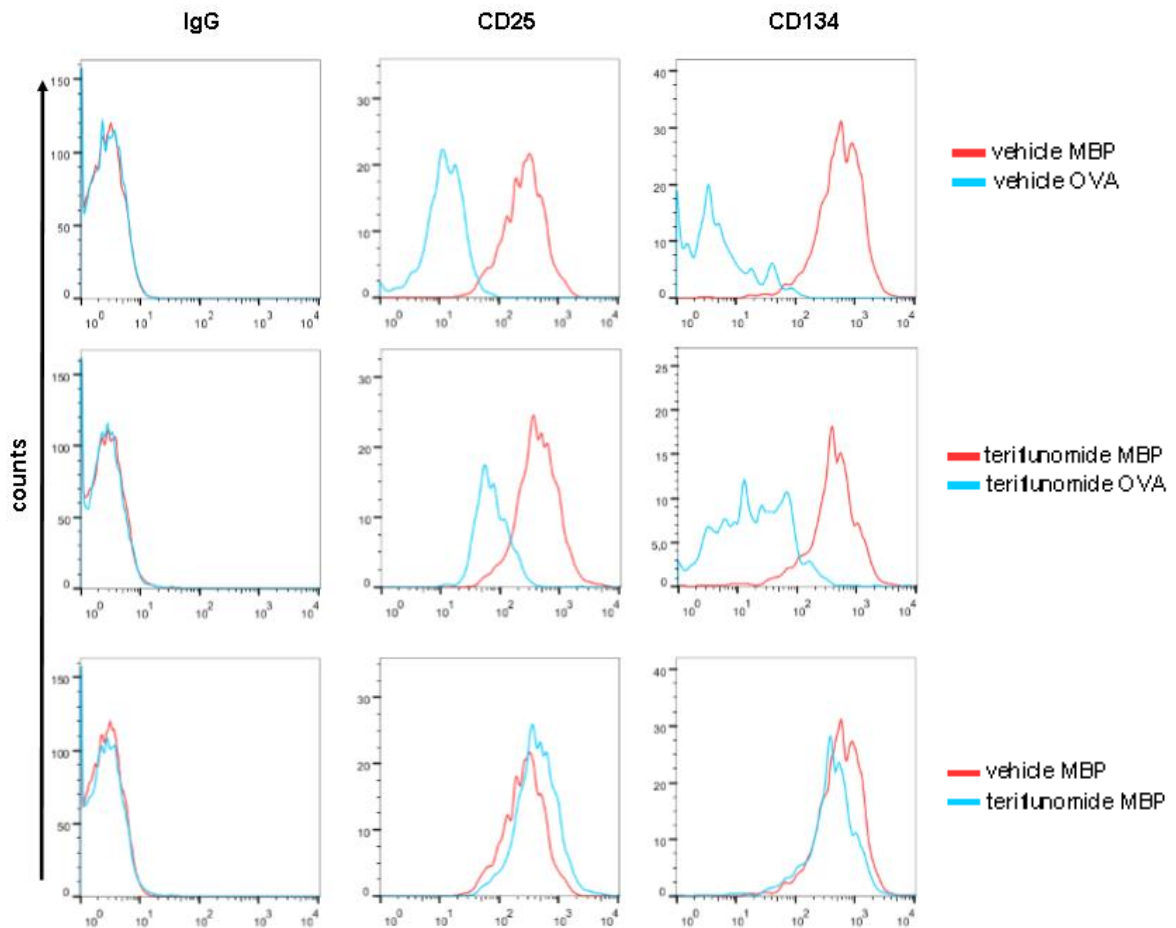


**Figure 24**  $T_{\text{MBP-GFP}}$  cells extracted from mediastinal lymph nodes from animals treated with vehicle- or teriflunomide and re-stimulated *in vitro* with MBP show the same activation levels

$T_{\text{MBP-GFP}}$  cells extracted from mediastinal lymph nodes of vehicle- or teriflunomide-treated animals on day 2 p.t. were cultured *in vitro* with MBP or OVA. At day 2 after re-stimulation, T cells were stained for expression of surface markers CD134 (right column) and CD25 (middle column). As the control, cells were stained with isotype control antibody (IgG) (left column). Overlay histograms gated for  $T_{\text{MBP-GFP}}$  cells are depicted. The results are of one representative experiment ( $n=1$ ). The experiment was done in triplicate.

Under the same conditions as for expression of cell surface markers, the influence of teriflunomide on cytokine production in  $T_{\text{MBP-GFP}}$  cells was investigated. The expression levels of pro-inflammatory cytokines  $\text{IFN}\gamma$  and IL-17 and cell surface marker CD25 were measured by qPCR.

In both the vehicle-treated group and the teriflunomide-treated group, the expressions of IFN $\gamma$  (**Fig. 25A**), IL-17 (**Fig. 25B**), and CD25 (**Fig. 25C**) were upregulated when T<sub>MBP-GFP</sub> cells were challenged *in vitro* with their cognate antigen MBP. OVA served as the control antigen. For IL-17 and CD25, no significant difference in the expression of the pro-inflammatory cytokines could be detected between the teriflunomide- and vehicle-treated animals. In the case of IFN $\gamma$  a significantly lower expression was detected in the teriflunomide-treated animals.

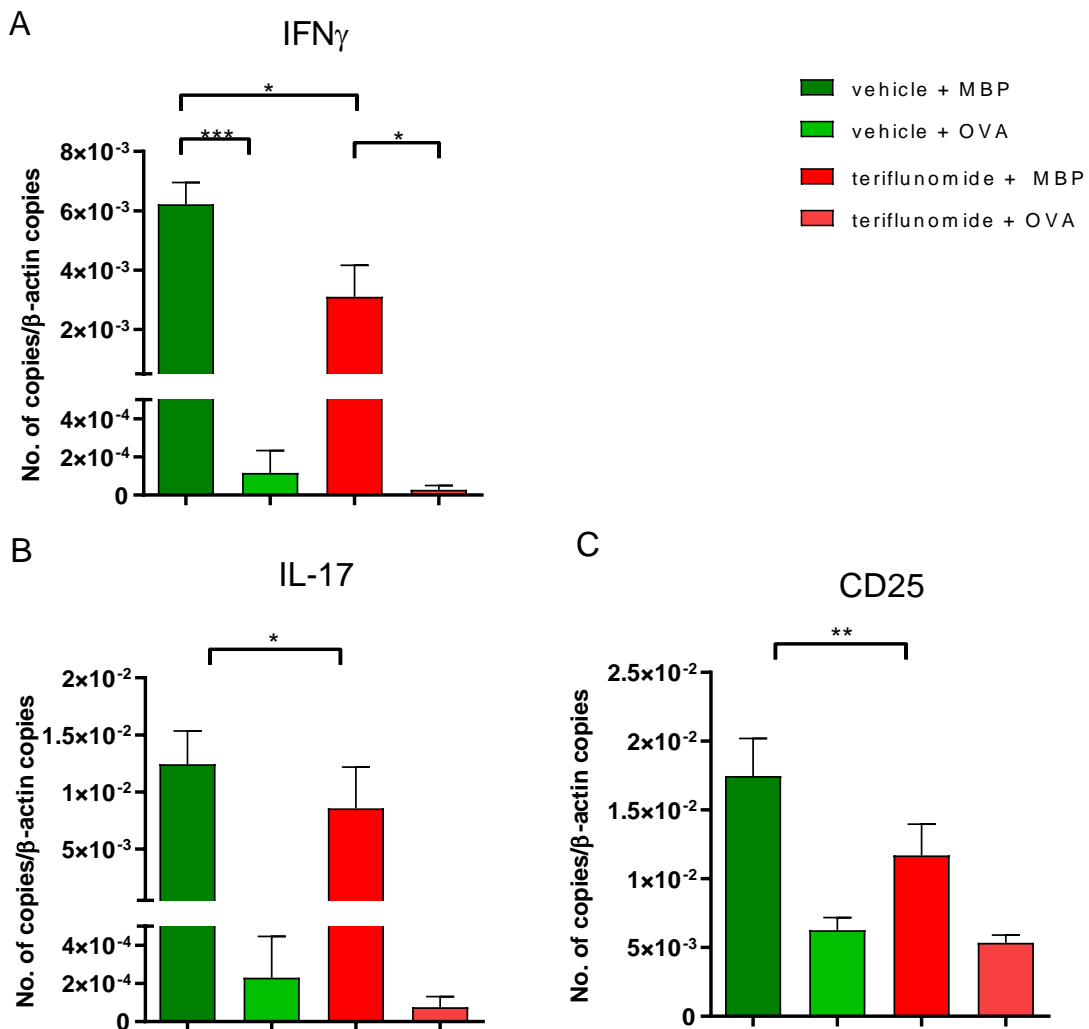


**Figure 25** Expression levels of inflammatory cytokines in T<sub>MBP-GFP</sub> cells extracted from vehicle- or teriflunomide-treated animals on day 2 after antigen encounter

Results of quantitative PCR for IFN $\gamma$ , IL-17, and CD25 at day 2 after challenge with either MBP or OVA. The animals were either treated with teriflunomide 3mg/kg/d (red) or received the vehicle (green); T<sub>MBP-GFP</sub> cells were then isolated from mediastinal LNs and cultured as illustrated in Fig. 14. The bars show the relative copy numbers compared to  $\beta$ -actin as the housekeeping gene. The mean + s.e.m. of four independent experiments are presented (n=4). The statistical significance was tested by 1-way ANOVA and multiple comparison by Turkey's HSD. \*p<0.05, \*\*p<0.01 \*\*\*p<0.001.

### 3.5 Effect of teriflunomide on the clinical phase in the EAE model in Lewis rats

The next question to be answered was whether teriflunomide affects the diseases course when administered in a therapeutic way at the start of the disease, i.e. between day 3 and 3.5 when animals started to lose body weight.

Upon transfer, the vehicle-treated animals started to lose body weight at day 3 and developed a paralytic disease that peaked on days 5 to 6 (**Fig. 26**). As seen before (**Fig. 15**), the prophylactic treatment with teriflunomide completely prevented clinical symptoms (**Fig. 26**). On the contrary, in animals that were treated in a therapeutic regimen (3 mg/kg/d) starting on day 3, disease onset and the peak of the disease were identical to those observed in the vehicle group. The disease duration of therapeutically treated animals, however, was slightly shortened compared to that of the vehicle-treated animals (**Fig. 26**).

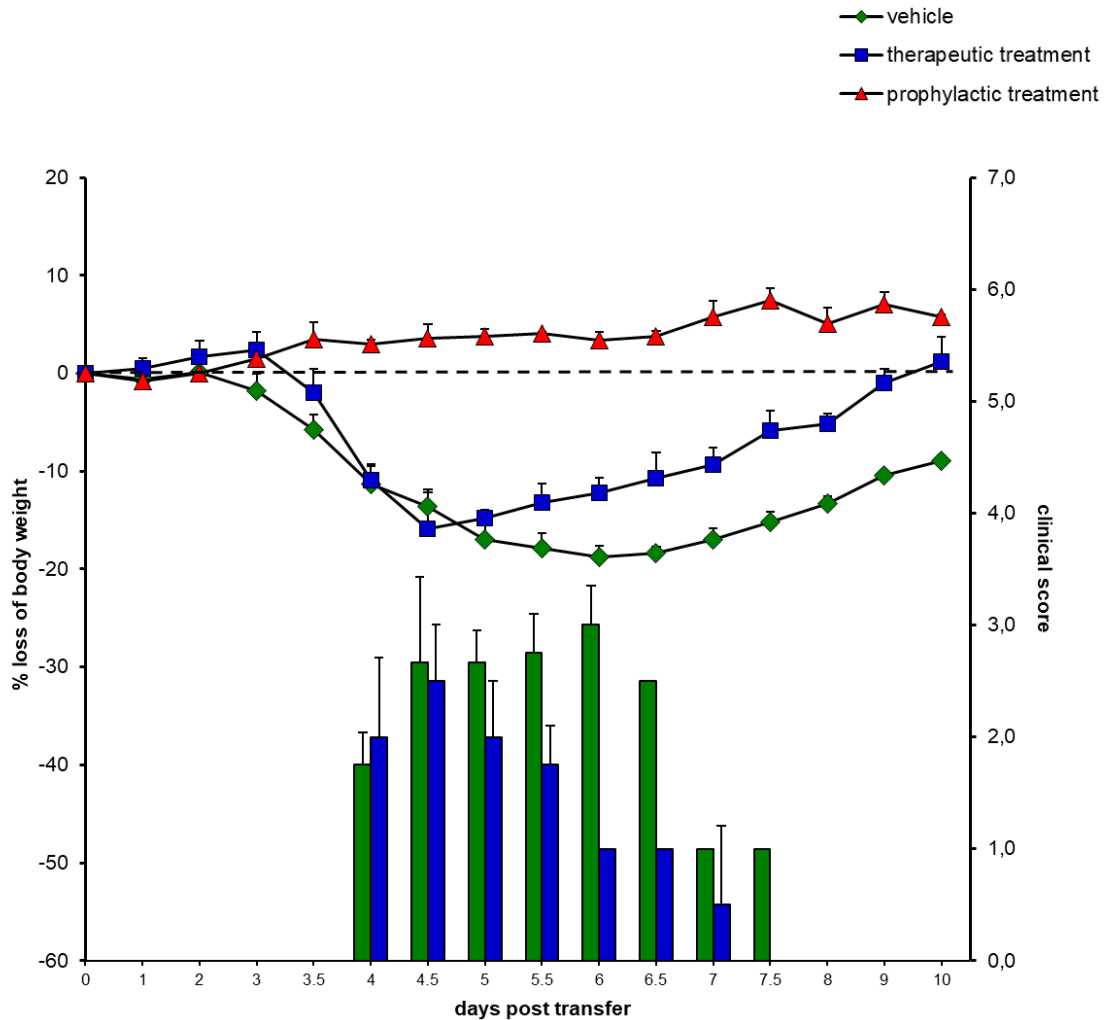


**Figure 26** Clinical effect of teriflunomide administered either as therapeutic or prophylactic treatment during atEAE

Activated  $T_{MBP-GFP}$  cells were i.v. injected into animals, which were treated with 3 different regimens: (1) vehicle treatment (green); (2) teriflunomide treatment at a dose of 3 mg/kg/d starting on day 0 (prophylactic treatment, red); and (3) teriflunomide treatment at a dose of 3 mg/kg/d starting on day 3 (therapeutic treatment, blue). The clinical data of one experiment are depicted. Mean + S.D. For each data point  $n \geq 2$ .

The infiltration kinetic of  $T_{MBP-GFP}$  cells between the vehicle group, therapeutic group, and prophylactic group was further investigated by flow cytometry.

In line with this study's clinical data, a reduced number of  $T_{MBP-GFP}$  cells could be measured in the s.c. parenchyma, s.c. meninges, and blood of prophylactically treated animals (**Fig. 27**).

Between the vehicle-treated and the therapeutically treated group, no significant differences could be observed. In contrast to the vehicle-treated group, the number of  $T_{\text{MBP-GFP}}$  cells in s.c. parenchyma and blood was slightly decreased in therapeutically treated animals. Compared to vehicle-treated animals, the number of  $T_{\text{MBP-GFP}}$  cells was slightly elevated in the s.c. meninges of therapeutically treated animals (Fig. 27).

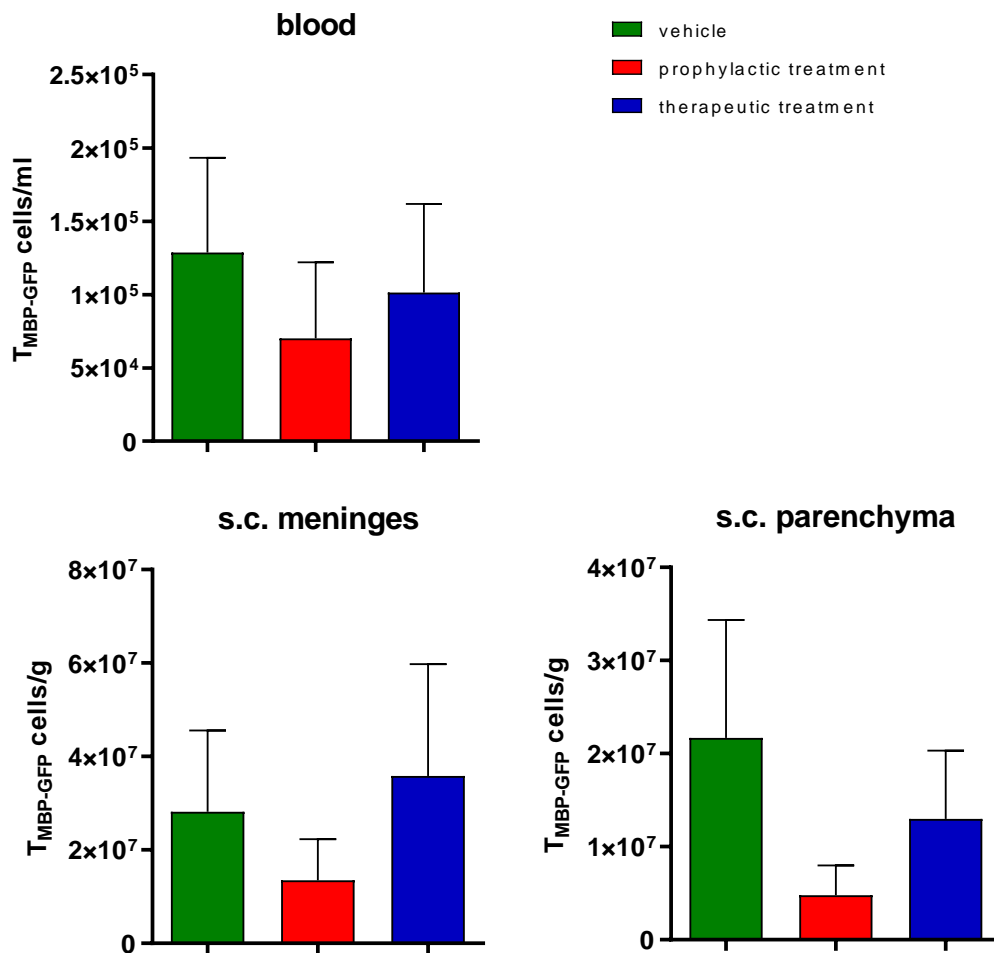


**Figure 27** Number of  $T_{\text{MBP-GFP}}$  cells in the s.c. parenchyma, s.c. meninges, and blood under vehicle treatment, prophylactic treatment, and therapeutic treatment at day 4 p.t.

Numbers of  $T_{\text{MBP-GFP}}$  cells quantified by flow cytometry in the indicated tissues at day 4 p.t. Three different teriflunomide regimens were performed: prophylactic (red), therapeutic (blue), and vehicle treatment (green). The results of three independent experiments are shown. Mean + s.e.m. (n=5)

The next step was to investigate whether teriflunomide influences the expression of pro-inflammatory cytokines in either total s.c. tissue or in  $T_{\text{MBP-GFP}}$  cells sorted from s.c. parenchyma, s.c. meninges, and blood (Fig. 28 and 29) on day 4 p.t.

In  $T_{\text{MBP-GFP}}$  cells sorted from s.c. parenchyma of both groups, a similar level of cytokine expression could be observed as analyzed by quantitative PCR.  $\text{IFN}\gamma$  as well as IL-17 were expressed at the same level in vehicle-treated and therapeutically treated animals

(**Fig. 28A**). The  $T_{\text{MBP-GFP}}$  cells of the therapeutically treated animals showed a slightly higher expression of  $\text{IFN}\gamma$  and IL-17 in the blood (**Fig. 28B**).

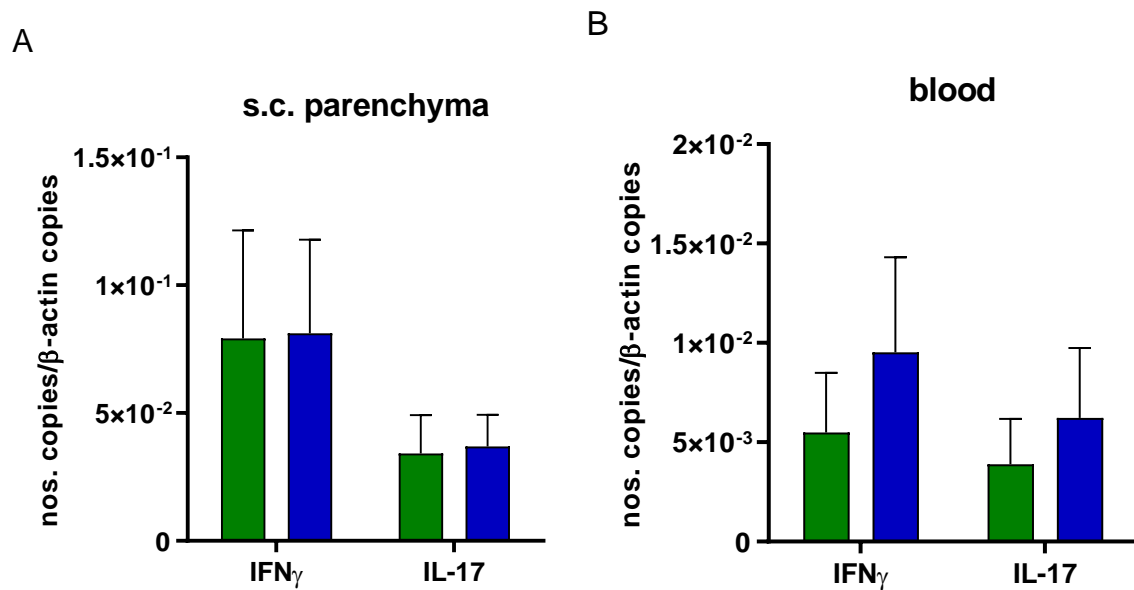


**Figure 28** Quantitative RNA analyses of pro-inflammatory cytokines in  $T_{\text{MBP-GFP}}$  cells sorted from s.c. parenchyma and blood from either vehicle-treated or therapeutically treated animals on day 4 p.t.

The  $T_{\text{MBP-GFP}}$  cells were sorted from the indicated organs at day 4 p.t. and analyzed for the expression level of  $\text{IFN}\gamma$  and IL-17 by qPCR. The animals were either vehicle-treated or treated with 3–7 mg/kg/d teriflunomide starting at day 3 p.t. Shown are the relative copy numbers compared to  $\beta$ -actin as the housekeeping gene. Mean + s.e.m. of three independent experiments with  $n \geq 4$ .

In accordance with expression levels of cytokines in sorted cells (**Fig. 28**) the expression of  $\text{IFN}\gamma$  and IL-17 in total tissue of s.c. parenchyma of the vehicle-treated and the therapeutically treated group did not differ. Again, in the s.c. meninges a lower level of

cytokines could be detected in the vehicle-treated group compared to the therapeutic treatment (Fig. 29).

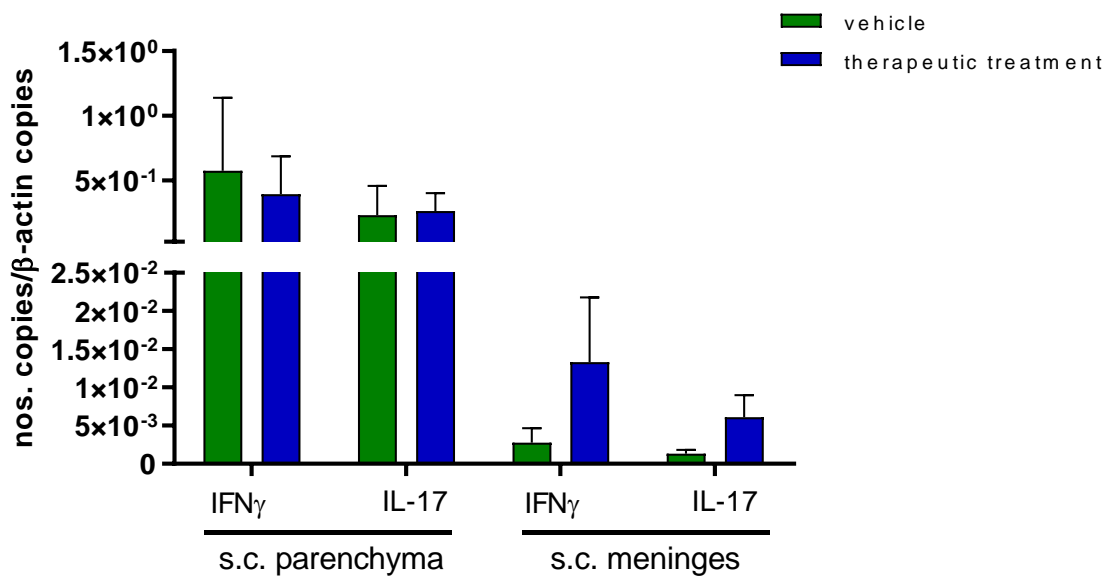


**Figure 29** Quantitative RNA analyses of pro-inflammatory cytokines in the total tissue of s.c. parenchyma and meninges on day 4 p.t.

Spinal cords were explanted from Lewis rats on day 4 post transfer. The vehicle-treated group (green) received only the vehicle. The therapeutic treatment (blue) started on day 3 with 3–7 mg/kg/d. The s.c. parenchyma showed similar levels of pro-inflammatory cytokines in both groups. In the s.c. meninges of the therapeutically treated animals, higher levels of both cytokines were expressed. Shown are relative copy numbers compared to  $\beta$ -actin as the housekeeping gene. Mean + s.e.m. of at least 2 different experiments with  $n=3$ .



## 4 Discussion

Teriflunomide, one of the new oral disease-modifying agents, was introduced for the treatment of multiple sclerosis in the European Union in 2013.

So far, the effect of teriflunomide has been mainly studied *in vitro* or in active immunization EAE in animal models of MS. Furthermore, most of these studies were conducted with leflunomide, the precursor of teriflunomide. The data of the present work displays the effect of teriflunomide in adoptive transfer EAE in Lewis rats both *in vitro* and *ex vivo*, particularly focusing on the effect of the drug on the antigen-specific effector T cell population.

### 4.1 Effect of teriflunomide on T<sub>MBP-GFP</sub> cells *in vitro*

Due to the T cells' main role in the pathogenesis of MS, much attention has been focused on identifying drugs that are able to selectively or at least primarily interfere with T cell function (see 1.5). One of these drugs is teriflunomide. Teriflunomide blocks T cell proliferation by inhibiting DHODH, a key enzyme of the pyrimidine metabolism (see 1.5.2). This pathway is predominantly active in strongly proliferating cells because resting lymphocytes can supply their pyrimidine pool from the salvage pathway which is DHODH-independent. Besides the antiproliferative effect, several other effects of teriflunomide have been investigated *in vitro*, e.g. the inhibition of Jak1 and Jak3 tyrosine kinase activity. To inhibit phosphorylation of Jak1 and Jak3, two major janus tyrosine kinases downstream of cytokine receptors, an IC<sub>50</sub> of 50  $\mu$ M teriflunomide was necessary. In comparison, an IC<sub>50</sub> of 2  $\mu$ M teriflunomide is required for inhibition of proliferation, as tested *in vitro* in a murine cytotoxic T cell line (CTLL-4) (Elder et al. 1997). Therefore, the antiproliferative effect through inhibition of DHODH likely takes precedence over other effects (Breedveld and Dayer 2000; Claussen and Korn 2012).

In this study, the drug strongly reduced proliferation of T cells *in vitro* in a dose-dependent manner, starting from a concentration of 1  $\mu$ M up to a concentration of 100  $\mu$ M, at which nearly no proliferation could be detected (**Fig. 11 and 12**). In several studies, the abrogation of proliferation by teriflunomide could be overcome by adding exogenous uridine *in vitro* (Zielinski et al. 1995; Williamson et al. 1995; Silva et al. 1996; Korn et al. 2004). This effect was shown in either murine T and B cell lines (Zielinski et al. 1995), mouse spleen cells (Williamson et al. 1995), rat MBP-specific T cells (Korn et al. 2004), and peripheral blood mononuclear cells (Li et al. 2013). In line with the

literature, this effect could be reproduced using our T<sub>MBP-GFP</sub> cell line. The antiproliferative effect could be overcome for teriflunomide concentrations of up to 50  $\mu$ M by supplying exogenous uridine *in vitro* (**Fig. 11 and 12**). The concentration at which the antiproliferative effect cannot be reversed *in vitro* is comparable to data acquired in previous studies (Elder et al. 1997; Rückemann et al. 1998).

Two conclusions can be drawn from these experiments: firstly, the block of pyrimidine synthesis is presumably responsible for the antiproliferative effect *in vitro*, and secondly, the concentration of teriflunomide needed for an effective blockage of our cell line is comparable to that used in previous studies.

Furthermore, it has been described in previous studies that a significant decrease of the IFN- $\gamma$  production occurs in rat MBP specific T cells when treated with teriflunomide (Korn et al. 2004). The activation of T cells takes place after recognition of the specific antigen (in this study MBP) via the surface-expressed T cell receptor and co-stimulatory molecules. This is followed by a downstream signaling cascade leading to cytokine production (e.g. IL-17 and IFN $\gamma$ ) and expression of cell surface molecules (e.g. CD25 and CD134) (Brownlie and Zamoyska 2013; Lodygin et al. 2013). After re-stimulation of T cells with specific antigen *in vitro*, no difference in cytokine secretion upon treatment with teriflunomide could be found (**Fig. 14**). Moreover, surface markers for activation, CD25 and CD134, were not altered by the treatment with teriflunomide (see 3.2 and **Fig. 13**).

All in all, the signaling cascade leading to expression of CD134 and CD25 as well as the cytokine production of IFN $\gamma$  and IL-17 seems not to be affected *in vitro*. Therefore, this study suggests that the effect of teriflunomide on changes in lymphocyte proliferation is rather a consequence of reduced proliferation than impaired activation. Studies have shown *in vitro* for human lymphocytes (Li et al. 2013) and rat MBP-specific T cells (Ringheim et al. 2013) that teriflunomide affects proliferation with little impact on T cell function.

#### 4.2 *In vivo* effect of teriflunomide on transfer EAE

Next, the effect of teriflunomide was assessed *in vivo*. To our knowledge, this is the first study addressing the effects of teriflunomide on autoreactive T cells in an atEAE model.

In order to directly investigate the effect of the drug on MBP specific T cells, a transfer model of EAE in Lewis rats was used. The EAE was induced by i.v. injection of activated MBP-specific T cells.

Usually, drugs are administered at the minimal effective dose to avoid/minimize side effects. At high doses, teriflunomide can induce off-target effects independent from the DHODH inhibition. The drug was titrated in order to identify the most suitable dose in rats. Five different doses were tested: 0.5, 1, 3, 5, and 10 mg/kg/d teriflunomide. The minimal effective dose in this study was 3 mg/kg/d teriflunomide (**Table 5, Fig. 15**). The disease course could not be altered at lower doses (0.5 and 1 mg/kg/d). A dose-dependent reduction in loss of body weight and in clinical score could be observed. At 5 and 10 mg/kg/d, no clinical symptoms were observed and no transferred  $T_{\text{MBP-GFP}}$  cells were found in the tissues analyzed. The dose-dependent effect on the clinical symptoms coincides with the dose-dependent linear increase of the teriflunomide plasma level ( $C_{\text{max}}$ ). Steady state seems to be reached in rats after supplying the drug for approximately three months, which lies outside of the trial period of this study (data supplied by Genzyme EU B.V., 2015).

The chosen dose of 3 mg/kg/d is in accordance with the dose used in previous studies in DA rats (Merrill et al. 2009). In active EAN in Lewis rats, leflunomide was used at a concentration of 1.5–20 mg/kg/d (Korn et al. 2001), and in atEAE leflunomide was used at a concentration of 20 mg/kg/d (Korn et al. 2004). Considering that 86 % of leflunomide is converted to its active metabolite teriflunomide (Merrill et al. 2009), this dose roughly equals to 17 mg/kg/d teriflunomide (Korn et al. 2004; Merrill et al. 2009), which is much higher than the dose used in this study. These differences might be due to different pathogenicity or numbers of cells transferred into the rats.

At the chosen dose of 3 mg/kg/d teriflunomide, the infiltration of  $T_{\text{MBP-GFP}}$  cells into the CNS (**Fig. 16**) and the resulting inflammation were clearly reduced (**Fig. 17**). These effects could also be shown in previous studies in an active EAE model in DA rats (Merrill et al. 2009; Ringheim et al. 2013). In addition, a lower demyelination and axonal loss was observed (Merrill et al. 2009).

Due to the known effect of teriflunomide on cell proliferation, the number of T cells in different organs, namely, the lung, mediastinal lymph nodes, spleen, blood, s.c. meninges, and s.c. parenchyma, was assessed during different phases of EAE (**Fig. 18**). Both flow cytometric (see 3.4.2) and histological data (see 3.2.3) clearly showed a strong reduction

of about 80 % T<sub>MBP-GFP</sub> cells in all investigated compartments and at all investigated time points compared to vehicle treatment.

In attempt to overcome the block of proliferation, exogenous uridine was substituted. However, in contrast to the *in vitro* results, quantification of T<sub>MBP-GFP</sub> cell number showed no significant increase in the indicated organs (**Fig. 18**). Also, only a slight effect on the disease duration, the maximum score, and disease severity could be seen (**Table 5**). The same lack of effect upon uridine administration was observed in the paper by Korn et al. (2004) for leflunomide treatment. Furthermore, application of uridine has been established for other treatment regimens, e.g. for tumor treatment with 5-fluorouracil (5-FU), a classical antimetabolite. An additional treatment with uridine raised the sensitivity of the tumor for 5-FU (Martin et al. 1982; Klubes and Cerna 1983) in mice, and led to a rescue of the side effects caused by 5-FU in humans. It proved efficient to administer uridine either i.v., i.p., or orally (van Groeningen et al. 1986; van Groeningen et al. 1993). All these results indicate that the treatment and metabolism of externally supplied uridine per se is working.

It is possible that uridine can overcome only part of the teriflunomide effect *in vivo* explaining the partial effect on EAE. Results can be interpreted in light of studies showing that the effect of leflunomide on B cell and Th cell activity could be reversed by uridine but not the suppression of cytotoxic effector T cells in a mouse model for autoimmune diabetes (Pinschewer et al. 2001). Further studies need to be carried out to investigate the discrepancy between the *in vitro* and *in vivo* effect of uridine on treatment with teriflunomide.

#### 4.3 Impairment of T cell migration

Considering the low numbers of T<sub>MBP-GFP</sub> cells infiltrating the s.c. meninges and s.c. parenchyma, the effect of teriflunomide on the distribution pattern of autoreactive T cells during their migratory phase in the periphery and in their target organ (CNS) was investigated.

Interestingly, teriflunomide seemed to change the homing pattern of T cells during EAE. In vehicle-treated animals the transferred T cells mainly homed into the lung at day 3 after injection, first distributing around the alveoli and later localizing around the bronchial structures. After that, they emigrate out of the lung, pass through the spleen, and arrive at the meningeal blood vessels, from where they extravasate into in the CNS

parenchyma (**Fig. 18**). In the teriflunomide-treated animals the distribution of cells inside the lung was not affected but the egression of the T cells from the lung seemed impaired: the majority of cells was trapped in the lung (**Fig. 19, 20**).

To further analyze the diminished T cell egression from the lung, known factors facilitating this process were investigated. In the preclinical phase of atEAE it was shown that  $T_{\text{MBP-GFP}}$  cells change their expression profile in the lung, upregulating adhesion molecules, chemokine receptors, as well as S1P1. S1P1 is essential for egression from peripheral lymphoid organs and the lung (Odoardi et al. 2012). During proliferation it becomes downregulated, trapping cells in lymphatic tissue. After proliferation, T cells upregulate S1P1 (Rosen and Goetzl 2005; Cyster and Schwab 2012). For this, T cells must enter the cell cycle to induce the expression of molecules involved in T cell egression (Pham, Trung H M et al. 2008). It is therefore possible that blocking the proliferation with teriflunomide in the G1 phase of the cell cycle (Tanasescu et al. 2013; Breedveld and Dayer 2000) can also prevent T cells from acquiring the necessary phenotype to leave the lung tissue.

The expression of chemokine receptors and S1P1 was evaluated in T cells isolated from lung of teriflunomide-treated and vehicle-treated animals. Interestingly, the effector T cells isolated from the lung of teriflunomide-treated animals showed a lower expression of S1P1 compared to the vehicle-treated animals. No differences in the expression of chemokine receptors CCR7 and CXCR3 were observed. Moreover, the transcription factor KLF2, a master regulator of S1P1 expression (Carlson et al. 2006), which is strictly linked to the regulation of the cell cycle, was downregulated (**Fig. 22**) in T cells treated with teriflunomide.

Whether teriflunomide leads to apoptosis was also tested since this could also contribute to the lower numbers of T cells observed after treatment. Higher levels of apoptosis could not be observed compared to vehicle-treated animals (**Fig. 21**). Studies that showed that teriflunomide mediates cytostatic but not cytotoxic effects (Rückemann et al. 1998; Korn et al. 2004) and can even prevent apoptosis (Korn et al. 2004) support the findings of the present study. The functionality of T cells transferred could be confirmed by extracting  $T_{\text{MBP-GFP}}$  cells from lung draining lymph nodes. Upon stimulation with the cognate antigen (MBP), cells were still able to proliferate (**Fig. 23**), showing a comparable level in activation (**Fig. 24**). Contrary to *in vitro*-stimulated  $T_{\text{MBP-GFP}}$  cells treated with teriflunomide, cells isolated from teriflunomide-treated animals showed a significantly

lower production of IFN $\gamma$  compared to cells isolated from vehicle-treated animals; in contrast, there was no difference in IL17 production (**Fig. 25**) between the two groups. However, after transfer in naive rats, these T cells were able to provoke mild EAE (flaccid tail) (data not shown). Similar studies support the findings of this study: T cells extracted from animals treated with HWA 486 (leflunomide) are still completely functional (Bartlett 1986; Merrill et al. 2009; Korn et al. 2001), as highlighted by the fact that abrogation of treatment with leflunomide still leads to development of an EAN (Korn et al. 2001).

All in all, the data indicate that teriflunomide, when administered in a prophylactic way, induces a block of MBP-specific T cell proliferation without affecting T cell activation. However, it also impairs their migratory capacity.

#### 4.4 Teriflunomide in therapeutic treatment

It has been shown that teriflunomide is very effective in preventive treatment of EAE (Merrill et al. 2009; Ringheim et al. 2013). In this study, teriflunomide was very effective in preventing disease in atEAE when administered before clinical onset (**Table 5, Fig. 15**). When administered after onset of disease in a therapeutic setting, the clinical effect was limited (**Fig. 26**).

Therapeutic treatment with teriflunomide started shortly after the appearance of the first clinical symptoms (weight loss), which coincides with the entry of T cells into the CNS (Odoardi et al. 2012). Under a therapeutic regime, onset and peak of the disease were identical to those in the vehicle-treated group. No significant differences in the invasion of T<sub>MBP-GFP</sub> cells into s.c. meninges and s.c. parenchyma could be detected at the early stage of the disease (**Fig. 27**). However, the disease duration was slightly shortened, and recovery seemed to be faster. On the contrary, when animals were treated prophylactically, EAE could be completely prevented (**Fig. 15 and 26**). Furthermore, there was no significant difference in the severity of inflammation in the CNS when treated therapeutically (**Fig. 29**), and no influence on the production of proinflammatory cytokines (**Fig. 28**). However, more data needs to be acquired in a greater cohort of animals to obtain conclusive results.

In this study, the discrepancy between preventive and therapeutic treatment in the reduction of symptoms can be interpreted in light of the peculiarity of the CNS milieu. As described above, the major mechanism of teriflunomide is the block of proliferation.

However, in atEAE, after invading the CNS, almost no T cells proliferate indicating that reactivation of T cells in the CNS is not sufficient to trigger proliferation (Lodygin et al. 2013). Nevertheless, it leads to production of pro-inflammatory cytokines. Without proliferation, there will be no impact of teriflunomide on T cells, therefore explaining the lack of a clinical effect.

Previously, it has been shown that in the active EAE/EAN models, leflunomide and teriflunomide both influence the clinical course when administered in a therapeutic manner. An inhibition in the maximal clinical score was shown as well as a faster recovery of treated animals (Korn et al. 2001; Merrill et al. 2009; Ringheim et al. 2013). Because of differences in the set-up, the comparability to this study is limited. The previous studies all worked with an active EAE/EAN model, in which animals are immunized, whereas the study at hand used an atEAE model. Furthermore, Merrill et al. (2009) and Ringheim et al. (2013) both worked with Dark Agouti rats, a model that resembles a RRMS. Moreover, for this clinical study, a dose of 3 mg/kg/d was used, whereas in the study by Ringheim et al. (2009) animals were treated with 10 mg/kg/d teriflunomide and in the study by Korn et al. (2001) with 20 mg/kg/d leflunomide (approx. 17 mg/kg/d teriflunomide see 4.2.). Only Merrill et al. (2009) showed a significant reduction of the median maximal disease score and median cumulative disease score under a treatment with 10 mg/kg/d as well as 3 mg/kg/d teriflunomide (Korn et al. 2001; Merrill et al. 2009; Ringheim et al. 2013).

However, also in this study, a slight tendency of a faster recovery could be seen in the group of therapeutically treated animals (**Fig. 26**). Previous studies showed an impact of teriflunomide on bystander cells supporting the impact of teriflunomide on the late phase of atEAE, e.g. recruitment of macrophages (Gold et al. 2006), migration of neutrophils and macrophages (Cutolo et al. 2003; Kraan et al. 2000; Claussen and Korn 2012), and cytokine production of macrophages and microglial cells (Korn et al. 2004; Claussen and Korn 2012). It was shown that in the development of active EAE, teriflunomide seems to influence the number of recruited macrophages/microglia and neutrophils in the CNS as well as in the periphery (Ringheim et al. 2013).

## 5 Summary and conclusion

In this study the effect of teriflunomide, a recently approved drug for MS, on antigen-specific CD4<sup>+</sup> T cells was investigated *in vitro* and *in vivo* using a classical model of MS, namely the transfer EAE in Lewis rats. Moreover, the time of action of the drug was addressed in the same model.

Regarding the *in vitro* effect, according to published literature our data could confirm that teriflunomide has a strong anti-proliferating effect on antigen-specific T cells. Interestingly, the activation profile of the T cells remained unaffected. These data were also confirmed *in vivo*. Indeed, in transfer EAE in Lewis rats, myelin-reactive T cells were strongly impaired in their proliferation. However, the few T cells able to reach the CNS switched to an activatory profile with increased expression of pro-inflammatory chemokines. Notably, we observed that *in vivo*, beside the well-known anti-proliferating effect, teriflunomide impairs T cell migration capacity prejudicing the egression of T cells from the lung. The tendency of a diminished expression of KLF2 and S1P1 in myelin-reactive T cells isolated from treated animals suggest that these genes may represent potential key factors for the observed impaired T cell migration.

Regarding the time of action, in our EAE model, teriflunomide was very effective in preventing EAE if it was given in a preventive treatment manner. If teriflunomide was given as a therapeutic regime, only modest clinical effects not associated with changes in T cell infiltration and activation could be observed. The discrepancy of the results can be interpreted in light of the peculiarity of the CNS milieu where the infiltrating T cells undergo activation but not proliferation. This failure to proliferate will impact the major mechanism of action of teriflunomide, i.e. the inhibition of the enzyme DHODH, which could explain the observed lack of clinical effect in the therapeutic treatment.

The understanding the MOA of drugs for multiple sclerosis is focus of current scientific research. Knowledge on this effect might empower medicine in the future to develop personalized therapy specifically framed for individual patients depending on their pathogenesis process. In this context, the present study indicates further potential MOAs of teriflunomide, but future research should focus on and further investigate this potential in order to increase the current scientific knowledge.



## 6 Abstract

Multiple sclerosis (MS), the most common autoimmune disorder of the CNS, is characterized by the infiltration of autoreactive inflammatory cells. Nowadays, more and more immune modulating drugs are entering the European market, one of them being teriflunomide. Teriflunomide (A77 1726) is the active metabolite of leflunomide, an anti-inflammatory drug that has been used for a long time in the treatment of rheumatoid arthritis and psoriasis. In MS, teriflunomide has been shown to significantly reduce the relapse rate in clinical studies. The drug is known to be a potent inhibitor of the enzyme DHODH, a mitochondrial enzyme critical for *de novo* pyrimidine synthesis. The *de novo* pyrimidine synthesis pathway is essential for the expansion of cells with high-proliferating capacity, and it has been proposed that teriflunomide's main mechanism of action is an anti-proliferative effect on rapidly dividing cells such as lymphocytes. However, other mechanisms like the inhibition of tyrosine kinases can also play a role.

Therefore, in the present study, we aim to investigate the effect of teriflunomide on CD4<sup>+</sup> MBP-reactive T cells both *in vitro* and *in vivo* using the experimental autoimmune encephalomyelitis (EAE) model in Lewis rats. Moreover, we aim to understand in which phase of the disease the drug exercises its therapeutic action.

Our *in vivo* and *in vitro* data confirmed that the block of proliferation of antigen-specific T cells is the main mechanism of teriflunomide. In addition, this study revealed that teriflunomide interferes with antigen-specific T cell migration during the pre-clinical phase, impairing T cell egression from the lung. At the molecular level, the reduced egression was associated with a differential expression of S1P1 and KLF2, which are important genes in mediating leukocyte egression from lymphoid and non-lymphoid organs.

Furthermore, regarding the time of action, the data indicate that teriflunomide is very effective in preventing disease when administered before clinical onset of EAE, but less effective if administered after onset.

In summary, the data reveal an unexpected mechanism of action of teriflunomide on T cell migration beside the well-known anti-proliferative effect. Additionally, the data reinforce the use of teriflunomide for prophylactic treatment.

## 7 References

- Aharoni R, Teitelbaum D, Leitner O, Meshorer A, Sela M, Arnon R (2000): Specific Th2 cells accumulate in the central nervous system of mice protected against experimental autoimmune encephalomyelitis by copolymer 1. *Proc Natl Acad Sci U S A* 97, 11472–11477
- Ascherio A, Munger KL, White R, Köchert K, Simon KC, Polman CH, Freedman MS, Hartung HP, Miller DH, Montalbán X (2014): Vitamin D as an early predictor of multiple sclerosis activity and progression. *JAMA Neurol* 71, 306–314
- Atlas of MS 2013: Mapping multiple sclerosis around the world. Multiple Sclerosis International Federation. [<https://www.msif.org/about-us/who-we-are-and-what-we-do/advocacy/atlas/>] Accessed on: 01.12.2016
- Babbe H, Roers A, Waisman A, Lassmann H, Goebels N, Hohlfeld R, Friese M, Schröder R, Deckert M, Schmidt S (2000): Clonal expansions of Cd8 + T cells dominate the T cell infiltrate in active multiple sclerosis lesions as shown by micromanipulation and single cell polymerase chain reaction. *J Exp Med* 192, 393–404
- Bar-Or A (2014): Teriflunomide (Aubagio®) for the treatment of multiple sclerosis. Special Issue: Progress in MS pathophysiology and treatment. *Exp Neurol* 262, 57–65
- Bar-Or A, Pachner A, Menguy-Vacheron F, Kaplan J, Wiendl H (2014): Teriflunomide and its mechanism of action in multiple sclerosis. *Drugs* 74, 659–674
- Bartholomäus I, Kawakami N, Odoardi F, Schläger C, Miljkovic D, Ellwart JW, Klinkert WE, Flügel-Koch C, Issekutz TB, Wekerle H (2009): Effector T cell interactions with meningeal vascular structures in nascent autoimmune CNS lesions. *Nature* 462, 94–98
- Bartlett RR (1986): Immunopharmacological profile of HWA 486, a novel isoxazol derivative--II. In vivo immunomodulating effects differ from those of cyclophosphamide, prednisolone, or cyclosporin A. *Int J Immunopharmacol* 8, 199–204
- Beecham AH, Patsopoulos NA, Xifara DK, Davis MF, Kempainen A, Cotsapas C, Shah TS, Spencer C, Booth D, Goris A (2013): Analysis of immune-related loci identifies 48 new susceptibility variants for multiple sclerosis. *Nat Genet* 45, 1353–1360

- Ben-Nun A, Wekerle H, Cohen IR (1981): The rapid isolation of clonable antigen-specific T lymphocyte lines capable of mediating autoimmune encephalomyelitis. *Eur J Immunol* 11, 195–199
- Bielekova B, Sung MH, Kadom N, Simon R, McFarland H, Martin R (2004): Expansion and functional relevance of high-avidity myelin-specific CD4+ T cells in multiple sclerosis. *J Immunol* 172, 3893–3904
- Bjartmar C, Kidd G, Mörk S, Rudick R, Trapp BD (2000): Neurological disability correlates with spinal cord axonal loss and reduced N-acetyl aspartate in chronic multiple sclerosis patients. *Ann Neurol* 48, 893–901
- Bogie JFJ, Stinissen P, Hendriks JJA (2014): Macrophage subsets and microglia in multiple sclerosis. *Acta Neuropathol* 128, 191–213
- Booss J, Esiri MM, Tourtellotte WW, Mason DY (1983): Immunohistological analysis of T lymphocyte subsets in the central nervous system in chronic progressive multiple sclerosis. *J Neurol Sci* 62, 219–232
- Boyd AS (2012): Leflunomide in dermatology. *J Am Acad Dermatol* 66, 673–679
- Breedveld FC, Dayer JM (2000): Leflunomide: mode of action in the treatment of rheumatoid arthritis. *Ann Rheum Dis* 59, 841–849
- Brinkmann V (2009): FTY720 (fingolimod) in multiple sclerosis: therapeutic effects in the immune and the central nervous system. *Br J Pharmacol* 158, 1173–1182
- Brownlie RJ, Zamojska R (2013): T cell receptor signalling networks: branched, diversified and bounded. *Nat Rev Immunol* 13, 257–269
- Bruneau JM, Yea CM, Spinella-Jaegle S, Fudali C, Woodward K, Robson PA, Sautès C, Westwood R, Kuo EA, Williamson RA (1998): Purification of human dihydro-orotate dehydrogenase and its inhibition by A77 1726, the active metabolite of leflunomide. *Biochem J* 336, 299–303
- Cao W, Kao P, Chao AC, Gardner P, Ng J, Morris RE (1995): Mechanism of the antiproliferative action of leflunomide. A77 1726, the active metabolite of leflunomide, does not block T-cell receptor-mediated signal transduction but its antiproliferative effects are antagonized by pyrimidine nucleosides. *J Heart Lung Transplant* 14, 1016–1030

- Carlson CM, Endrizzi BT, Wu J, Ding X, Weinreich MA, Walsh ER, Wani MA, Lingrel JB, Hogquist KA, Jameson SC (2006): Kruppel-like factor 2 regulates thymocyte and T-cell migration. *Nature* 442, 299–302
- Chen H, Assmann JC, Krenz A, Rahman M, Grimm M, Karsten CM, Kohl J, Offermanns S, Wettschureck N, Schwaninger M (2014): Hydroxycarboxylic acid receptor 2 mediates dimethyl fumarate's protective effect in EAE. *J Clin Invest* 124, 2188–2192
- Chen JJ, Jones ME (1976): The cellular location of dihydroorotate dehydrogenase: Relation to de novo biosynthesis of pyrimidines. *Arch Biochem Biophys* 176, 82–90
- Cherwinski HM, Byars N, Ballaron SJ, Nakano GM, Young JM, Ransom JT (1995a): Leflunomide interferes with pyrimidine nucleotide biosynthesis. *Inflamm Res* 44, 317–322
- Cherwinski HM, McCarley D, Schatzman R, Devens B, Ransom JT (1995b): The immunosuppressant leflunomide inhibits lymphocyte progression through cell cycle by a novel mechanism. *J Pharmacol Exp Ther* 272, 460–468
- Cherwinski HM, Cohn RG, Cheung P, Webster DJ, Xu YZ, Caulfield JP, Young JM, Nakano G, Ransom JT (1995c): The immunosuppressant leflunomide inhibits lymphocyte proliferation by inhibiting pyrimidine biosynthesis. *J Pharmacol Exp Ther* 275, 1043–1049
- Chong AS, Rezai K, Gebel HM, Finnegan A, Foster P, Xu X, Williams JW (1996): Effects of leflunomide and other immunosuppressive agents on T cell proliferation in vitro. *Transplantation* 61, 140–145
- Claussen MC, Korn T (2012): Immune mechanisms of new therapeutic strategies in MS: teriflunomide. *Clin Immunol* 142, 49–56
- Compston A, Coles A (2002): Multiple sclerosis. *Lancet* 359, 1221–1231
- Compston A, Coles A (2008): Multiple sclerosis. *Lancet* 372, 1502–1517
- Confavreux C, O'Connor P, Comi G, Freedman MS, Miller AE, Olsson TP, Wolinsky JS, Bagulho T, Delhay JL, Dukovic D (2014): Oral teriflunomide for patients with relapsing multiple sclerosis (TOWER): A randomised, double-blind, placebo-controlled, phase 3 trial. *Lancet Neurol* 13, 247–256

- Cross AH, Cannella B, Brosnan CF, Raine CS (1990): Homing to central nervous system vasculature by antigen-specific lymphocytes. I. Localization of <sup>14</sup>C-labeled cells during acute, chronic, and relapsing experimental allergic encephalomyelitis. *Lab Invest* 63, 162–170
- Cross AH, Naismith RT (2014): Established and novel disease-modifying treatments in multiple sclerosis. *J Intern Med* 275, 350–363
- Cutolo M, Sulli A, Ghiorzo P, Craviotto C, Villagio B (2003): Anti-inflammatory effects of leflunomide on cultured synovial macrophages from patients with rheumatoid arthritis. *Ann Rheum Dis* 62, 297–302
- Cyster JG, Schwab SR (2012): Sphingosine-1-phosphate and lymphocyte egress from lymphoid organs. *Annu Rev Immunol* 30, 69–94
- Davis JP, Cain GA, Pitts WJ, Magolda RL, Copeland RA (1996): The immunosuppressive metabolite of leflunomide is a potent inhibitor of human dihydroorotate dehydrogenase. *Biochemistry* 35, 1270–1273
- DGN 2012: Leitlinie für Diagnose und Therapie der Multiplen Sklerose. S2e-Leitlinie der Deutschen Gesellschaft für Neurologie. Ergänzt am 12. April 2014 [<https://www.dgn.org/leitlinien/2333-ll-31-2012-diagnose-und-therapie-der-multiplen-sklerose>] Accessed on: 04.12.2018
- Dhib-Jalbut S, Marks S (2010): Interferon- $\beta$  mechanisms of action in multiple sclerosis. *Neurology* 74, S17-S24
- Duda PW, Schmied MC, Cook SL, Krieger JI, Hafler DA (2000): Glatiramer acetate (Copaxone) induces degenerate, Th2-polarized immune responses in patients with multiple sclerosis. *J Clin Invest* 105, 967–976
- Elder RT, Xu X, Williams JW, Gong H, Finnegan A, Chong AS (1997): The immunosuppressive metabolite of leflunomide, A77 1726, affects murine T cells through two biochemical mechanisms. *J Immunol* 159, 22–27
- Engelhardt B, Ransohoff RM (2005): The ins and outs of T-lymphocyte trafficking to the CNS: anatomical sites and molecular mechanisms. *Trends Immunol* 26, 485–495
- Engelhardt B, Kappos L (2008): Natalizumab: targeting alpha4-integrins in multiple sclerosis. *Neurodegener Dis* 5, 16–22

- Engelhardt B, Ransohoff RM (2012): Capture, crawl, cross: the T cell code to breach the blood-brain barriers. *Trends Immunol* 33, 579–589
- Eylar EH, Kniskern PJ, Jackson JJ (1974): Myelin basic proteins. *Methods Enzymol* 32, 323–341
- Farez MF, Fiol MP, Gaitan MI, Quintana FJ, Correale J (2015a): Sodium intake is associated with increased disease activity in multiple sclerosis. *J Neurol Neurosurg Psychiatry* 86, 26–31
- Farez MF, Mascanfroni ID, Mendez-Huergo SP, Yeste A, Murugaiyan G, Garo LP, Balbuena Aguirre ME, Patel B, Ysraelit MC, Zhu C (2015b): Melatonin contributes to the seasonality of multiple sclerosis relapses. *Cell* 162, 1338–1352
- Flügel A, Willem M, Berkowicz T, Wekerle H (1999): Gene transfer into CD4+ T lymphocytes: green fluorescent protein-engineered, encephalitogenic T cells illuminate brain autoimmune responses. *Nat Med* 5, 843–847
- Flügel A, Berkowicz T, Ritter T, Labeur M, Jenne DE, Li Z, Ellwart JW, Willem M, Lassmann H, Wekerle H (2001): Migratory activity and functional changes of green fluorescent effector cells before and during experimental autoimmune encephalomyelitis. *Immunity* 14, 547–560
- Freund J, McDermott K (1942): Sensitization to horse serum by means of adjuvants. *Exp Biol and Med* 4, 548–553
- Garg N, Smith TW (2015): An update on immunopathogenesis, diagnosis, and treatment of multiple sclerosis. *Brain Behav* 5, e00362
- GBD 2013 Mortality and Causes of Death Collaborators (2015): Global, regional, and national age–sex specific all-cause and cause-specific mortality for 240 causes of death, 1990–2013: A systematic analysis for the global burden of disease study 2013. *Lancet* 385, 117–171
- Goebels N (2000): Repertoire dynamics of autoreactive T cells in multiple sclerosis patients and healthy subjects: Epitope spreading versus clonal persistence. *Brain* 123, 508–518
- Gold R, Linington C, Lassmann H (2006): Understanding pathogenesis and therapy of multiple sclerosis via animal models: 70 years of merits and culprits in experimental autoimmune encephalomyelitis research. *Brain* 129, 1953–1971

- Gonsette RE (2012): Self-tolerance in multiple sclerosis. *Acta Neurol Belg* 112, 133–140
- Gourraud PA, Harbo HF, Hauser SL, Baranzini SE (2012): The genetics of multiple sclerosis: an up-to-date review. *Immunol Rev* 248, 87–103
- Greene S, Watanabe K, Braatz-Trulson J, Lou L (1995): Inhibition of dihydroorotate dehydrogenase by the immunosuppressive agent leflunomide. *Biochem Pharmacol* 50, 861–867
- He D, Zhang C, Zhao X, Zhang Y, Dai Q, Li Y, Chu L (2016): Teriflunomide for multiple sclerosis. *Cochrane Database Syst Rev* 3, CD009882
- Hedström AK, Olsson T, Alfredsson L (2015): The role of environment and lifestyle in determining the risk of multiple sclerosis. In: La Flamme AC, Orian JM (Eds.): *Emerging and evolving topics in multiple sclerosis pathogenesis and treatments (Current Topics in Behavioral Neurosciences)*. Springer, Cham 2015, 87-104
- Hemmer B, Cepok S, Nessler S, Sommer N (2002): Pathogenesis of multiple sclerosis: an update on immunology. *Curr Opin Neurol* 15, 227–231
- Hernán MA, Jick SS, Logroscino G, Olek MJ, Ascherio A, Jick H (2005): Cigarette smoking and the progression of multiple sclerosis. *Brain* 128, 1461–1465
- Hong J, Li N, Zhang X, Zheng B, Zhang JZ (2005): Induction of CD4+CD25+ regulatory T cells by copolymer-I through activation of transcription factor Foxp3. *Proc Natl Acad Sci U S A* 102, 6449–6454
- Hu Y, Turner MJ, Shields J, Gale MS, Hutto E, Roberts BL, Siders WM, Kaplan JM (2009): Investigation of the mechanism of action of alemtuzumab in a human CD52 transgenic mouse model. *Immunology* 128, 260–270
- Jones ME (1980): Pyrimidine nucleotide biosynthesis in animals: genes, enzymes, and regulation of UMP biosynthesis. *Annu Rev Biochem* 49, 253–279
- Kamm CP, Uitdehaag BM, Polman CH (2014): Multiple sclerosis: current knowledge and future outlook. *Eur Neurol* 72, 132–141
- Kasper LH, Reder AT (2014): Immunomodulatory activity of interferon-beta. *Ann Clin Transl Neurol* 1, 622–631

- Kebir H, Ifergan I, Alvarez JI, Bernard M, Poirier J, Arbour N, Duquette P, Prat A (2009): Preferential recruitment of interferon-gamma-expressing TH17 cells in multiple sclerosis. *Ann Neurol* 66, 390–402
- Kemppinen A, Sawcer S, Compston A (2011): Genome-wide association studies in multiple sclerosis: lessons and future prospects. *Brief Funct Genomics* 10, 61–70
- Kitamura D, Roes J, Kuhn R, Rajewsky K (1991): A B cell-deficient mouse by targeted disruption of the membrane exon of the immunoglobulin mu chain gene. *Nature* 350, 423–426
- Klubes P, Cerna I (1983): Use of uridine rescue to enhance the antitumor selectivity of 5-fluorouracil. *Cancer Res* 43, 3182–3186
- Köhler H, Hoffmann FA: Klinik. In: Schmidt RM, Hoffmann F, Faiss J, Köhler W (Eds.): *Multiple Sklerose*. 6. Edition; Elsevier Urban & Fischer, München 2015, 55-73
- Kolber P, Luessi F, Meuth SG, Klotz L, Korn T, Trebst C, Tackenberg B, Kieseier B, Kümpfel T, Fleischer V (2015): Aktuelles zur Therapieumstellung bei Multipler Sklerose. *Nervenarzt* 86, 1236–1247
- Koritschoner R, Schweinburg F (1925): Induktion von Paralyse und Rückenmarksentzündung durch Immunisierung von Kaninchen mit menschlichem Rückenmarksgewebe. *Z Immunitätsforsch ExpTher* 42, 217–283
- Korn T, Toyka K, Hartung HP, Jung S (2001): Suppression of experimental autoimmune neuritis by leflunomide. *Brain* 124, 1791–1802
- Korn T, Magnus T, Toyka K, Jung S (2004): Modulation of effector cell functions in experimental autoimmune encephalomyelitis by leflunomide--mechanisms independent of pyrimidine depletion. *J Leukoc Biol* 76, 950–960
- Kraan MC, Koster BM de, Elferink JGR, Post WJ, Breedveld FC, Tak PP (2000): Inhibition of neutrophil migration soon after initiation of treatment with leflunomide or methotrexate in patients with rheumatoid arthritis: Findings in a prospective, randomized, double-blind clinical trial in fifteen patients. *Arthritis Rheum* 43, 1488–1495
- Kuhlmann T, Lingfeld G, Bitsch A, Schuchardt J, Brück W (2002): Acute axonal damage in multiple sclerosis is most extensive in early disease stages and decreases over time. *Brain* 125, 2202–2212



- Kuo EA, Hambleton PT, Kay DP, Evans PL, Matharu SS, Little E, McDowall N, Jones CB, Hedgecock CJ, Yea CM (1996): Synthesis, structure-activity relationships, and pharmacokinetic properties of dihydroorotate dehydrogenase inhibitors: 2-cyano-3-cyclopropyl-3-hydroxy-N-3'-methyl-4'-(trifluoromethyl)phenyl propenamide and related compounds. *J Med Chem* 39, 4608–4621
- Langer-Gould A, Brara SM, Beaber BE, Koebnick C (2013): Childhood obesity and risk of pediatric multiple sclerosis and clinically isolated syndrome. *Neurology* 80, 548–552
- Lassmann H (2013): Pathology and disease mechanisms in different stages of multiple sclerosis. *J Neurol Sci* 333, 1–4
- Lassmann H, Bruck W, Lucchinetti CF (2007): The immunopathology of multiple sclerosis: an overview. *Brain Pathol* 17, 210–218
- Leitlinie MS see DGN
- Levin LI, Munger KL, O'Reilly EJ, Falk KI, Ascherio A (2010): Primary infection with the Epstein-Barr virus and risk of multiple sclerosis. *Ann Neurol* 67, 824–830
- Levine RL, Hoogenraad NJ, Kretchmer N (1974): A review: biological and clinical aspects of pyrimidine metabolism. *Pediatr Res* 8, 724–734
- Li L, Liu J, Delohery T, Zhang D, Arendt C, Jones C (2013): The effects of teriflunomide on lymphocyte subpopulations in human peripheral blood mononuclear cells in vitro. *J Neuroimmunol* 265, 82–90
- Linington C, Bradl M, Lassmann H, Brunner C, Vass K (1988): Augmentation of demyelination in rat acute allergic encephalomyelitis by circulating mouse monoclonal antibodies directed against a myelin/oligodendrocyte glycoprotein. *Am J Pathol* 130, 443–454
- Linker RA, Lee DH (2009): Models of autoimmune demyelination in the central nervous system: on the way to translational medicine. *Exp Transl Stroke Med* 1, 5
- Linker RA, Lee DH, Ryan S, van Dam AM, Conrad R, Bista P, Zeng W, Hronowsky X, Buko A, Chollate S (2011): Fumaric acid esters exert neuroprotective effects in neuroinflammation via activation of the Nrf2 antioxidant pathway. *Brain* 134, 678–692
- Lipton MM, Freund J, Brady E (1953): The transfer of experimental allergic encephalomyelitis in the rat by means of parabiosis. *J Immunol* 71, 380–384

- Lodygin D, Odoardi F, Schläger C, Körner H, Kitz A, Nosov M, van den Brandt J, Reichardt HM, Haberl M, Flügel A (2013): A combination of fluorescent NFAT and H2B sensors uncovers dynamics of T cell activation in real time during CNS autoimmunity. *Nat Med* 19, 784–790
- Löffler M, Jöckel J, Schuster G, Becker C (1997): Dihydroorotat-ubiquinone oxidoreductase links mitochondria in the biosynthesis of pyrimidine nucleotides. *Mol Cell Biochem* 17, 125-129
- Lublin FD, Reingold SC, Cohen JA, Cutter GR, Sorensen PS, Thompson AJ, Wolinsky JS, Balcer LJ, Banwell B, Barkhof F (2014): Defining the clinical course of multiple sclerosis: the 2013 revisions. *Neurology* 83, 278–286
- Lucchinetti C, Bruck W, Parisi J, Scheithauer B, Rodriguez M, Lassmann H (2000): Heterogeneity of multiple sclerosis lesions: implications for the pathogenesis of demyelination. *Ann Neurol* 47, 707–717
- Mandala S, Hajdu R, Bergstrom J, Quackenbush E, Xie J, Milligan J, Thornton R, Shei GJ, Card D, Keohane C (2002): Alteration of lymphocyte trafficking by sphingosine-1-phosphate receptor agonists. *Science* 296, 346–349
- Markowitz D, Goff S, Bank A (1988): Construction and use of a safe and efficient amphotropic packaging cell line. *Virology* 167, 400–406
- Martin DS, Stolfi RL, Sawyer RC, Spiegelman S, Young CW (1982): High-dose 5-fluorouracil with delayed uridine "rescue" in mice. *Cancer Res* 42, 3964–3970
- Martinelli V, Dalla Costa G, Colombo B, Dalla Libera D, Rubinacci A, Filippi M, Furlan R, Comi G (2014): Vitamin D levels and risk of multiple sclerosis in patients with clinically isolated syndromes. *Mult Scler* 20, 147–155
- Matyszak MK, Perry VH (1996): The potential role of dendritic cells in immune-mediated inflammatory diseases in the central nervous system. *Neuroscience* 74, 599–608
- McRae BL, Vanderlugt CL, Dal Canto MC, Miller SD (1995): Functional evidence for epitope spreading in the relapsing pathology of experimental autoimmune encephalomyelitis. *J Exp Med* 182, 75–85
- Merrill JE, Hanak S, Pu SF, Liang J, Dang C, Iglesias-Bregna D, Harvey B, Zhu B, McMonagle-Strucko K (2009): Teriflunomide reduces behavioral, electrophysiological,

and histopathological deficits in the Dark Agouti rat model of experimental autoimmune encephalomyelitis. *J Neurol* 256, 89–103

Miller A, Wolinsky J, Kappos L, Comi G, Freedman M, Olsson T, Liang J, Bauer D, Benamor M, Wamil B (2014): TOPIC: Efficacy and safety of once-daily oral teriflunomide in patients with first clinical episode consistent with multiple sclerosis (PL2.002). *Neurology* 82 (10 Supplement)

Munger KL, Bentzen J, Laursen B, Stenager E, Koch-Henriksen N, Sorensen TIA, Baker JL (2013): Childhood body mass index and multiple sclerosis risk: a long-term cohort study. *Mult Scler* 19, 1323–1329

Munger KL, Kochert K, Simon KC, Kappos L, Polman CH, Freedman MS, Hartung HP, Miller DH, Montalban X, Edan G (2014): Molecular mechanism underlying the impact of vitamin D on disease activity of MS. *Ann Clin Transl Neurol* 1, 605–617

Munier-Lehmann H, Vidalain P-O, Tangy F, Janin YL (2013): On dihydroorotate dehydrogenases and their inhibitors and uses. *J Med Chem* 56, 3148–3167

Neuhaus O, Farina C, Yassouridis A, Wiendl H, Then Bergh F, Dose T, Wekerle H, Hohlfeld R (2000): Multiple sclerosis: comparison of copolymer-1- reactive T cell lines from treated and untreated subjects reveals cytokine shift from T helper 1 to T helper 2 cells. *Proc Natl Acad Sci U S A* 97, 7452–7457

O'Connor P, Wolinsky JS, Confavreux C, Comi G, Kappos L, Olsson TP, Benzerdjeb H, Truffinet P, Wang L, Miller A (2011): Randomized trial of oral teriflunomide for relapsing multiple sclerosis. *N Engl J Med* 365, 1293–1303

Odoardi F, Sie C, Streyl K, Ulaganathan VK, Schläger C, Lodygin D, Heckelsmiller K, Nietfeld W, Ellwart J, Klinkert WE (2012): T cells become licensed in the lung to enter the central nervous system. *Nature* 488, 675–679

O'Gorman C, Broadley SA (2014): Smoking and multiple sclerosis: evidence for latitudinal and temporal variation. *J Neurol* 261, 1677–1683

Oh J, O'Connor PW (2014): Teriflunomide in the treatment of multiple sclerosis: current evidence and future prospects. *Ther Adv Neurol Disord* 7, 239–252

Oldstone MB (1987): Molecular mimicry and autoimmune disease. *Cell* 50, 819–820

Ousman SS, Kubes P (2012): Immune surveillance in the central nervous system. *Nat Neurosci* 15, 1096–1101

- Pender MP, Burrows SR (2014): Epstein-Barr virus and multiple sclerosis: potential opportunities for immunotherapy. *Clin Transl Immunology* 3, e27
- Perry VH (1998): A revised view of the central nervous system microenvironment and major histocompatibility complex class II antigen presentation. *J Neuroimmunol* 90, 113–121
- Peters GJ, Veerkamp JH (1983): Purine and pyrimidine metabolism in peripheral blood lymphocytes. *Int J Biochem* 15, 115–123
- Peterson JW, Bo L, Mork S, Chang A, Trapp BD (2001): Transected neurites, apoptotic neurons, and reduced inflammation in cortical multiple sclerosis lesions. *Ann Neurol* 50, 389–400
- Pham TH, Trung HM, Okada T, Matloubian M, Lo CG, Cyster JG (2008): S1P1 receptor signaling overrides retention mediated by G alpha i-coupled receptors to promote T cell egress. *Immunity* 28, 122–133
- Pinschewer DD, Ochsenbein AF, Fehr T, Zinkernagel RM (2001): Leflunomide-mediated suppression of antiviral antibody and T cell responses: Differential restoration by uridine. *Transplantation* 72, 712–719
- Popescu BFG, Pirko I, Lucchinetti CF (2013): Pathology of multiple sclerosis: where do we stand? *Continuum (Minneap Minn)* 19, 901–921
- Posevitz V, Chudyka D, Kurth F, Wiendl H (2012): Teriflunomide suppresses antigen induced T-cell expansion in a TCR avidity dependent fashion (P1107). *Mult Scler J* 2012, 509–520
- Ransohoff RM (2012): Immunology: Licensed in the lungs. *Nature* 488, 595–596
- Rice GPA, Hartung HP, Calabresi PA (2005): Anti-alpha4 integrin therapy for multiple sclerosis: mechanisms and rationale. *Neurology* 64, 1336–1342
- Ringheim GE, Lee L, Laws-Ricker L, Delohery T, Liu L, Zhang D, Colletti N, Soos TJ, Schroeder K, Fanelli B (2013): Teriflunomide attenuates immunopathological changes in the dark agouti rat model of experimental autoimmune encephalomyelitis. *Front Neurol* 4, 169
- Rivers TM (1935): Encephalomyelitis accompanied by myelin destruction experimentally produced in monkeys. *J Exp Med* 61, 689–702

- Rodi M, Dimisianos N, Lastic AL de, Sakellaraki P, Deraos G, Matsoukas J, Papathanasopoulos P, Mouzaki A (2016): Regulatory cell populations in relapsing-remitting multiple sclerosis (RRMS) Patients: effect of disease activity and treatment regimens. *Int J Mol Sci* 17, 1398
- Rodig SJ, Abramson JS, Pinkus GS, Treon SP, Dorfman DM, Dong HY, Shipp MA, Kutok JL (2006): Heterogeneous CD52 expression among hematologic neoplasms: implications for the use of alemtuzumab (CAMPATH-1H). *Clin Cancer Res* 12, 7174–7179
- Rosen H, Goetzl EJ (2005): Sphingosine 1-phosphate and its receptors: an autocrine and paracrine network. *Nat Rev Immunol* 5, 560–570
- Rückemann K, Fairbanks LD, Carrey EA, Hawrylowicz CM, Richards DF, Kirschbaum B, Simmonds HA (1998): Leflunomide inhibits pyrimidine de novo synthesis in mitogen-stimulated T-lymphocytes from healthy humans. *J Biol Chem* 273, 21682–21691
- Salzer J, Hallmans G, Nystrom M, Stenlund H, Wadell G, Sundstrom P (2013): Smoking as a risk factor for multiple sclerosis. *Mult Scler* 19, 1022–1027
- Sarchielli P, Zaffaroni M, Floridi A, Greco L, Candelieri A, Mattioni A, Tenaglia S, Di Filippo M, Calabresi P (2007): Production of brain-derived neurotrophic factor by mononuclear cells of patients with multiple sclerosis treated with glatiramer acetate, interferon-beta 1a, and high doses of immunoglobulins. *Mult Scler* 13, 313–331
- Schneider A, Long SA, Cerosaletti K, Ni CT, Samuels P, Kita M, Buckner JH (2013): In active relapsing-remitting multiple sclerosis, effector T cell resistance to adaptive T(regs) involves IL-6-mediated signaling. *Sci Transl Med* 5
- Schwentker FF, Rivers TM (1934): The antibody response of rabbits to injections of emulsions and extracts of homologous brain. *J Exp Med* 60, 559–574
- Siemasko KF, Chong AS, Williams JW, Bremer EG, Finnegan A (1996): Regulation of B cell function by the immunosuppressive agent leflunomide. *Transplantation* 61, 635–642
- Siemasko K, Chong AS, Jäck Hans-Martin, Gong H, Williams JW, Finnegan A (1998): Inhibition of JAK3 and STAT6 tyrosine phosphorylation by the immunosuppressive drug leflunomide leads to a block in IgG1 production. *J Immunol* 160, 1581–1588

- Silva HT, Cao W, Shorthouse R, Morris RE (1996): Mechanism of action of leflunomide: in vivo uridine administration reverses its inhibition of lymphocyte proliferation. *Transplant Proc* 28, 3082–3084
- Steinman L (2007): A brief history of T(H)17, the first major revision in the T(H)1/T(H)2 hypothesis of T cell-mediated tissue damage. *Nat Med* 13, 139–145
- Stromnes IM, Cerretti LM, Liggitt D, Harris RA, Goverman JM (2008): Differential regulation of central nervous system autoimmunity by T(H)1 and T(H)17 cells. *Nat Med* 14, 337–342
- Sykes DB, Kfoury YS, Mercier FE, Wawer MJ, Law JM, Haynes MK, Lewis TA, Schajnovitz A, Jain E, Lee D (2016): Inhibition of dihydroorotate dehydrogenase overcomes differentiation blockade in acute myeloid leukemia. *Cell* 167, 171–186
- Tanasescu R, Evangelou N, Constantinescu CS (2013): Role of oral teriflunomide in the management of multiple sclerosis. *Neuropsychiatr Dis Treat* 9, 539–553
- Teitelbaum D, Meshorer A, Hirshfeld T, Arnon R, Sela M (1971): Suppression of experimental allergic encephalomyelitis by a synthetic polypeptide. *Eur J Immunol* 1, 242–248
- van Groeningen CJ, Leyva A, Kraal I, Peters GJ, Pinedo HM (1986): Clinical and pharmacokinetic studies of prolonged administration of high-dose uridine intended for rescue from 5-FU toxicity. *Cancer Treat Rep* 70, 745–750
- van Groeningen CJ, Peters GJ, Pinedo HM (1993): Reversal of 5-fluorouracil-induced toxicity by oral administration of uridine. *Ann Oncol* 4, 317–320
- Vermersch P, Czlonkowska A, Grimaldi LME, Confavreux C, Comi G, Kappos L, Olsson TP, Benamor M, Bauer D, Truffinet P (2014): Teriflunomide versus subcutaneous interferon beta-1a in patients with relapsing multiple sclerosis: a randomised, controlled phase 3 trial. *Mult Scler Journal* 20, 705–716
- Warnke C, Meyer Zu Horste G, Menge T, Stuve O, Hartung H-P, Wiendl H, Kieseier BC (2013): Teriflunomide zur Behandlung der Multiplen Sklerose. *Nervenarzt* 84, 724–731
- Weber MS, Hohlfeld R, Zamvil SS (2007): Mechanism of action of glatiramer acetate in treatment of multiple sclerosis. *Neurotherapeutics* 4, 647–653

Wekerle H, Sun DM (2010): Fragile privileges: autoimmunity in brain and eye. *Acta Pharmacol Sin* 31, 1141–1148

Williamson RA, Yea CM, Robson PA, Curnock AP, Gadher S, Hambleton AB, Woodward K, Bruneau JM, Hambleton P, Moss D (1995): Dihydroorotate dehydrogenase is a high affinity binding protein for A77 1726 and mediator of a range of biological effects of the immunomodulatory compound. *J Biol Chem* 270, 22467–22472

Williamson RA, Yea CM, Robson PA, Curnock AP, Gadher S, Hambleton AB, Woodward K, Bruneau JM, Hambleton P, Spinella-Jaegle S (1996): Dihydroorotate dehydrogenase is a target for the biological effects of leflunomide. *Transplant Proc* 28, 3088–3091

Wucherpfennig KW, Strominger JL (1995): Molecular mimicry in T cell-mediated autoimmunity: Viral peptides activate human T cell clones specific for myelin basic protein. *Cell* 80, 695–705

Xu M, Lu X, Fang J, Zhu X, Wang J (2016): The efficacy and safety of teriflunomide based therapy in patients with relapsing multiple sclerosis: A meta-analysis of randomized controlled trials. *J Clin Neurosci* 33, 28–31

Xu X, Williams JW, Gong H, Finnegan A, Chong AS (1996): Two activities of the immunosuppressive metabolite of leflunomide, A77 1726. *Biochem Pharmacol* 52, 527–534

Yong VW, Chabot S, Stuve O, Williams G (1998): Interferon beta in the treatment of multiple sclerosis mechanisms of action. *Neurology* 51, 682–689

Zielinski T, Zeitter D, Müllner S, Bartlett RR (1995): Leflunomide, a reversible inhibitor of pyrimidine biosynthesis? *Inflamm Res* 44, 207-S208

## Acknowledgments

I would like to thank Prof. Dr. Alexander Flügel, director of the Institute for Neuroimmunology and Multiple Sclerosis Research (IMSF), for giving me the opportunity to write my thesis in his department and also for his guidance and support during this project.

I owe my deepest gratitude to my supervisor, Dr. Francesca Odoardi. She has been an outstanding mentor throughout the project. I cannot be grateful enough for her great support in theoretical and practical issues. Whenever I needed assistance, she was there.

I thank my former colleagues Dr. Christian Schläger, Dr. Alexandra Kitz, and Michael Haberl for sharing their theoretical and practical knowledge with me. I thank Dr. Anne Flach for her help with the sometimes tricky sorter. I thank Dr. Manuel von Osten for his support, especially for PP support. I would like to thank Maike Sonneck for introducing me to the technique of acute slicing. I thank Dr. Tanja Litke for her support during night shifts in the laboratory.

I thank Adriane Stas, Simon Mole, Nancy Meyer, Simone Hamann, and Birgit Curdt for their excellent technical assistance.

For her endless support, I am particularly grateful to my colleague and friend, Dr. Henrike Körner. She was a thorough proofreader and supported me in structuring and developing this thesis.



## Lebenslauf

Mein Name ist Jasemin Beate Dannheim. Ich bin am 05.06.1990 in Stade geboren, bin verheiratet und habe zwei Kinder (4 Jahre, 1 Jahr).

Am Gymnasium in Nordenham habe ich 2009 das Abitur mit der Note 1,2 abgelegt. Im selben Jahr begann ich an der Christian-Albrechts-Universität in Kiel Medizin zu studieren und bestand dort 2011 erfolgreich mein 1. Staatsexamen. Danach wechselte ich an die Georg-August-Universität Göttingen an der ich im Juni 2017 mein Studium der Humanmedizin mit der Note 1,6 abschloss.

Im Rahmen meines klinischen Studienabschnittes war ich im Sommersemester 2014 sowie im Sommersemester 2015 Vollzeit zur Datenerhebung für meine Promotionsarbeit „Analysis of teriflunomide therapy on EAE“ am Institut für Neuroimmunologie und Multiple-Sklerose-Forschung tätig. Zur Verbesserung meiner Englischkenntnisse famulierte ich im Februar 2014 für drei Monate am Sinai Hospital in Baltimore. Meine weiteren Famulaturen absolvierte ich im März 2012 in der allgemeinmedizinischen Praxis von Herrn Dr. Bethge in Nordenham, im Juli 2012 im Evangelischen Krankenhaus Weende in Göttingen in der Abteilung Anästhesie und anschließend eineinhalb Monate in der Inneren Medizin sowie im April 2014 für 14 Tage im GIZ Nord (Pharmakologie und Toxikologie).

Während meines Studiums wurde ich durch die Stiftung der deutschen Wirtschaft gefördert, in der ich mich zunächst um die Eingliederung neuer Mitglieder in unsere Regionalgruppe kümmerte und im April 2016 für ein Semester den Gruppenvorsitz übernahm. Des Weiteren besuchte ich mehrere Seminare u. a. zum Thema Strukturierung und Arbeitsverteilung in der Projektarbeit sowie Analyse von Persönlichkeitstypen, Konfliktmanagement, Teamsupport und Motivation.

Parallel zu meinem Studium engagierte ich mich ehrenamtlich in der Uniklinik Göttingen. Dort rief ich aus eigener Initiative heraus ein Zirkusprojekt für Kinder im stationären Aufenthalt ins Leben und betreute es zwei Jahre lang.

Nach meinem Studium begann ich im August 2018 in der Klinik für Kardiologie und Pneumologie der Universitätsmedizin Göttingen zu arbeiten. Nach der Geburt meines zweiten Sohnes und der Elternzeit wechselte ich an das Evangelische Krankenhaus in Oldenburg in die Abteilung Innere Medizin.